# A viral toolbox for conditional and transneuronal gene expression in zebrafish

**Chie Satou[1,*], Rachael L. Neve[2], Hassana K. Oyibo[1], Pawel Zmarz[1,7], Kuo-Hua Huang[1,8], Estelle Arn Bouldoires[1], Takuma Mori[3], Shin-ichi Higashijima[4,5], Georg B. Keller[1,6], Rainer W. Friedrich[1,6,*]**

**Affiliations**

1. Friedrich Miescher Institute for Biomedical Research, Basel, Switzerland
2. Gene Delivery Technology Core, Massachusetts General Hospital, MA, USA
3. Department of Molecular and Cellular Physiology, Institute of Medicine, Academic Assembly, Shinshu University, Nagano, JAPAN
4. National Institutes of Natural Sciences, Exploratory Research Center on Life and Living Systems, National Institute for Basic Biology, Okazaki, Japan
5. Graduate University for Advanced Studies, Okazaki, Aichi, Japan
6. Faculty of Natural Sciences, University of Basel, Basel, Switzerland
7. Present address: Department of Organismic and Evolutionary Biology and Center for Brain Science, Harvard University, Cambridge, MA, USA
8. Present address: Institute of Molecular Biology, Academia Sinica, Taipei, Taiwan

*** Corresponding authors:** chie.satou@fmi.ch, rainer.friedrich@fmi.ch

**Contact:**

Rainer Friedrich, Friedrich Miescher Institute for Biomedical Research, Maulbeerstrasse 66, 4058 Basel, Switzerland.
Phone: +41 79 666 8072
Email: rainer.friedrich@fmi.ch

**Abstract:**

**The zebrafish is an important model in systems neuroscience but a key limitation is the lack of viral tools to dissect the structure and function of neuronal circuitry. We developed methods for efficient gene transfer and retrograde tracing in adult and larval zebrafish by herpes simplex viruses (HSV1). HSV1 can be combined with the Gal4/UAS system to target cell types with high spatial, temporal and molecular specificity. We also established methods for efficient transneuronal tracing by modified rabies viruses in zebrafish. We demonstrate that HSV1 and rabies viruses can be used to visualize and manipulate genetically or anatomically identified neurons within and across different brain areas of adult and larval zebrafish. An expandable library of viruses is provided to express fluorescent proteins, calcium indicators, optogenetic probes, toxins and other molecular tools. This toolbox creates new opportunities to interrogate neuronal circuits in zebrafish through combinations of genetic and viral approaches.**

## Introduction

The zebrafish is an important vertebrate model in systems neuroscience because its small, optically accessible brain provides unique opportunities to analyze neuronal circuits and behavior[1,2]. Key methods established in zebrafish include large-scale imaging of neuronal population activity, behavioral approaches including virtual realities, and genetic manipulations[1–8], but efficient methods for viral gene transfer are still lacking. Viral vectors are important experimental tools in mammals because they enable the visualization and manipulation of defined neurons with high spatial, temporal and molecular specificity, and because they can bypass the need to generate transgenic animals[9,10]. Moreover, engineered viral tools that cross synapses allow for the visualization and physiological analysis of synaptically connected neuronal cohorts[11–13]. Our goal was to establish similar methods for specific viral gene transfer and transneuronal tracing in zebrafish.

## Results

### Optimization of the temperature regime for viral gene transfer

Previous studies demonstrated that adeno-associated viruses (AAVs), which are widely used for gene transfer in mammals and other amniotes, fail to infect neurons in the zebrafish brain[14]. Infection of zebrafish neurons by other viruses has been reported but efficiency was usually low and viral vectors for conditional gene expression in transgenic fish have not been described. To improve upon these points, we

first focused on herpes simplex virus 1 (HSV1), a DNA virus that can infect zebrafish neurons both locally and retrogradely via projecting axons without obvious signs of cytotoxicity[15]. We first explored whether HSV1-mediated gene transfer can be further improved by optimizing the temperature regime. Zebrafish are usually kept at 26 – 28.5 ºC but the temperature range of natural habitats is broad (up to >38 ºC) and temperature tolerance in the laboratory extends up to ~41 ºC[16,17]. We therefore tested whether viral gene expression is more efficient at temperatures near those of mammalian hosts (37 ºC).

After injection of amplicon type HSV1 viruses into the brain of adult or larval zebrafish using established procedures[15], swimming behavior appeared normal both at standard laboratory temperatures (26 - 28.5 ºC) and when fish were kept at 35 – 37 ºC (Supplementary Movies 1 – 3). To further examine effects of temperature on behavior we trained two groups of adult zebrafish in an odor discrimination task[6,18] that comprised one day of acclimatization to the setup followed by five days of appetitive conditioning (nine training trials with a rewarded odor [CS+] and with a non-rewarded odor [CS-] each per day). Group 1 (control) underwent no surgery and was kept at the standard laboratory temperature. Group 2 was injected with an HSV1 and subsequently kept at 36 ºC for two days before training commenced (Fig. S1a). Learning was assessed by a standard discrimination score and not significantly different between groups. These results confirm that swimming behavior and olfactory discrimination learning were not significantly impaired by virus injection or subsequent incubation at temperatures near 37 ºC.

To examine the temperature-dependence of HSV1-mediated gene expression we injected adult zebrafish expressing green fluorescent protein (GFP) under the *vglut1* promoter (Tg[*vglut1*:GFP]) with HSV1[*LTCMV*:DsRed], an HSV1 with an insert encoding the red-fluorescent protein DsRed under the control of a non-specific promoter for long-term expression (*LTCMV*). Injections were targeted unilaterally into the olfactory bulb (OB) and fish were then maintained at 26 ºC or 36 ºC for 6 days after injection (Fig. 1a). Consistent with previous results[15], reporter expression (DsRed) was observed in the injected OB (Fig. S1c). Moreover, retrogradely labeled neurons were present in telencephalic areas that project to the OB, most notably in the posterior zone of the dorsal telencephalon (Dp), the homolog of mammalian olfactory cortex (Fig. S1c). After incubation at 36 ºC, substantially more neurons expressed DsRed (Fig. 1b). In addition, retrograde labeling was detected in a small but distinct population of neurons in the dorsal telencephalon that was not seen at 26 ºC (Fig. 1b, c). DsRed expression at 36 ºC was first detected ~12 hours after injection and stable for at least 10 days (Fig. S1d). Moreover, increasing the temperature from 26 ºC to 36 ºC three days after the injection failed to enhance expression (Fig. 1a, c). These results show that adjusting the temperature to that of mammalian hosts can substantially increase the efficiency of HSV1-mediated viral gene transfer in zebrafish.

64 To explore viral gene delivery at earlier developmental stages we injected HSV1[*LTCMV*:GFP] into the
65 optic tectum of zebrafish larvae at 3 days post fertilization (dpf) and examined expression 48 h later.
66 Consistent with previous observations[15], expression of GFP was observed when fish were kept at 28.5 ºC
67 (N = 3 fish) but the number of GFP-positive cells further increased when temperature was raised to 32 ºC
68 (N = 5) or 35 ºC (N = 10; Fig. S2a). Strong and widespread expression was also observed when the virus
69 was injected at 5 dpf (N = 14) or 14 dpf (N = 9) and fish were subsequently kept at 35 ºC for 48 h (Fig.
70 S2b,c). When HSV1[*LTCMV*:GFP] was injected into muscles of the trunk at 5 dpf, strong and selective
71 retrograde labeling was observed in motor neurons in the spinal cord after keeping fish at 35 ºC for 48 h
72 (N = 4; Fig. S2d). These results indicate that HSV1 can be used for gene delivery and retrograde neuronal
73 tracing throughout development.

74

75 **Intersection of HSV1 with the Gal4/UAS system**

76 Viral vectors are often combined with transgenic lines to target specific cell types using two-component
77 expression systems (e.g., injection of a Cre-dependent viral construct into Cre-expressing mice). In
78 zebrafish, the most widely used two-component expression system is the Gal4/UAS system. We therefore
79 explored the possibility to combine viral delivery of UAS-dependent expression constructs with Gal4-
80 expressing driver lines. We first created a Gateway expression vector[20] to simplify the construction of
81 HSV1 for UAS-dependent expression (Fig. 2a). We then generated HSV1[*UAS*:TVA-mCherry] to
82 expresses a fusion of the transmembrane protein TVA and the red fluorescent protein mCherry under
83 UAS control. This virus did not drive expression when injected into the brain of wt zebrafish (N = 3; not
84 shown).

85 We injected HSV1[*UAS*:TVA-mCherry] into the cerebellum of adult Tg[*gad1b*:GFP; *gad1b*:Gal4] fish[18],
86 which express Gal4 and GFP under the control of the *gad1b* promoter, a marker of GABAergic neurons.
87 Consistent with the distribution of GABAergic neurons in the cerebellum, GFP was expressed in Purkinje
88 neurons and in a sparse neuronal population in the granular layer, presumably Golgi cells. mCherry was
89 co-expressed with GFP in a subset of Purkinje neurons and putative Golgi cells (97.7 ± 1.2 % of
90 mCherry-positive neurons were also GFP-positive; mean ± s.d.; N = 4 fish; Fig. 2b,c). No expression was
91 detected in the dense population of GFP-negative granule cells in the granular layer.

92 Co-expression of mCherry and GFP was observed also when the injection of HSV1[*UAS*:TVA-mCherry]
93 was directed at a cluster of GABAergic neurons near Dp in adult Tg[*gad1b*:GFP; *gad1b*:Gal4] fish (94.8
94 ± 4.5 % of mCherry+ neurons coexpressed GFP; mean ± s.d.; N = 5 fish; Fig. 2c, Fig. S3). Interestingly,
95 mCherry-expressing neurites arborized extensively in the lateral pallium but spared a region of Dp

immediately adjacent to the *gad1b*-positive cluster, indicating that the dorsal telencephalon contains specific long-range projections of GABAergic neurons (Fig. S3a). In zebrafish larvae (7 dpf) we injected HSV1[*UAS*:GFP] into the hindbrain of Tg[*gad1b*:Gal4; *gad1b*:DsRed] fish (N = 3) and detected expression of GFP selectively in DsRed-positive cells in the hindbrain and cerebellum (Fig. S2e). These observations indicate that HSV1 can be combined with the Gal4/UAS system to enhance the specificity of cellular targeting.

To corroborate this conclusion we designed experiments to target sparse neuronal populations. We first injected HSV1[*UAS*:Venus-CAAX] into the optic tectum of Tg[*th*:Gal4; *UAS*:tdTomato-CAAX] fish, which express Gal4 and the red-fluorescent protein tdTomato-CAAX under the control of the tyrosine hydroxylase-1 promoter, a marker for catecholaminergic neurons. This procedure resulted in the selective expression of the membrane-associated protein Venus-CAAX in a small number of tdTomato-CAAX-positive neurons in the locus coeruleus with complex long-distance axonal projections, indicating that expression was specifically directed to catecholaminergic (noradrenergic) neurons (Fig. 2d; N = 4 fish). In additional experiments we first injected HSV1[*LTCMV*:Gal4] into the OB of wt zebrafish and subsequently injected HSV1[*UAS*:GFP] into the dorsal telencephalon. Expression of GFP was observed specifically in OB-projecting neurons of the dorsal telencephalon without expression elsewhere (Fig. 2e). To assess the efficiency of this intersectional targeting approach we compared the number of labeled neurons using either the Gal4/UAS system or the one-component approach (injection of HSV1[*LTCMV*:DsRed] into OB). Both approaches yielded similar numbers of labeled neurons in the dorsal telencephalon (Fig. 2f). We therefore conclude that HSV1 can be combined with the Gal4/UAS system in intersectional approaches with high efficiency and low leakiness.

We next explored strategies for co-expression of multiple transgenes in the same neurons. When red and green reporter constructs were co-packaged into the same virus (HSV1[*UAS*:TVA-mCherry & *UAS*:GFP]), injection into the cerebellum of Tg[*gad1b*:Gal4] resulted in a high rate of co-expression, as expected (89.5 ± 8.7 % co-expression; mean ± s.d.; N = 3 fish; Fig. S4a, c). However, the rate of co-expression did not reach 100 %, possibly because not all virus particles received both constructs during packaging. Interestingly, co-injection of the same responder constructs packaged into separate viruses (HSV1[*UAS*:TVA-mCherry] and HSV1[*UAS*:GFP]) produced a similar rate of co-expression, even when overall expression was sparse (84.3 ± 6.0 % co-expression; mean ± s.d.; N = 3 fish; Fig. S4b, c). These results indicate that co-packaging and co-injection of viruses can be used to express multiple transgenes in the same neurons.

We also tested HSV1 as a tool for functional manipulations of neurons and behavior. We first injected HSV1[*LTCMV*:Gal4] into the OB of wt zebrafish and subsequently co-injected HSV1[*UAS*:GCaMP6f]

129 and HSV1[*UAS*:Chrimson-tdTomato] into the dorsal telencephalon. This procedure resulted in the co-
130 expression of the green-fluorescent calcium indicator GCaMP6f [21] and the red-light-gated cation channel
131 Chrimson-tdTomato[22] in OB-projecting neurons of the dorsal telencephalon. Brief (500 ms) illumination
132 with red light evoked GCaMP6f fluorescence transients that increased in amplitude with increasing light
133 intensity (Fig. S5; 11 neurons in N = 1 fish). Hence, transgene-expressing neurons were functional and
134 responsive to optogenetic stimulation. To explore strategies for neuronal ablations we expressed tetanus
135 toxin light chain (TeNT) in GABAergic neurons of the cerebellum by injecting HSV1[*UAS*:TeNT-GFP]
136 into the cerebellum of Tg[*gad1b*:Gal4] fish. Injected fish showed abnormal body posture and swimming
137 patterns while control fish injected with HSV1[*UAS*:GFP] swam normally (Supplementary Movie 4).
138 HSV1-mediated gene transfer thus offers a wide range of opportunities for anatomical and functional
139 experiments in zebrafish.

140 We have so far assembled a collection of 26 different HSV1s for applications in zebrafish
141 (Supplementary Table1). 15 of these drive expression of fluorescent markers, calcium indicators, Gal4 or
142 optogenetic probes under the control of the non-specific LTCMV promoter for regional transgene
143 expression and retrograde tracing. The remaining 11 HSV1s drive expression of fluorescent markers,
144 optogenetic probes, toxins and other proteins under UAS control for intersectional targeting of neurons
145 using the Gal4/UAS system. This toolbox is available and can be further expanded using our UAS-
146 containing expression vector (Fig. 2a).

147

148 **Transneuronal viral tracing in zebrafish**

149 The ability of some viruses to cross synapses has been exploited to express transgenes in synaptically
150 connected cohorts of neurons. In zebrafish and other species, neurons were traced across one or multiple
151 synapses using engineered vesicular stomatitis viruses (VSVs) but these tools have not been used widely
152 as biological tools, possibly because they can exhibit toxicity[23–25]. In rodents, modified rabies viruses
153 have become important tools to analyze connectivity and structure-function relationships in neuronal
154 circuits. These vectors can infect specific "starter" neurons and are transmitted retrogradely to presynaptic
155 neurons across one synapse. Specific infection is achieved by expressing the receptor protein TVA in the
156 starter neuron and pseudotyping the virus with the envelope protein EnvA[11]. To limit retrograde transfer
157 to one synapse, an essential glycoprotein (G) is deleted from the viral genome and supplied in *trans* only
158 in the starter neurons. In zebrafish, the G-deleted rabies virus (RVΔG) has been reported to infect
159 neurons[14] and to cross synapses when complemented with G but the efficiency of retrograde synaptic
160 transfer appeared very low[26].

161 To enhance the efficiency of viral infection and transneuronal tracing we first explored the effect of
162 temperature. When we injected EnvA-coated RVΔG expressing GFP (EnvA-RVΔG-GFP) into the
163 telencephalon of wt fish at 36 ºC, no GFP expression was observed (Fig. S6). We then injected EnvA-
164 RVΔG-GFP into the telencephalon of Tg[*gad1b*:Gal4; *UAS*:TVA-mCherry] fish that express TVA-
165 mCherry in GABAergic neurons. After 6 days, efficient and selective infection of neurons expressing
166 GFP was observed at 36 ºC but not at 26 ºC, nor when the temperature was raised from 26 ºC to 36 ºC
167 three days post injection (Fig. S7). Hence, infection of zebrafish neurons by EnvA-RVΔG-GFP required
168 TVA and was substantially more efficient when the temperature was close to the body temperature of
169 natural hosts. Subsequent experiments were therefore performed at 35 – 37 ºC.

170 To assess potential toxicity of RVΔG we injected EnvA-RVΔG-GFP into the OB of Tg[*gad1b*:Gal4;
171 *UAS*:TVA-mCherry] fish as before, dissociated the OB, and performed RNA sequencing after
172 fluorescence-activated cell sorting. This approach allowed us to compare transcriptomes of GABAergic
173 neurons infected by RVΔG (green and red) to transcriptomes of non-infected GABAergic neurons
174 expressing only the TVA receptor (red only; Fig. S8). Of 19'819 endogenous genes analyzed, 522 were
175 significantly downregulated while 27 were significantly upregulated in infected cells. Among these, stress
176 markers occurred with approximately average frequency (downregulated: 27 out of 471 stress marker
177 genes; upregulated: 1/471) and cell death markers were underrepresented (downregulated: 14/651 genes;
178 upregulated: 4/651; Fig. 3a-c; Supplementary Table2). The 65 gene ontology (GO) terms that were
179 significantly associated with the set of regulated genes were primarily related to immune responses while
180 GO terms related to stress, cell death, electrophysiological properties or synapses were rare or absent
181 (Supplementary Table 3). These results indicate that RVΔG does not have major effects on the health or
182 physiological status of infected neurons.

183 To directly compare neuronal activity of infected and uninfected neurons we targeted the dense
184 population of GABAergic interneurons in the deep layers of the OB. We injected EnvA-RVΔG-mCherry
185 into the OB of adult Tg[*gad1b*:Gal4; *UAS*:TVA-mCherry] fish and detected infection in a subset of
186 neurons by the strong cytoplasmic and nuclear expression of mCherry, which could easily be
187 distinguished from the weak, membrane-associated background expression of TVA-mCherry (Fig. 3c).
188 We then loaded neurons non-specifically with the green-fluorescent calcium indicator Oregon Green 488
189 BAPTA-1 (OGB1) by bolus injection of the AM ester[27] and measured odor responses of all neurons
190 simultaneously (Fig. 3d). No obvious differences were detected in the time course or amplitude
191 distribution of odor responses between infected neurons (N = 1293 neurons from four fish) and uninfected
192 neurons (N = 559 from the same four fish; Fig. 3e-g). Together, these results indicate that infection with
193 RVΔG did not compromise the health or physiological function of neurons.

194 Efficient transneuronal spread of the rabies virus depends on the expression level of the viral glycoprotein
195 in starter cells[28,29]. We therefore took two steps to enhance glycoprotein expression. First, we optimized
196 codon usage for zebrafish. Second, we expressed TVA and the codon-optimized glycoprotein (zoSADG)
197 using HSV1 because viral vectors typically reach higher expression levels than transgenics[15]. In rodents,
198 starter neurons expressing high levels of G often disappear in parallel with the emergence of
199 transneuronal expression, presumably because long-term expression of G is toxic[30,31]. We therefore
200 determined the time course of transgene expression under different experimental conditions. We first
201 focused on the cerebellum where GABAergic Purkinje neurons receive local synaptic input from different
202 types of cerebellar neurons and long-range input from neurons in the contralateral inferior olive (climbing
203 fibers; Fig. 4a). We injected a mixture of HSV1[*UAS*:TVA-mCherry] and EnvA-RVΔG-GFP into the
204 cerebellum of Tg[*gad1b*:Gal4] fish and examined expression for up to 10 days. As observed before
205 (Fig. 2b), mCherry expression was localized to Purkinje neurons and putative Golgi cells. Neurons
206 expressing GFP were concentrated around the injection site and usually co-expressed mCherry (Fig 4b,
207 d). Rarely, GFP expression was observed in mCherry-negative neurons (Fig. 4d), which may indicate
208 TVA-independent viral entry. However, as no GFP expression was observed when EnvA-RVΔG-GFP
209 was injected into wt animals (Fig. S6), it appears more likely that GFP+/mCherry- neurons initially
210 expressed TVA but subsequently lost expression due to the slight decline of expression driven by the viral
211 promoter (Fig. S1b). Co-expression of mCherry and GFP was stable for at least 10 days after injection
212 and GFP+/mCherry- neurons remained very rare (Fig. 4d). These results confirm the specificity of EnvA-
213 RVΔG-GFP infection and provide additional evidence that expression of TVA-mCherry or the infection
214 by RVΔG alone are not toxic in the absence of glycoprotein. No expression of GFP was observed in the
215 inferior olive, consistent with the expectation that RVΔG does not spread in the absence of glycoprotein.

216 To examine whether the delivery of glycoprotein to starter cells can drive transneuronal spread, we
217 injected a mixture of HSV1[*UAS*:TVA-mCherry], HSV1[*UAS*:zoSADG] and EnvA-RVΔG-GFP into the
218 cerebellum of Tg[*gad1b*:Gal4] fish. Unlike in the absence of glycoprotein, the number of mCherry-
219 expressing Purkinje neurons and putative Golgi cells now declined over the incubation period of 10 days.
220 The number of neurons expressing GFP, in contrast, was low initially but increased steeply between 6 and
221 10 days after injection (Fig. 4d). In the cerebellum, GFP was expressed in Purkinje cells and throughout
222 the granular layer (Fig. 4c). The number and spatial distribution of GFP-expressing neurons in the
223 granular layer was clearly different from mCherry expression in the absence of glycoprotein
224 (Tg[*gad1b*:Gal4] fish injected with HSV1[*UAS*:TVA-mCherry]; Fig. 2b), indicating that GFP was
225 expressed in granule cells. Moreover, GFP-positive neurons were found in the contralateral inferior olive
226 (Fig. 4c). We therefore conclude that *trans*-complementation with zoSADG in starter cells promoted
227 transneuronal spread of the rabies virus.

228 Transneuronal viral transfer for synaptic inputs to Purkinje neurons from the inferior olive was quantified
229 in each individual by a convergence index that is defined as the number of transneuronally labeled
230 neurons (here: GFP+/mCherry- neurons in the inferior olive) normalized to the number of starter cells
231 (here: GFP+/mCherry+ Purkinje neurons)[29,32]. This index does not reflect the true convergence because
232 an unknown number of starter neurons has disappeared at the time when neurons are counted. We
233 nevertheless used this index to assess transneuronal spread because it has been established previously as a
234 benchmark in rodents[29,32]. The convergence index was 1.00 ± 0.95 (mean ± s.d.; N = 4 fish; Fig. 4e),
235 which is comparable to values reported in mammals[29].

236 To corroborate these results we also examined transneuronal tracing from starter neurons in telencephalic
237 area Dp. In this area, both glutamatergic principal neurons and GABAergic interneurons receive long-
238 range input from mitral cells in the OB (Fig. 4f). In addition, Dp receives other telencephalic inputs that
239 are not well characterized. When a mixture of HSV1[*UAS*:TVA-mCherry] and EnvA-RVΔG-GFP was
240 injected into Tg[*gad1b*:Gal4] fish (Fig. 4g), GFP expression was largely restricted to a cluster of neurons
241 that co-expressed mCherry (Fig. 4g). This cluster was located near a prominent furrow that separates an
242 anterior from a posterior compartment of Dp, consistent with the known location of GABAergic neurons
243 in Dp[18]. When HSV1[*UAS*:zoSADG] was added to the injected virus mixture, mCherry expression
244 became rare while a large number of neurons in different telencephalic areas expressed GFP (Fig. 4h, i).
245 Moreover, GFP was expressed in the olfactory bulb by neurons with the characteristic morphology of
246 mitral cells, but not by other cells (Fig. 4h).

247 Similar observations were made when the infection was targeted to glutamatergic starter neurons by
248 injecting the cocktail of viruses into Dp of Tg[*vglut1*:Gal4] fish (Fig. S9). In the absence of
249 HSV1[*UAS*:zoSADG], GFP was co-expressed with mCherry and restricted to the injection site, while in
250 the presence of HSV1[*UAS*:zoSADG], expression of mCherry disappeared and GFP expression became
251 more widespread, including neurons in the OB (Fig. S9 ). Note that *vglut1* is expressed in excitatory
252 neurons in the telencephalon but not in the OB (Fig. S10), implying that labeling of OB neurons cannot
253 be explained by direct infection. Convergence indices for projections of mitral cells to GABAergic or
254 glutamatergic starter neurons in Dp were 0.70 ± 0.21 and 1.31 ± 1.20 (mean ± s.d.; N = 5 and N = 4 fish,
255 respectively; Fig. 4j). These results confirm that EnvA-RVΔG selectively infects TVA-expressing target
256 neurons and undergoes monosynaptic retrograde transneuronal transfer when complemented with
257 zoSADG.

258 To examine transneuronal viral spread at early developmental stages we injected EnvA-RVΔG-GFP into
259 the spinal cord of Tg[*gad1b*:Gal4; *UAS*:TVA-mCherry] fish at 10 dpf and analyzed fluorescence after
260 6 – 7 days. In the absence of zoSADG, GFP expression was restricted to mCherry-positive neurons

261 around the injection site (Fig. 5a). When zoSADG was supplied in *trans* by co-injecting EnvA-RVΔG-
262 GFP with HSV1[*UAS*:zoSADG], GFP expression was observed throughout the spinal cord and in the
263 brainstem (Fig. 5b). GFP-positive neurons distant from the injection site did usually not co-express
264 mCherry. We therefore conclude that glycoprotein-dependent retrograde transneuronal transfer also
265 occurs at larval stages.

266

267 **Discussion**

268 In summary, we found that viral infection and transgene expression in zebrafish can be significantly
269 enhanced by adjusting the temperature to that of the natural viral host. HSV1 vectors can be combined
270 with the Gal4/UAS system for intersectional gene expression strategies without obvious leakiness. We
271 applied HSV1s to target the expression of multiple transgenes to different brain areas and neuron types in
272 the adult zebrafish brain and in larvae. Hence, HSV1-mediated gene transfer and retrograde tracing has a
273 wide range of potential of applications in zebrafish.

274 We have generated a collection of HSV1s for the direct or conditional expression of different transgenes
275 including fluorescent markers, calcium indicators, optogenetic probes, and toxins (Supplementary
276 Table1). This toolbox opens novel opportunities for the fast and flexible interrogation of neurons in
277 zebrafish. Intersectional strategies can be used to target narrowly defined types of neurons by combining
278 the genetic specificity of promoters and the Gal4/UAS system with the spatial and temporal precision of
279 injections. For example, anatomically defined sets of projection neurons can be targeted by retrograde
280 HSV1-mediated delivery of Gal4 and subsequent HSV1-mediated delivery of a UAS responder.
281 Importantly, expression can be directed to specific neurons by injecting HSV1 with UAS-dependent
282 inserts into existing Gal4 driver lines. Such approaches can immediately capitalize on the broad spectrum
283 of Gal4 driver lines that has been created using defined promoters and random insertion strategies[33–35].
284 Conceivably, viral delivery of UAS responders may also be useful to overcome the slow loss of
285 expression observed in some Gal4/UAS transgenic lines over generations because it bypasses epigenetic
286 silencing of the highly repetitive UAS elements[36,37].

287 We further established procedures for retrograde monosynaptic tracing using rabies viruses that greatly
288 enhanced the efficiency of transneuronal transfer compared to a previous study in zebrafish[26].
289 Temperature adjustments were important but unlikely to be the only factor underlying the enhanced
290 transneuronal spread because the temperature difference to the previous study was only 1.5 ºC[26]. We
291 therefore assume that increased glycoprotein expression by codon optimization, viral gene delivery, and
292 possibly small differences in the experimental schedule also contributed significantly. Transcriptomics

293 and measurements of odor-evoked activity revealed no signs of toxicity of RVΔG alone, indicating that
294 transneuronally labeled neurons are healthy even though starter neurons disappear.

295 Transneuronal spread of rabies viruses was glycoprotein-dependent and labeled substantial numbers of
296 putative presynaptic neurons from different starter neurons, both in adult zebrafish and in larvae.
297 Convergence ratios were similar to those observed in rodents despite the fact that zebrafish neurons are
298 smaller and probably receive fewer synaptic inputs. These results suggest that the efficiency of
299 transneuronal tracing was in the same range as in rodents although quantitative comparisons are difficult.
300 In the future, further improvements may be achieved by modifications that are currently explored in
301 rodents such as the design of optimized glycoproteins[29] or trans-complementation with a second viral
302 gene[38]. The apparent long-term toxicity of the glycoprotein may be circumvented by transient expression
303 using a negative feedback system[39]. Hence, rabies-based transneuronal tracers are promising tools for the
304 structural and functional dissection of neuronal circuitry in zebrafish.

305 Retrograde tracing of connected neuronal cohorts using rabies viruses has become an important approach
306 to decipher the functional logic of neuronal connectivity in rodents. Our results pave the way for
307 applications of this approach in zebrafish. The small size of zebrafish facilitates the combination of
308 neuronal circuit tracing with other methods such high-resolution imaging of neuronal activity patterns
309 throughout large brain areas. Transneuronal tracing in the anterograde direction from starter neurons that
310 were not genetically defined has previously been achieved using VSVs in larval zebrafish[23,24]. Recently, it
311 has been reported that the cytotoxicity of VSVs used in initial studies can be reduced[25], suggesting that
312 anterograde transneuronal tracing using VSVs may complement retrograde transneuronal tracing by
313 rabies viruses. Our experiments were designed primarily to explore HSV1 and rabies viruses as tools for
314 structural and functional analyses of neuronal circuits and behavior. Moreover, the ability of HSV1 and
315 rabies viruses, as well as VSVs, to infect larval neurons may be exploited for studies of development,
316 although the temporal resolution will be limited by the time required for viral gene expression (days).
317 Viral tools and their combination with transgenic lines and optical approaches therefore offer a wide
318 range of experimental opportunities that have not been available in zebrafish so far.

## References


1. Friedrich, R. W., Jacobson, G. A. & Zhu, P. Circuit Neuroscience in Zebrafish. *Curr. Biol.* **20**, R371–R381 (2010).

2. Vanwalleghem, G. C., Ahrens, M. B. & Scott, E. K. Integrative whole-brain neuroscience in larval zebrafish. *Curr. Opin. Neurobiol.* **50**, 136–145 (2018).

3. Aoki, T. *et al.* Imaging of neural ensemble for the retrieval of a learned behavioral program. *Neuron* **78**, 881–894 (2013).

4. Cherng, B. W., Islam, T., Torigoe, M., Tsuboi, T. & Okamoto, H. The Dorsal Lateral Habenula-Interpeduncular Nucleus Pathway Is Essential for Left-Right-Dependent Decision Making in Zebrafish. *Cell Rep.* **32**, 108143 (2020).

5. Huang, K. H. *et al.* A virtual reality system to analyze neural activity and behavior in adult zebrafish. *Nat. Methods* **17**, 343–351 (2020).

6. Namekawa, I., Moenig, N. R. & Friedrich, R. W. Rapid olfactory discrimination learning in adult zebrafish. *Exp. Brain Res.* **236**, 2959–2969 (2018).

7. Satou, C. *et al.* Functional Diversity of Glycinergic Commissural Inhibitory Neurons in Larval Zebrafish. *Cell Rep.* **30**, 3036-3050.e4 (2020).

8. Amo, R. *et al.* The habenulo-raphe serotonergic circuit encodes an aversive expectation value essential for adaptive active avoidance of danger. *Neuron* **84**, 1034–1048 (2014).

9. Jüttner, J. *et al.* Targeting neuronal and glial cell types with synthetic promoter AAVs in mice, non-human primates and humans. *Nat. Neurosci.* **22**, 1345–1356 (2019).

10. Luo, L., Callaway, E. M. & Svoboda, K. Genetic Dissection of Neural Circuits : A Decade of Progress. *Neuron* **98**, 256–281 (2018).

11. Wickersham, I. R. *et al.* Monosynaptic Restriction of Transsynaptic Tracing from Single, Genetically Targeted Neurons. *Neuron* **53**, 639–647 (2007).

12. Ghanem, A. & Conzelmann, K. K. G gene-deficient single-round rabies viruses for neuronal circuit analysis. *Virus Res.* **216**, 41–54 (2016).

13. Callaway, E. M. & Luo, L. Monosynaptic circuit tracing with glycoprotein-deleted rabies viruses. *J. Neurosci.* **35**, 8979–8985 (2015).

14. Zhu, P. *et al.* Optogenetic dissection of neuronal circuits in zebrafish using viral gene transfer and the tet system. *Front. Neural Circuits* **3**, 1–12 (2009).

15. Zou, M., De Koninck, P., Neve, R. L. & Friedrich, R. W. Fast gene transfer into the adult zebrafish brain by herpes simplex virus 1 (HSV-1) and electroporation: Methods and optogenetic applications. *Front. Neural Circuits* **8**, 1–16 (2014).

16. López-Olmeda, J. F. & Sánchez-Vázquez, F. J. Thermal biology of zebrafish (Danio rerio). *J. Therm. Biol.* **36**, 91–104 (2011).

17. Engeszer, R. E., Patterson, L. B., Rao, A. A. & Parichy, D. M. Zebrafish in the wild: A review of natural history and new notes from the field. *Zebrafish* **4**, 21–40 (2007).

18. Frank, T., Mönig, N. R., Satou, C., Higashijima, S. ichi & Friedrich, R. W. Associative conditioning remaps odor representations and modifies inhibition in a higher olfactory brain area. *Nat. Neurosci.* **22**, 1844–1856 (2019).

19. Dana, H. *et al.* High-performance calcium sensors for imaging activity in neuronal populations and microcompartments. *Nat. Methods* **16**, 649–657 (2019).

361 20. Reece-hoyes, J. S. & Walhout, A. J. M. Gateway Recombinational Cloning. (2018)
362 doi:10.1101/pdb.top094912.

363 21. Chen, T. W. *et al.* Ultrasensitive fluorescent proteins for imaging neuronal activity. *Nature* **499**, 295–300
364 (2013).

365 22. Klapoetke, N. C. *et al.* Independent optical excitation of distinct neural populations. *Nat. Methods* **11**, 338–
366 346 (2014).

367 23. Mundell, N. A. *et al.* Vesicular Stomatitis Virus Enables Gene Transfer and Transsynaptic Tracing in a
368 Wide Range of Organisms. **1663**, 1639–1663 (2015).

369 24. Ma, M., Kler, S. & Pan, Y. A. Structural Neural Connectivity Analysis in Zebrafish With Restricted
370 Anterograde Transneuronal Viral Labeling and Quantitative Brain Mapping. *Front. Neural Circuits* **13**,
371 (2020).

372 25. Kler, S., Ma, M., Narayan, S., Ahrens, M. B. & Albert, Y. Cre-Dependent Anterograde Transsynaptic
373 Labeling and Functional Imaging in Zebrafish Using VSV With Reduced Cytotoxicity. *Front. Neuroanat.*
374 **15**, 1–10 (2021).

375 26. Dohaku, R. *et al.* Tracing of afferent connections in the zebrafish cerebellum using recombinant rabies virus.
376 *Front. Neural Circuits* **13**, 1–15 (2019).

377 27. Yaksi, E. & Friedrich, R. W. Reconstruction of firing rate changes across neuronal populations by
378 temporally deconvolved Ca2+ imaging. *Nat. Methods* **3**, 377–383 (2006).

379 28. Miyamichi, K. *et al.* Dissecting local circuits: Parvalbumin interneurons underlie broad feedback control of
380 olfactory bulb output. *Neuron* **80**, 1232–1245 (2013).

381 29. Kim, E. J. *et al.* Improved Monosynaptic Neural Circuit Tracing Using Engineered Rabies Virus
382 Glycoproteins Report Improved Monosynaptic Neural Circuit Tracing Using Engineered Rabies Virus
383 Glycoproteins. *CellReports* **15**, 692–699 (2016).

384 30. Faber, M. *et al.* Overexpression of the Rabies Virus Glycoprotein Results in Enhancement of Apoptosis and
385 Antiviral Immune Response. *J. Virol.* **76**, 3374–3381 (2002).

386 31. Ohara, S., Sato, S., Oyama, K., Tsutsui, K. I. & Iijima, T. Rabies virus vector transgene expression level and
387 cytotoxicity improvement induced by deletion of glycoprotein gene. *PLoS One* **8**, (2013).

388 32. Miyamichi, K. *et al.* Cortical representations of olfactory input by trans-synaptic tracing. *Nature* **472**, 191–
389 199 (2011).

390 33. Satou, C. *et al.* Transgenic tools to characterize neuronal properties of discrete populations of zebrafish
391 neurons. *Development* **140**, 3927–3931 (2013).

392 34. Asakawa, K. *et al.* Genetic dissection of neural circuits by Tol2 transposon-mediated Gal4 gene and
393 enhancer trapping in zebrafish. *Proc. Natl. Acad. Sci. U. S. A.* **105**, 1255–1260 (2008).

394 35. Förster, D. *et al.* Genetic targeting and anatomical registration of neuronal populations in the zebrafish brain
395 with a new set of BAC transgenic tools. *Sci. Rep.* **7**, 1–11 (2017).

396 36. Akitake, C. M., Macurak, M., Halpern, M. E. & Goll, M. G. Transgenerational analysis of transcriptional
397 silencing in zebrafish. *Dev. Biol.* **352**, 191–201 (2011).

398 37. Goll, M. G., Anderson, R., Stainier, D. Y. R., Spradling, A. C. & Halpern, M. E. Transcriptional silencing
399 and reactivation in transgenic zebrafish. *Genetics* **182**, 747–755 (2009).

400 38. Chatterjee, S. *et al.* Nontoxic, double-deletion-mutant rabies viral vectors for retrograde targeting of
401 projection neurons. *Nat. Neurosci.* **21**, 638–646 (2018).

402 39. Ciabatti, E., González-Rueda, A., Mariotti, L., Morgese, F. & Tripodi, M. Life-Long Genetic and Functional
403 Access to Neural Circuits Using Self-Inactivating Rabies Virus. *Cell* **170**, 382-392.e14 (2017).

404 40. Li, J. *et al.* Intron targeting-mediated and endogenous gene integrity-maintaining knockin in zebrafish using
405 the CRISPR/Cas9 system. *Cell Res.* **25**, 634–637 (2015).

406 41. Miyasaka, N. *et al.* Olfactory projectome in the zebrafish forebrain revealed by genetic single-neuron
407 labelling. *Nat. Commun.* **5**, (2014).

408 42. Urasaki, A., Morvan, G. & Kawakami, K. Functional dissection of the Tol2 transposable element identified
409 the minimal cis-sequence and a highly repetitive sequence in the subterminal region essential for
410 transposition. *Genetics* **174**, 639–649 (2006).

411 43. Watabe-Uchida, M., Zhu, L., Ogawa, S. K., Vamanrao, A. & Uchida, N. Whole-Brain Mapping of Direct
412 Inputs to Midbrain Dopamine Neurons. *Neuron* **74**, 858–873 (2012).

413 44. Kimura, Y., Hisano, Y., Kawahara, A. & Higashijima, S. I. Efficient generation of knock-in transgenic
414 zebrafish carrying reporter/driver genes by CRISPR/Cas9-mediated genome engineering. *Sci. Rep.* **4**, 1–7
415 (2014).

416 45. Wertz, A. *et al.* Network Modules. *Science (80-. ).* **349**, 70–74 (2015).

417 46. Vélez-Fort, M. *et al.* The stimulus selectivity and connectivity of layer six principal cells reveals cortical
418 microcircuits underlying visual processing. *Neuron* **83**, 1431–1443 (2014).

419 47. Susaki, E. A. *et al.* Whole-brain imaging with single-cell resolution using chemical cocktails and
420 computational analysis. *Cell* **157**, 726–739 (2014).

421 48. Attinger, A., Wang, B., Keller Correspondence, G. B. & Keller, G. B. Visuomotor Coupling Shapes the
422 Functional Development of Mouse Visual Cortex. *Cell* **169**, 1291-1302.e14 (2017).

423 49. Dombeck, D. A., Khabbaz, A. N., Collman, F., Adelman, T. L. & Tank, D. W. Imaging Large-Scale Neural
424 Activity with Cellular Resolution in Awake, Mobile Mice. *Neuron* **56**, 43–57 (2007).

425 50. Jacobson, G. A., Rupprecht, P. & Friedrich, R. W. Experience-Dependent Plasticity of Odor Representations
426 in the Telencephalon of Zebrafish. *Curr. Biol.* 1–14 (2017) doi:10.1016/j.cub.2017.11.007.

427 51. Mathieson, W. B. & Maler, L. Joumal of Sensory, Morphological and electrophysiological properties of a
428 novel in vitro preparation: the electrosensory lateral line lobe brain slice. *J Comp Physiol A* **163**, 489–506
429 (1988).

430 52. Rupprecht, P. & Friedrich, R. W. Precise Synaptic Balance in the Zebrafish Homolog of Olfactory Cortex.
431 *Neuron* **100**, 669-683.e5 (2018).

432 53. Pologruto, T. A., Sabatini, B. L. & Svoboda, K. ScanImage: Flexible software for operating laser scanning
433 microscopes. *Biomed. Eng. Online* **2**, 1–9 (2003).

434 54. Hempel, C. M., Sugino, K. & Nelson, S. B. A manual method for the purification of fluorescently labeled
435 neurons from the mammalian brain. *Nat. Protoc.* **2**, 2924–2929 (2007).

436 55. Picelli, S. *et al.* Full-length RNA-seq from single cells using Smart-seq2. *Nat. Protoc.* **9**, 171–181 (2014).

437 56. Picelli, S. *et al.* Tn5 transposase and tagmentation procedures for massively scaled sequencing projects.
438 *Genome Res.* **24**, 2033–2040 (2014).

439 57. Gaidatzis, D., Lerch, A., Hahne, F. & Stadler, M. B. QuasR: Quantification and annotation of short reads in
440 R. *Bioinformatics* **31**, 1130–1132 (2015).

441 58. Wickersham, I. R., Finke, S., Conzelmann, K. K. & Callaway, E. M. Retrograde neuronal tracing with a
442 deletion-mutant rabies virus. *Nat. Methods* **4**, 47–49 (2007).

443 59. Robinson, M. D., McCarthy, D. J. & Smyth, G. K. edgeR: A Bioconductor package for differential
444 expression analysis of digital gene expression data. *Bioinformatics* **26**, 139–140 (2009).

445 60. Eggermont, J. & Proudfoot, N. J. Poly(A) signals and transcriptional pause sites combine to prevent

interference between RNA polymerase II promoters. *EMBO J.* **12**, 2539–2548 (1993).

**Acknowledgements**

We thank Hans-Rudolf Hotz for offering the QuasR tools in the FMI Galaxy, Hubertus Kohler for FACS experiments, and Sébastien Smallwood and Stéphane Thiry for RNA sequencing. We thank Aya Takeoka for comments on the manuscript and the Friedrich group for stimulating discussions. This work was supported by the Novartis Research Foundation, by fellowships from the European Union (Marie Curie) and JSPS (C.S.), by the European Research Council (ERC) under the European Union's Horizon 2020 research and innovation program (grant agreement no. 742576), and by the Swiss National Science Foundation (grant no. 31003A_172925/1).

**Author contributions**

C.S. developed the methodology, designed and performed experiments, analyzed data and wrote the manuscript. R.L.N. produced HSV1. H.K.O. produced rabies virus. P. Z. performed and analyzed optogenetic and calcium imaging experiments. K.H. developed head-fix preparation and in vivo imaging technique. E.A.B. helped molecular biology to establish HSV1[*UAS*:GFP], M.T. helped to establish rabies virus tracing in zebrafish. S.H. created transgenic fish. G.B.K. supervised the project. R.W.F. supervised the project and wrote the manuscript.

**Competing interests**

R.L.N. is the head of the Gene Delivery Technology Core at Massachusetts General Hospital where HSV1 can be obtained commercially.

## Methods

### Animals

Experiments were performed in adult (5 – 15 month old) zebrafish (*Danio rerio*) of both sexes. Fish were bred under standard laboratory conditions (26 – 27°C, 13 h/11 h light/dark cycle). All experiments were approved by the Veterinary Department of the Canton Basel-Stadt (Switzerland).

The following transgenic fish lines were used: Tg[*gad1b*:GFP][33], Tg[*gad1b*:Gal4][18], Tg [*vglut2a*:loxP-DsRed-loxP-GFP][33], Tg[*th*:Gal4][40], Tg[*vglut1*:GFP] (created in this study), Tg[*vglut1*:Gal4] (created in this study), Tg[*UAS*:tdTomato-CAAX][41] and Tg[*UAS*:TVA-mCherry] (created in this study). Note that Tg[*gad1b*:GFP] and Tg[*gad1b*:Gal4] were created using the same BAC (zC24M22).

Optogenetic experiments and odor discrimination training were performed in fish with low pigmentation that were derived by selection from a wt population. We refer to this genetic background as "Basel-golden". These fish facilitate non-invasive optical access to the brain in adults and show no obvious impairments or behavioral alterations.

### Transgenic fish, DNA constructs and virus production

Tg[*UAS*:TVA-mCherry] fish were created using standard procedures based on the Tol2 transposon[42]. TVA-mCherry was amplified by PCR from a plasmid (gift from Dr. Uchida, Addgene plasmid #38044 ; http://n2t.net/addgene:38044 ; RRID:Addgene_38044, ref[43]) and inserted into a 5xUAS vector[34]. Tg[*vglut1*:GFP] fish were established using the CRISPR/Cas9 method[44]. Insertion of a construct containing the hsp70 promoter was targeted at a site upstream of the *vglut1* gene using the target sequence gagagagactcgggcgcgcg. The same procedure and target sequence was used to generate Tg[*vglut1:*loxP-mCherry-loxP-Gal4]. This line was then crossed to Tg[*hspa8*:Cre-mCherry-NLS] (ZFIN ID: ZDB-ALT-201210-1), which expresses Cre ubiquitously, to generate Tg[*vglut1:*Gal4].

For HSV1 production, constructs containing *LTCMV*:DsRed, *LTCMV*:GFP, *LTCMV*:Gal4 and *LTCMV*:jGCaMP7b were created at the Gene Delivery Technology Core of the Massachusetts General Hospital. Constructs containing *UAS*:GFP, *UAS*:Venus-CAAX, *UAS*:GCamp6f, *UAS*:tdTomato, *UAS*:TeNTGFP, *UAS*:TVA-mCherry, and *UAS*:zoSADG were created using the Gateway construct described in Fig. 2A. The transcriptional blocker (Fig. 2a) and zoSADG were synthesized with the following sequences:

Transcriptional blocker:
caataaaatatctttattttcattacatctgtgtgttggttttttgtgtgaatcgatagtactaacatacgctctccatcaaaacaaaacgaaacaaaacaaactagcaaa
ataggctgtccccagtgcaagtgcaggtgccagaacatttctct

zoSADG:
atggtgcctcaggctctgctgtttgtgcctctgctggtgttccctctgtgcttcggaaaattccctatctacacaatcccggataaactgggaccttggagccctatcg
acatccaccacctgagctgtcctaacaacctggtggtggaggatgagggatgcactaacctgagcggattctcctacatggagctgaaagtgggatacatcctg
gctatcaaggtgaacggattcacctgtacaggagtggtgactgaggctgagacatacacaaacttcgtgggatacgtgacaaccacattcaaaaggaaacactt
cagacctacacctgatgcttgtagagctgcctacaactggaagatggctggtgaccctagatatgaggagtccctgcacaacccttaccctgactacagatggct
gcgtacagtgaagacaacaaaagagagcctcgttatcatcagcccttccgtggccgatctcgatccatatgacagaagcctgcactctagagtgttcccaagcgg
aaagtgctctggcgtggcagtgtcttccacttactgctcaaccaaccacgactacaccatctggatgccagagaacccaagactgggaatgtcttgtgacatcttc
actaactctagaggaaaaagagcttctaaaggatctgagacctgcggattcgtggatgagagaggactgtacaagtctctgaagggagcttgtaaactgaagctg
tgtggagtgctgggactgagactgatggacggaacctgggtcagcatgcagacaagcaacgagaccaagtggtgtcctccagacaaactggtgaacctgcac
gactttagaagcgatgagattgagcaccttgtggtggaggagctggtgagaaaaagagaggagtgtctggacgctctggagagcatcatgacaacaaaaagc
gtgtctttcagaagactgagccacctgagaaaactggtgcctggattcggaaaggcttatacaatcttcaacaaaacactgatggaggctgatgctcactacaaga
gcgtgagaacatggaacgagatcctgccttctaaaggatgcctgagagtgggaggaagatgtcacccacacgtgaacggagtgttctttaacgggatcattttgg

513 gtcccgacggcaatgtgctcatcccggaaatgcagagcagcctgctccagcaacacatggagttgctcgagagtagtgtgataccccttagtccatccactcgca
514 gatccttccacagtgttcaaggatggtgacgaggctgaggactttgtagaggttcatctccctgatgtgcacaaccaggtgtctggagtggatctgggactgccaa
515 actggggaaagtacgtgctgctgtctgctggagctctgaccgctctgatgctgatcatcttcctgatgacatgttgtagaagagtgaacagatctgagcctacacag
516 cacaacctgagaggaactggaagagaggtgagcgtgacacctcagagcggaaagatcatctctagctgggagtcacataagtctggaggtgaaactagactgt
517 ga.

518 All HSV1 viruses were produced by Gene Delivery Technology Core in the Massachusetts General Hospital
519 (https://researchcores.partners.org/mvvc/about, titer: 5 x $10^9$ iu/ml). EnvA-RVΔG-GFP (titer: 2.2 x $10^9$ iu/ml)
520 and EnvA-RVΔG-mCherry (titer: 4.2 x $10^8$ iu/ml) were produced by the FMI viral core.

521

522 **Virus injection**

523 Virus injections were performed as described[15] with minor modifications. Adult fish were anesthetized in
524 0.03 % tricaine methanesulfonate (MS-222) and placed under a dissection microscope. MS-222 (0.01 %) was
525 continuously delivered into the mouth through a small cannula. A small craniotomy was made over the dorsal
526 telencephalon near the midline, over the OBs, or over the cerebellum. If multiple viruses were injected in the
527 same region, virus suspensions were mixed. Phenol red (0.05 %) was added to the suspension to visualize the
528 injection. Micropipettes pulled from borosilicate glass were inserted vertically through the craniotomy. The
529 depth of injections was approximately 100 µm in the dorsal telencephalon, 50 µm in the OB, 100-150 µm in
530 the cerebellum, 300-500 µm in Dp and 50 – 200 µm in the tectum. The injected volume was 50 nl – 100 nl.
531 After surgery, fish were kept in standard holding tanks at 35 °C – 37 °C unless noted otherwise.

532 Larval fish were anesthetized in 0.03 % tricaine methanesulfonate (MS-222) and placed on an agarose plate
533 under a dissection microscope. Micropipettes pulled from borosilicate glass were inserted vertically into the
534 target region (spinal cord, muscle or brain) without a craniotomy. The injected volume was 250 pl – 500 pl.
535 After retraction of the pipette, fish were kept in standard tanks in an incubator at 28.5 °C, 32 °C or 35 °C.

536 For transneuronal rabies tracing, all components were co-injected. To test whether the efficiency of infection
537 and transneuronal labeling can be enhanced when HSV1[*UAS*:TVA-mCherry] and HSV1[*UAS*:zoSADG]
538 are expressed prior to the injection of EnvA-RVΔG-GFP, we also performed experiments with two separate
539 injections. However, the number of GFP-positive neurons was not increased when EnvA-RVΔG-GFP
540 was injected two (n = 3 fish) or four (n = 3 fish) days after HSV1[*UAS*:TVA-mCherry] and
541 HSV1[*UAS*:zoSADG] (not shown), consistent with observations in rodents[45,46]. We assume that this
542 observation can be explained by at least two factors. First, rabies virus appears to remain close to the
543 injection site for an extended period of time, possibly because it has high affinity for membranes. Second,
544 it is difficult to precisely target the two separate injections at the same neurons.

545 Transneuronal spread of the rabies virus was determined by quantitative analyses of neurons that expressed
546 GFP but not TVA-mCherry. In theory, some of these neurons could be two (or more) synapses away from the
547 starter cell if they target other neurons that received only the glycoprotein but not TVA-mCherry, if these
548 neurons in turn were presynaptic to a starter neuron. However, because labeling was sparse and because the
549 number of neurons receiving G only should be low, the probability of such events should be very low.
550 Moreover, because transneuronal gene expression is observed only after a delay of >6 days, multi-step events
551 should be very rare 10 days post infection. Multi-step events were therefore not taken into account in our
552 quantitative analyses.

553

554 **Clearing of brain samples**

555 We adapted the original Cubic protocol[47] to small samples such as adult zebrafish brains. After fixation with
556 4 % paraformaldehyde overnight, samples were soaked with reagent 1A (10%w/v Triton, 5wt% NNNN-
557 tetrakis (2HP) ethylenediamine and 10 %w/v urea) for 2.5 h at room temperature and for 6 h at 37 °C with
558 mild shaking and multiple solution exchanges. Subsequently, samples were washed in PBS overnight at room
559 temperature. On the next day, samples were treated with reagent 2 (25 % w/v urea, 50 % w/v sucrose and 10 %
560 w/v triethanolamine) for refractive index matching, mounted in glass bottom dishes, and covered by 16 x 16
561 mm cover glasses to avoid drift. Images were acquired using a Zeiss 10x water-immersion objective lens (N.A.
562 = 0.45) on an upright Zeiss LSM 700 confocal microscope.

563

564 **Immunohistochemistry**

565 For rabies virus tracing in the cerebellar circuit, GFP and mCherry signals were detected by
566 immunocytochemistry. Brain samples were fixed overnight in 4 % paraformaldehyde and sectioned (100 µm)
567 on a Leica VT1000 vibratome. Primary antibodies were anti-GFP (Thermofisher, A10262, 1:200) and anti-
568 RFP (5F8, chromotek, 1:200). Secondary antibodies were conjugated to Alexa Fluor 488 or 594 (Invitrogen,
569 1:200).

570

571 **Neuron counts**

572 For whole brain imaging (Fig. 1c, 1g and S1d), z stacks (7-10 µm steps) were acquired using an upright Zeiss
573 LSM 700 confocal microscope with a 10x objective (water, N.A. = 0.45, pixel size 1.25 µm). GFP or DsRed-
574 expressing neurons in the dorsal telencephalon were counted manually.

575 Z stacks from individual brain slices (1 – 2 um steps, Fig. 2f, 4d, 4i, 4j, and S4c) were acquired using an
576 upright Zeiss LSM 700 confocal microscope with a 20x objective (air, N.A. = 0.8, pixel size 0.625 um). For
577 non-rabies injections, a single slice, containing the largest number of labelled neurons, was chosen from each
578 brain sample for cell counting. For rabies injections, all slices were used for cell counting. Cells expressing
579 GFP and/or mCherry in specific regions (cerebellum, telencephalon, olfactory bulb) were counted manually.

580

581 **Optogenetics and imaging *in vivo***

582 Multiphoton calcium imaging and simultaneous ChrimsonR stimulation was performed as described[48] using a
583 modified B-scope (Thorlabs) with a 12 kHz resonant scanner (Cambridge Technology) at excitation
584 wavelengths of 930 nm (GCaMP6f) or 1100 nm (tdTomato) and an average power under the objective of
585 30 mW at 930 nm. Optogenetic stimulation with ChrimsonR was performed using an LED (UHP-T-595,
586 Prizmatix; 595 nm). Light paths for imaging and stimulation were combined using a dichroic mirror (ZT775sp-
587 2p, Chroma). Emitted light was split using a second dichroic mirror (F38-555SG, Semrock), band-pass filtered
588 with a 525/50 filter (Semrock) for GCaMP6f imaging and with a 607/70 filter (Semrock) for tdTomato, and
589 focused onto a GaAsP photomultiplier (H7422, Hamamatsu). The signal was amplified (DHPCA-100, Femto),
590 digitized at 800 MHz (NI5772, National Instruments), and band-pass filtered around 80 MHz using a digital
591 Fourier-transform filter implemented on an FPGA (NI5772, National Instruments). LED activation was
592 synchronized to the turnaround phase of the resonant scanner when no data were acquired. Images were
593 acquired at 60 Hz with a resolution of 750 x 400 pixels, corresponding to a field of view of 300 µm x 250 µm.
594 Images were acquired sequentially in four different focal planes by moving the objective (Nikon 16x, 0.8 NA)
595 with a piezo-electric linear actuator (Physik Instrumente; effective frame rate: 15 Hz per plane). Anatomical
596 snapshots were generated by averaging 1000 images in the absence of optogenetic stimulation.

597 Basel-golden fish were head-fixed in a custom chamber and neurons in the dorsal telencephalon were imaged
598 through the intact skull[5]. Optogenetic stimuli (500 ms duration) were applied randomly every 6 – 11 s. The
599 average power of each stimulus was chosen at random to be 1.3 mW, 2.4 mW, 4.7 mW, or 8.6 mW under the
600 objective. The total duration of an imaging session was 11 min.

601 Raw images were full frame registered to correct for motion. Regions of interest were manually selected based
602 on neuronal co-expression of GCaMP6f and ChrimsonR-tdTomato (N = 11 neurons). Raw fluorescence traces
603 were calculated as mean of the pixel values in a given region of interest in each imaging frame. Raw traces
604 were then corrected for slow drift in fluorescence using an 8th-percentile filtering with a 15 s window[49]. ΔF/F
605 traces were computed by dividing raw fluorescence trace by the median calculated over the entire fluorescence
606 distribution for each region of interest. Responses were pooled across neurons and pulses of the same intensity,
607 and the resulting population responses were normalized by subtracting average population activity in a 1 s
608 baseline window prior to the pulse. The standard error of the mean population response was computed over
609 average responses of individual neurons.

610

611 **Calcium imaging in the OB**

612 Calcium imaging in the adult OB was performed 4 – 10 days after viral injections in an explant preparation of
613 the entire brain and nose[18,50] that was continuously superfused with artificial cerebrospinal fluid (ACSF)
614 containing (in mM) 124 NaCl, 2 KCl, 1.25KH2PO4, 1.6 MgSO4, 22 D-(+)-Glucose, 2 CaCl2, 24 NaHCO3,
615 pH 7.2[51]. Oregon Green 488 1,2-bis-(*o*-aminophenoxy)-ethane-*N*,*N*,*N*,*N*-tetraacetic acid, tetraacetoxymethyl
616 ester (OGB-1; Thermo Fisher Scientific) was injected into the OB as described[18]. Two-photon calcium
617 imaging started >1 hr after dye injection. Odors were prepared and delivered to the nose for 5 s as described[52].
618 Inter-stimulus intervals (ISIs) were >2 min.

619 Multiphoton calcium imaging was performed using a custom-built microscope with a 20x water immersion
620 objective (NA 1.0; Zeiss) and galvo scanners[50]. Excitation wavelengths were 930 nm (OGB-1) or 1010 nm
621 (mCherry). The average power under the objective was 50 mW at 930 nm and 20 mW at 1010 nm. The emitted
622 light was split by a dichroic mirror (DMSP550L, Thorlabs), band-pass filtered with a 515/30 filter (Chroma) or
623 with a 641/75 filter (Semrock), and collected with a GaAsP photomultiplier (H7422-40MOD or H11706P-40,
624 Hamamatsu). Images were acquired at 8 Hz using Scanimage 5.5-1 (Vidrio Technologies, LLC)[53] with a
625 resolution of 256 x 256 pixels.

626

627 **Tissue dissociation and cell sorting**

628 EnvA-RVΔG-GFP was injected into one or both OBs of Tg[*gad1b*:Gal4;*UAS*:TVA-mCherry] fish. Cells were
629 dissociated and sorted as per previous protocol[54] with modification for fish. Briefly, after 3 – 4 days at 36 °C,
630 fish were anesthetized by cooling to 4 °C and decapitated in ACSF supplemented with 50 mM 2-Amino-5-
631 phosphonovaleric acid (APV), 20 mM 6,7-Dinitroquinoxaline-2,3-dione (DNQX), 5 mg/ml actinomycin D
632 (ACT-D), tetrodotoxin (TTX) 100 nM and 10 g/l Trehalose. OB samples were taken and harvested and kept in
633 ACSF. After pooling OB samples from 3 – 5 fish, samples were treated with pronase-mix (1 g/l protease type
634 xiv and 33 mg/l of collagenase in ACSF) for 10 minutes and the solution was replaced with fresh ACSF
635 containing 1 % FBS. Samples were then triturated gently with small custom-made glass pipettes and stored on
636 ice. DAPI was added to the samples to detect dead cells and cells were sorted based on GFP and mCherry
637 fluorescence using a 70 or 100 µm nozzle (BD FACSAria III; BD Biosciences). Sorted cells were kept in a
638 lysate buffer and stored at -80 °C until further processing.

639

640 **RNA sequencing**

641 RNA was purified using a single-cell RNA purification Kit (Norgen). mRNA-seq libraries were generated
642 using the SmartSeq2 approach[55] with the following modifications: For cDNA pre-amplification, up to 10 ng of
643 RNA was used as input and reverse transcription was performed using Superscript IV (Thermo Fisher
644 Scientific - 50 °C for 10 min, 80 °C for 10 min). Amplified cDNA (1 ng) was converted to indexed sequencing
645 libraries by tagmentation, using in-house purified Tn5[56] and Illumina Nextera primers. Libraries were
646 sequenced on an Illumina HiSeq2500, as 50 bp single-end reads.
647
648 Sequenced reads were pre-processed with preprocessReads from the Bioconductor package QuasR (version
649 1.24.2) [57])with default parameters except for Rpattern = "CTGTCTCTTATACACATCT". Processed reads
650 were then aligned against the chromosome sequences of fish genome (danRer11) using qAlign (QuasR) with
651 default parameters except for aligner = "Rhisat2", splicedAlignment = "TRUE", and auxiliaryFile =
652 "mCherry_GFP1.fa". mCherry and GFP sequences matched the sequences in the plasmids used to generate
653 transgenic fish (Tg[*UAS*:TVA-mCherry]) or rabies virus[58].
654
655 Raw gene counts were obtained using qCount (QuasR) with default parameters and ZFIN gene models
656 (https://zfin.org/downloads/zfin_genes.gff3, downloaded 18-Jul-2019) or the auxiliary file as query. The count
657 table was filtered to remove genes which had less than 2 samples with at least 1 cpm. Differential gene
658 expression was calculated with the Bioconductor package edgeR (version 3.26.4)[59] using the quasi-likelihood
659 F-test after applying the calcNormFactors function, obtaining the dispersion estimates and fitting the negative
660 binomial generalized linear models. The following threshold was applied: Significant differences in gene
661 expression were detected by applying a threshold of abs(logFC (fold change)) >3, logCPM (counts per million
662 reads mapped to the annotation) >3, and FDR (False Discovery Rate)<0.05. Stress marker genes
663 (GO:0033554) and cell death marker genes (GO:0008219) were chosen from Gene Ontology database
664 (AmiGo2: http://amigo.geneontology.org/amigo/landing). Gene ontology term for differentially expressed
665 genes were found using GENERIC GENE ONTOLOGY (GO) TERM FINDER (https://go.princeton.edu/cgi-
666 bin/GOTermFinder).
667

668 **Odor discrimination training and analysis of behavior**

669 In the experimental group, Basel-golden fish were injected with HSV1[*LTCMV*:jGCaMP7b] into both OBs and
670 kept at 36 °C for 2 days prior to behavioral training. Associative conditioning was performed as described[6,18].
671 Briefly, individual fish were acclimated to the behavioral setup without food for 1 – 3 days and subsequently
672 trained to associate one odor stimulus ($CS^+$: alanine) with a food reward, whereas a second odor stimulus ($CS^-$:
673 tryptophan) was not rewarded. Each odor was infused into the tank for 30 s nine times per day in an alternating
674 sequence (inter-trial interval: 20 min) for five consecutive days. A small amount of food was delivered at a
675 specific location at the end of the presentation of the $CS^+$ but not the $CS^-$. 3D swimming trajectories were
676 reconstructed from videos acquired by two orthogonal cameras (Logitech HD Pro C920). The following
677 behavioral components were extracted from the trajectories: swimming speed, elevation in water column,
678 presence in the reward zone, surface sampling, distance to the odor inflow and rhythmic circular swimming.
679 The components were combined into a compound score of appetitive behavior as described[6]. The learning
680 index was calculated as the difference between the mean behavioral scores in response to the $CS^+$ and $CS^-$
681 during the final day of training (last nine trials with each odor) in each fish.

682

683

684

685

686

687 **Data availability**

688 Transcriptomic data generated in this study have been deposited at ArrayExpress (accession number: E-
689 MTAB-11083).
690 Requests for HSV1 and the vectors shown in Fig. 2a should be addressed to R.L.N.
691 The data that support the findings of this study are available from the corresponding authors upon reasonable
692 request.

693

694 **Code availability**

695 All code used in this study is available from the corresponding authors upon reasonable request.

696

697 **Figure Legends**

698

699 **Fig 1. HSV1-mediated gene delivery in adult zebrafish**

700 **(a)** Procedure to test temperature-dependence of HSV1-mediated gene expression.

701 **(b)** Maximum intensity projection after injection of HSV1[*LTCMV*:DsRed] into one OB (arrow) of a
702 Tg[*vglut1*:GFP] fish and incubation at 36 ºC. White arrowhead indicates the OB-projecting area in the
703 dorsal telencephalon used for quantification in Fig. 1c and Fig. 2f**(f)**. *vglut1*:GFP expression served as a
704 morphological marker.

705 **(c)** Mean number of labeled neurons in the dorsal telencephalon after injection of HSV1[*LTCMV*:DsRed]
706 into the ipsilateral olfactory bulb and incubation at different temperatures. In this and similar plots, black
707 dots represent data from individual fish, box plot indicates median and 25$^{th}$ and 75$^{th}$ percentiles, circles
708 and error bars indicate mean and s.d., respectively, over individual fish. N: number of fish.

709

710 **Fig 2. Conditional HSV1-mediated gene expression using the Gal4/UAS system**

711 **(a)** Construction of the UAS vector for HSV packaging. Genes of interest (GOI) are inserted downstream
712 of the 5xUAS sequences by recombination cloning using the Gateway system. The transcriptional blocker
713 minimizes leaky expression[60].

714 **(b)** Injection of HSV1[*UAS*:TVA-mCherry] into the cerebellum of Tg[*gad1b*:Gal4; *gad1b*:GFP] double
715 transgenic fish. Note co-localization of mCherry and GFP in Purkinje cells (arrowheads) and putative
716 Golgi cells (arrows). ML: molecular layer; PL: Purkinje layer; GL: granular layer.

717 **(c)** Fraction of mCherry-positive neurons that co-expressed GFP after injection of HSV1[*UAS*:TVA-
718 mCherry] into the cerebellum or Dp of Tg[*gad1b*:Gal4; *gad1b*:GFP] double transgenic fish. N: number of
719 fish.

720 **(d)** Injection of HSV1[*UAS*:Venus-CAAX] into the optic tectum of Tg[*th*:Gal4; *UAS*:tdTomato-CAAX]
721 fish. Venus-CAAX was expressed by a small number of neurons with somata in the locus coeruleus and
722 extensive projections to the optic tectum and other brain areas. Images on the right are close-ups of the
723 boxed region showing co-expression of Venus-CAAX (green) with tdTomato (red) in the locus coeruleus.

724 **(e)** Injection of HSV1[*LTCMV*:Gal4] into the OB and HSV1[*UAS*:GFP] into the dorsal telencephalon of
725 wt fish. Note selective expression of GFP in OB-projecting neurons (arrowhead; dashed outline).

726 (**f**) Number of neurons labeled in the dorsal telencephalon by a single injection of HSV1[*LTCMV*:DsRed]
727 into the OB ('One way') or by two injections using the two-component Gal4/UAS system ('Gal4/UAS').
728 N: number of fish.

729

730 **Fig 3. Effects of RV infection on neuronal health and function**

731 (**a**) Fraction of genes that were significantly up- or down-regulated genes in RVΔG-infected cells out of
732 all 19'819 genes, out of the 471 stress markers (GO:0033554), and out of the 651 cell-death markers
733 (GO:0008219). Differences in expression level were considered significant when abs(logFC (fold
734 change)) >3, log(counts per million reads mapped) >3, and FDR<0.05. The FDR (False Discovery Rate)
735 corrects for multiple testing.

736 (**b**) Volcano plots displaying differential gene expression in RVΔG-infected and uninfected cells. Colored dots
737 indicate stress markers (left) and cell death markers (right) (orange: upregulated, blue: downregulated). Yellow
738 outline depicts statistically significant difference in expression level.

739 (**c**) OGB-1 labeling and mCherry expression in the deep (granule cell) layer of the adult zebrafish OB
740 after injection of EnvA-RVΔG-mCherry into the OB of Tg[*gad1b*:Gal4; *UAS*:TVA-mCherry] fish and
741 bolus loading of OGB-1.

742 (**d**) $Ca^{2+}$ signals evoked by two different odors in the same optical plane (single trials). Odors: alanine
743 (Ala), taurodeoxycholic acid (TDCA).

744 (**e**) Randomly selected responses of seven infected (magenta) neurons and seven uninfected (green)
745 neurons from the same optical plane to two odors (single trials).

746 (**f**) Odor-evoked $Ca^{2+}$ signals of infected (N = 559) and uninfected (N = 1293) OB cells from $N = 4$ fish,
747 averaged over all odors (N = 6) and repetitions (N = 3 for each odor). Shading indicates s.e.m.; bar
748 indicates odor stimulation.

749 (**g**) Distribution of response amplitudes in non-infected and infected cells to different odors (N = 6),
750 averaged over trials (N = 3). Distributions of were not significantly different (p = 0.24, Kolmogorov–
751 Smirnov test).

752

753 **Fig 4. Transneuronal tracing using pseudotyped rabies virus in adult zebrafish**

754 **(a)** Schematic of the cerebellar circuit. Glutamatergic neurons are shown in red colors, GABAergic
755 neurons in blue colors. Purkinje cells receive extra-cerebellar input exclusively from the inferior olive.

756 **(b)** Co-injection of EnvA-RVΔG-GFP and HSV1[*UAS*:TVA-mCherry] into the cerebellum of
757 Tg[*gad1b*:Gal4] fish in the absence of glycoprotein. Left: schematic. Center: expression of TVA-mCherry
758 (magenta) and GFP (green) in the cerebellum. Regions in the Purkinje and granular layers (dashed
759 rectangles) are enlarged. Unfilled white arrowheads indicate GFP+/mCherry+ neurons. Right: expression
760 of GFP in the hindbrain. Region covering the inferior olive (dashed rectangle) is enlarged. Expression of
761 GFP was restricted to putative starter neurons; no expression was detected in the inferior olive. ML:
762 molecular layer; PL: Purkinje layer; GL: granular layer.

763 **(c)** Same as in (b) but the glycoprotein (zoSADG) was supplied to starter neurons in *trans* by co-injection
764 of HSV1[*UAS*:zoSADG]. Filled white arrowheads indicate GFP+/mCherry- neurons. Note expression of
765 GFP in putative granule cells and in neurons of the inferior olive, indicating transneuronal spread.

766 **(d)** Number of neurons that expressed GFP and mCherry (putative starter neurons) or GFP alone (putative
767 presynaptic neurons) at different time points after injection of EnvA-RVΔG and HSV1[*UAS*:TVA-
768 mCherry] into the cerebellum of Tg[*gad1b*:Gal4] fish. Left: without glycoprotein; right: with trans-

complementation of zoSADG in starter neurons. Note that labeling of putative presynaptic neurons emerged between 6 and 10 days post injection only when zoSADG was trans-complemented in starter neurons. In all plots, black dots represent data from individual fish, box plot indicates median and the 25$^{th}$ and 75$^{th}$ percentiles, circles and error bars indicate mean and s.d. over individual fish. N: number of fish.

**(e)** Convergence index for the projection from the inferior olive to the cerebellum at different time points. The convergence index is the numerical ratio of transneuronally labeled neurons (GFP+/mCherry- neurons in the inferior olive) and putative starter cells in the cerebellum (GFP+/mCherry+ Purkinje neurons). N: number of fish.

**(f)** Schematic of the putative circuitry in telencephalic area Dp. Glutamatergic neurons are shown in red colors, GABAergic neurons in blue colors. Long-range projections from mitral cells in the olfactory bulb terminate on glutamatergic neurons and on GABAergic interneurons in Dp. Additional long-range projections originate in other telencephalic areas.

**(g)** Co-injection of EnvA-RVΔG and HSV1[*UAS*:TVA-mCherry] into Dp of Tg[*gad1b*:Gal4] fish in the absence of glycoprotein. Coronal section through the injected telencephalic hemisphere at the level of Dp. Area outlined by dashed rectangle is enlarged. Co-expression of GFP (green) and mCherry (magenta) indicates starter cells.

**(h)** Same as in (g) but with trans-complementation of zoSADG in starter neurons by co-injection of HSV1[*UAS*:zoSADG]. Left: coronal section through the injected telencephalic hemisphere. Right: coronal section through the ipsilateral OB. Expression of GFP only (green) indicates transneuronally labeled neurons.

**(i)** Number of neurons in the telencephalon that expressed GFP and mCherry (putative starter neurons) or GFP alone (putative presynaptic neurons) after injection of EnvA-RVΔG and HSV1[*UAS*:TVA-mCherry] into Dp with (+) or without (-) trans-complementation with zoSADG in starter neurons (HSV1[*UAS*:zoSADG]). Left: injection into Tg[*gad1b*:Gal4] fish; right: injection into Tg[*vglut1*:Gal4] fish (right). Expression was analyzed 10 days post injection. N: number of fish.

**(j)** Convergence index for the projection of transneuronally labeled neurons in the OB to Dp when EnvA-RVΔG was targeted to GABAergic neurons (viral injections into Tg[*gad1b*:Gal4] fish) or to glutamatergic neurons (injections into Tg[*vglut1*:Gal4] fish) in Dp. Expression was analyzed at 10 days post injection. N: number of fish.

**Fig 5. Transneuronal tracing using pseudotyped rabies virus in zebrafish larvae**

**(a)** Expression of GFP (green) and TVA-mCherry (red) 6 days after injection of EnvA-RVΔG-GFP into the spinal cord of Tg[*gad1b*:Gal4;*UAS*:TVA-mCherry] fish at 7 dpf. Boxed region is enlarged on the right.

**(b)** Same after co-injection of EnvA-RVΔG-GFP and HSV1[*UAS*:zoSADG] into the spinal cord of Tg[*gad1b*:Gal4;*UAS*:TVA-mCherry] fish at 7 dpf.

807 **Supplementary Figure Legends**

808 **Fig S1. Temperature-dependence and time course of HSV1-mediated gene expression**

809 **(a)** Sequence of virus injections, temperature changes and associative conditioning to assess effects of
810 experimental manipulations on discrimination learning.

811 **(b)** Learning index (behavioral discrimination score) on the last day of training. Plot symbols represent
812 data from individual fish; box plots show median and 25$^{th}$ and 75$^{th}$ percentiles, circles and error bars
813 indicate mean and s.d. over individual fish. N: number of fish. Control fish (group 1) were not injected
814 and kept at standard laboratory temperature. The experimental group (group 2) was injected with
815 HSV1[*LTCMV*:jGCaMP7b], an amplicon type of HSV1 with an insert encoding the calcium indicator
816 GCamp7b[19] under the control of a non-specific promoter for long-term expression (*LTCMV*), and
817 subsequently kept at 36 ºC for two days before training **(a)**. Performance was not significantly different
818 between groups (p = 0.76, Wilcoxon rank sum test).

819 **(c)** Expression of DsRed (magenta) six days after injection of HSV1[*LTCMV*:DsRed] into the OB (arrow)
820 of an adult Tg[*vglut1*:GFP] fish kept at 26 ºC (maximum projection of confocal stack). Boxed areas (OB
821 and Dp) are enlarged below. The number of DsRed-expressing neurons is low compared to DsRed
822 expression at 36 ºC (Fig. 1).

823 **(d)** DsRed expression in the dorsal telencephalon at different timepoints after injection of
824 HSV1[*LTCMV*:DsRed] into the ipsilateral OB. Fish were kept at 36 ºC. Black dots represent data from
825 individual fish, box plot indicates median and 25$^{th}$ and 75$^{th}$ percentiles, circles and error bars indicate
826 mean and s.d. over individual fish. N: number of fish.

827

828

829 **Fig S2. HSV1-mediated gene delivery in larvae zebrafish and Gal4/UAS**

830 **(a)** Expression of GFP 48 h after injection of HSV1[*LTCMV*:GFP] into the optic tectum of zebrafish
831 larvae (3 dpf; maximum intensity projection of confocal stack). Larvae were kept after the injection at
832 28.5, 32 or 35 ºC.

833 **(b)** Expression of GFP 48 h after injection of HSV1[*LTCMV*:GFP] into the optic tectum of a larva at 5
834 dpf (maximum intensity projection of confocal stack). The larva was kept after the injection at 35 ºC.

835 **(c)** Expression of GFP 48 h after injection of HSV1[*LTCMV*:GFP] into the optic tectum of a larva at 14
836 dpf (maximum intensity projection of confocal stack). The larva was kept after the injection at 35 ºC.

837 **(d)** Expression of GFP 48 h after injection of HSV1[*LTCMV*:GFP] into trunk muscles at 7 dpf (maximum
838 intensity projection of confocal stack). The larva was kept after the injection at 35 ºC. Note retrograde
839 labeling of motor neurons (M.N.).

840 **(e)** Expression of GFP 48 h after injection of HSV1[*UAS*:GFP] into the hindbrain of a Tg[*gad1b*:Gal4;
841 *gad1b*:DsRed] larva at 7 dpf (maximum intensity projection of confocal stack). The larva was kept after
842 the injection at 35 ºC. Note co-localization of DsRed and GFP in hindbrain and cerebellum.

843

844 **Fig S3. Targeting of GABAergic neurons in the telencephalon**

845 **(a)** Coronal section through the telencephalon at the level of Dp after injection of HSV1[*UAS*:TVA-
846 mCherry] into Tg[*gad1b*:Gal4; *gad1b*:GFP] double transgenic fish. The injection was targeted to a
847 volume around Dp. mCherry was expressed predominantly in a cluster of GFP-positive neurons
848 associated with Dp. Note long-range projections of mCherry-expressing neurons to multiple
849 telencephalic areas.

850 **(b)** Enlargements of boxed region in (a). Arrowheads indicate GFP+/mCherry+ neurons.

851

852 **Fig S4. Co-packaging of 2 different viruses does not facilitate co-infection of 2 viruses.**

853 **(a)** Expression of GFP and mCherry after injection of HSV1[*UAS*:GFP & *UAS*:TVA-mCherry] into the
854 cerebellum of Tg[*gad1b*:Gal4] fish. In this virus, two expression constructs, *UAS*:GFP and *UAS*:TVA-
855 mCherry, are packaged into the same virus particles. Expression is observed in Purkinje neurons and in
856 putative Golgi cells. Note high rate of co-expression of GFP and mCherry. ML: molecular layer; PL:
857 Purkinje layer; GL: granular layer.

858 **(b)** Expression of GFP and mCherry in the Purkinje layer after co-injection of two independent viruses
859 (HSV1[*UAS*:GFP] and HSV1[*UAS*:TVA-mCherry]) into the cerebellum of Tg[*gad1b*:Gal4] fish. Note
860 that the rate of co-expression was high even though GFP and mCherry were delivered by separate viruses.
861 Note also that the overall expression was sparse, implying that co-expression was unlikely to occur by
862 chance.

863 **(c)** Percentage of GFP and mCherry-expressing neurons among all fluorescent neurons. Filled circles
864 represent data from individual fish, box plot indicates median and the 25$^{th}$ and 75$^{th}$ percentiles, and open
865 circles indicate mean over individual fish. N: number of fish.

866

867 **Fig S5. Optogenetic manipulations using HSV1**

868 **(a)** Schematic: injection of HSV1[*LTCMV*:Gal4] into the OB and subsequent co-injection of
869 HSV1[*UAS*:GCaMP6f] and HSV1[UAS:Chrimson-tdTomato] into the dorsal telencephalon of wt fish.

870 **(b)** Simultaneously recorded calcium transients evoked by optical stimulation of different light intensity
871 (vertical lines) in three example neurons.

872 **(c)** Mean change GCaMP6f evoked by optical stimulation of different light intensity (N = 11 neurons;
873 11 – 18 light stimuli at each intensity). Shading shows SEM is over cell.

874

875 **Fig S6. Injection of pseudotyped rabies virus does not infect neurons in the absence of TVA**

876 **(a)** Absence of expression after injection of EnvA-RVΔG-GFP into the telencephalon of adult wt fish.

877 **(b)** Absence of expression after injection of EnvA-RVΔG-GFP into the optic tectum of wt fish at 7 dpf.

878

879 **Fig S7. Temperature-dependence of infection by rabies virus**

880 **(a)** Experimental scheme: Rabies virus (EnvA-RVΔG-GFP) was injected into the telencephalon of
881 transgenic fish expressing TVA-mCherry in GABAergic neurons (Tg[*gad1b*:Gal4; *UAS*:TVA-mCherry]).

882 **(b)** Expression of TVA-mCherry and GFP when fish were kept at 26 ºC for 6 days after injection. Note
883 almost complete absence of GFP expression.

884 **(c)** Expression of TVA-mCherry and GFP when fish were kept at 36 ºC for 6 days after injection. Note
885 strong GFP expression.

886 **(d)** Expression of TVA-mCherry and GFP six days after injection when the housing temperature was
887 increased from 26 ºC to 36 ºC 3 days after injection. GFP expression was weak and sparse.

888

889 **Fig S8. Analysis of gene expression in GABAergic neurons**

890 **(a)** Schematic: injection of EnvA-RVΔG-GFP into the OB of adult Tg[*gad1b*:Gal4;*UAS*:TVA-mCherry]
891 fish.

892 **(b)** Example of FACS analysis of GFP and mCherry expression. Boxes depict cells selected as
893 mCherry+/GFP+ (EnvA-RVΔG-GFP infected gad1b neurons), mCherry+/GFP- (non-infected gad1b
894 neurons), mCherry-/GFP- (negative control containing other OB cells). gad1b is one of two isoforms of
895 gad1 that are expressed differentially in GABAergic neurons.

896 **(c)** Expression of marker genes (x-axis) in infected gad1b neurons (mCherry+/GFP+; green), non-infected
897 gad1b neurons (mCherry+/GFP-; magenta), and other OB cells (mCherry-/GFP-; black). Cells classified
898 as gad1b-positive by fluorescence markers, but not other cells, expressed *gad1b* but not *gad1a*, the other
899 *gad1* isoform. Expression of fluorescent marker genes followed the detection of fluorescent markers by
900 FACS. The neuronal marker *elav3* was present in all three pools. Plot symbols represent data from
901 individual samples; box plots show median and $25^{th}$ and $75^{th}$ percentiles, circles and error bars indicate
902 mean and s.d. over individual samples (N = 8 samples).

903 **(d)** Expression of negative markers for GABAergic neurons. The selected marker genes (*slc17a6a*,
904 *slc17a6b*, *tbx21*, *lhx2b* and *lhx9*) should be expressed in mitral cells of the OB and other excitatory
905 neurons but not in GABAergic neurons. Consistent with this expectation, expression of all negative
906 markers was low or absent in pools of *gad1b* cells selected by FACS (N = 8 samples).

907

908 **Fig S9. Transneuronal tracing using pseudotyped rabies virus from *vglut1*+ neurons in Dp in adult**
909 **zebrafish**

910 **(a)** Co-injection of EnvA-RVΔG-GFP and HSV1[*UAS*:TVA-mCherry] into Dp of Tg[*vglut1*:Gal4] fish in
911 the absence of glycoprotein. Coronal section through the injected telencephalic hemisphere at the level of
912 Dp. Area outlined by dashed rectangle is enlarged. Co-expression of GFP (green) and mCherry (magenta)
913 indicates starter cells.

914 **(b)** Same as in (a) but with trans-complementation of zoSADG in starter neurons by co-injection of
915 HSV1[*UAS*:zoSADG]. Left: coronal section through the injected telencephalic hemisphere. Right:
916 coronal section through the ipsilateral olfactory bulb. Expression of GFP only (green) indicates
917 transneuronally labeled neurons.

918

919 **Fig S10. Expression pattern of *vglut1* and *vglut2* in olfactory bulb and Dp**

920 **(a)** Coronal cross sections through the OB and anterior telencephalon from Tg[*vglut2a*:RFP; *vglut1*:GFP]
921 double transgenic fish. Note that *vglut2a* (magenta) is expressed by axons of olfactory sensory neurons
922 innervating glomeruli in the OB and by a subset of mitral cells, while expression of *vglut1* (green) in the
923 OB is weak or absent. Dotted lines outline OBs.

924 **(b)** More posterior coronal cross sections through the telencephalon of the same fish at the level of Dp.
925 Note that expression of *vglut2a* and *vglut1* in the telencephalon are largely complementary. Neurons in
926 Dp express primarily *vglut1*. Dotted areas indicate the dorsal lateral telencephalic area (Dl) and Dp.

927

928

929

930

931

932

933 **Movie1:** Swimming behavior of adult zebrafish injected with an HSV1[*LTCMV*:DsRed] into the OB at
934 27 ºC. Fish were kept at 27 ºC for 10 days after the injection.

935

936 **Movie2:**

937 Swimming behavior of adult zebrafish injected with an HSV1[*LTCMV*:DsRed] into the OB at 37 ºC. Fish
938 were kept at 37 ºC for 10 days after the injection.

939

940 **Movie3:** Swimming behavior of zebrafish larvae injected with an HSV1[*LTCMV*:GFP] into the optic
941 tectum at 35 ºC. Fish were injected at 7 dpf and kept for 2 days at 35 ºC.

942

943 **Movie4:** Effect of TeNT expression in GABAergic neurons of the cerebellum on swimming behavior.
944 Left: Tg[*gad1b*:Gal4] fish 3 days after injection of HSV1[*UAS*:GFP] into the cerebellum (control). Right:
945 Tg[*gad1b*:Gal4] fish 3 days after injection of HSV1[*UAS*:TeNT-GFP] into the cerebellum. Top: side
946 view; bottom: top view of the same tanks.

947

948 **Table1**. List of HSV1 available. Requests for HSV1 and the destination vector shown in Fig. 2a should
949 be addressed to R.L.N.

950

951 **Table2**. List of genes that were significantly up- or downregulated in cells infected by RVΔG. Genes
952 associated with GO terms cellular response to stress (GO:0033554) and cell death (GO: 0008219) are
953 listed at the top (colored rows).

954

955 **Table3**. Gene ontology (GO) terms that showed a significant association with the set of regulated genes
956 in RVΔG-infected cells (Supplementary Table 2), sorted by probability (p-value). Note that most GO
957 terms are linked to immunity. GO terms linked to stress, cell death or synaptic functions are rare or
958 absent.

959

960

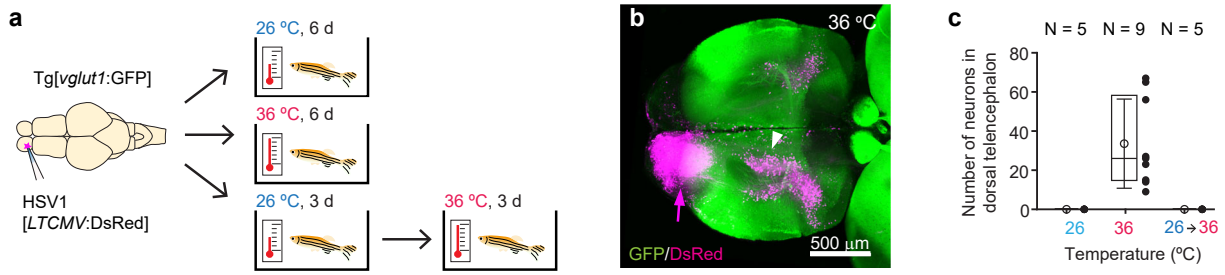


**Fig 1. HSV1-mediated gene delivery in adult zebrafish**

(a) Procedure to test temperature-dependence of HSV1-mediated gene expression.

(b) Maximum intensity projection after injection of HSV1[LTCMV:DsRed] into one OB (arrow) of a Tg[v-glut1:GFP] fish and incubation at 36 ºC. White arrowhead indicates the OB-projecting area in the dorsal telencephalon used for quantification in Fig. 1c and Fig. 2f. vglut1:GFP expression served as a morphological marker.

(c) Mean number of labeled neurons in the dorsal telencephalon after injection of HSV1[LTCMV:DsRed] into the ipsilateral olfactory bulb and incubation at different temperatures. In this and similar plots, black dots represent data from individual fish, box plot indicates median and 25th and 75th percentiles, circles and error bars indicate mean and s.d., respectively, over individual fish. N: number of fish.

Fig.1

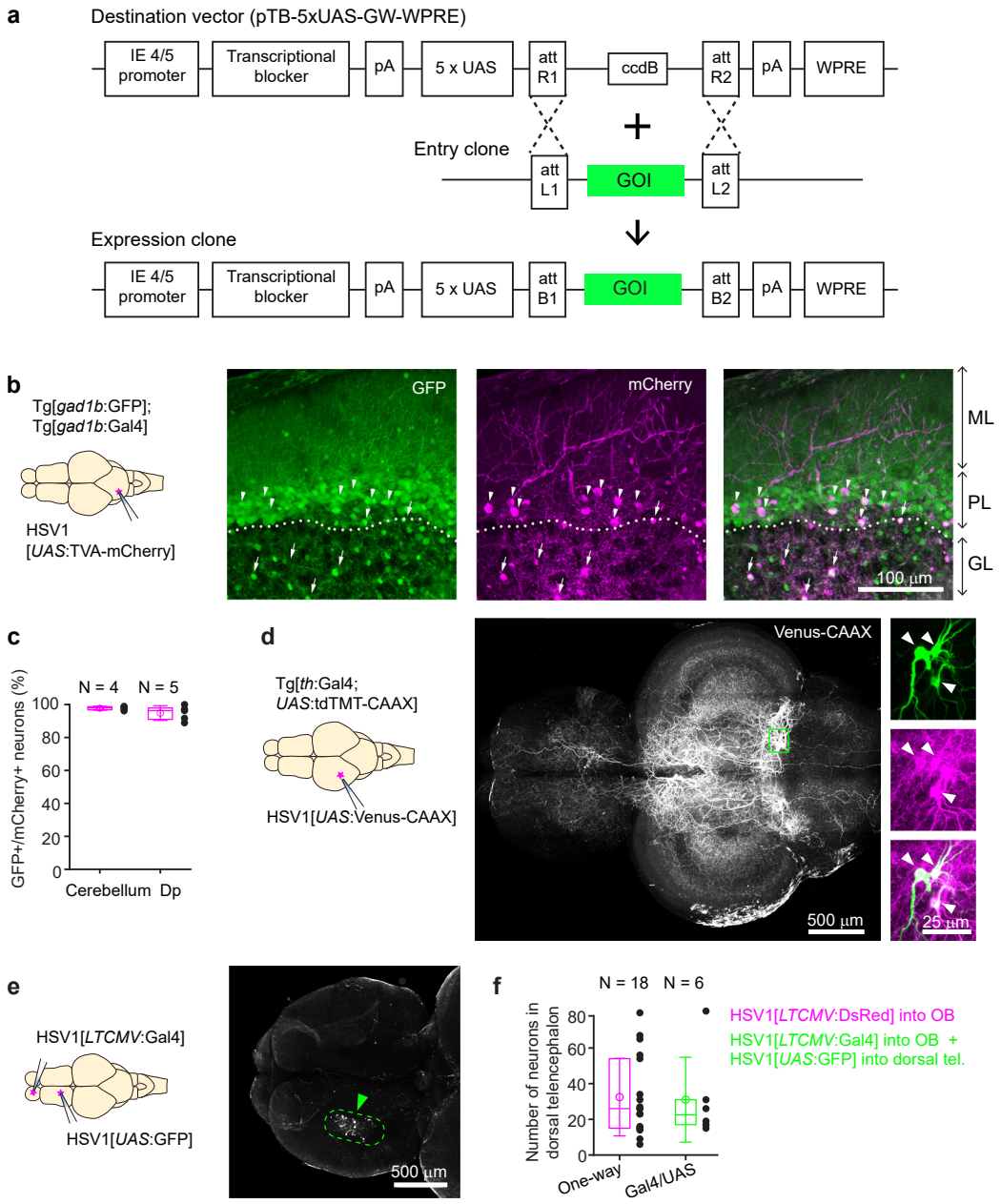


**Fig 2. Conditional HSV1-mediated gene expression using the Gal4/UAS system**

(a) Construction of the UAS vector for HSV packaging. Genes of interest (GOI) are inserted downstream of the 5xUAS sequences by recombination cloning using the Gateway system. The transcriptional blocker minimizes leaky expression60.

(b) Injection of HSV1[UAS:TVA-mCherry] into the cerebellum of Tg[gad1b:Gal4; gad1b:GFP] double transgenic fish. Note co-localization of mCherry and GFP in Purkinje cells (arrowheads) and putative Golgi cells (arrows). ML: molecular layer; PL: Purkinje layer; GL: granular layer.

(c) Fraction of mCherry-positive neurons that co-expressed GFP after injection of HSV1[UAS:TVA-mCherry] into the cerebellum or Dp of Tg[gad1b:Gal4; gad1b:GFP] double transgenic fish. N: number of fish.

(d) Injection of HSV1[UAS:Venus-CAAX] into the optic tectum of Tg[th:Gal4; UAS:tdTomato-CAAX] fish. Venus-CAAX was expressed by a small number of neurons with somata in the locus coeruleus and extensive projections to the optic tectum and other brain areas. Images on the right are close-ups of the boxed region showing co-expression of Venus-CAAX (green) with tdTomato (red) in the locus coeruleus.

(e) Injection of HSV1[LTCMV:Gal4] into the OB and HSV1[UAS:GFP] into the dorsal telencephalon of wt fish. Note selective expression of GFP in OB-projecting neurons (arrowhead; dashed outline).

(f) Number of neurons labeled in the dorsal telencephalon by a single injection of HSV1[LTCMV:DsRed] into the OB ('One way') or by two injections using the two-component Gal4/UAS system ('Gal4/UAS'). N: number of fish.

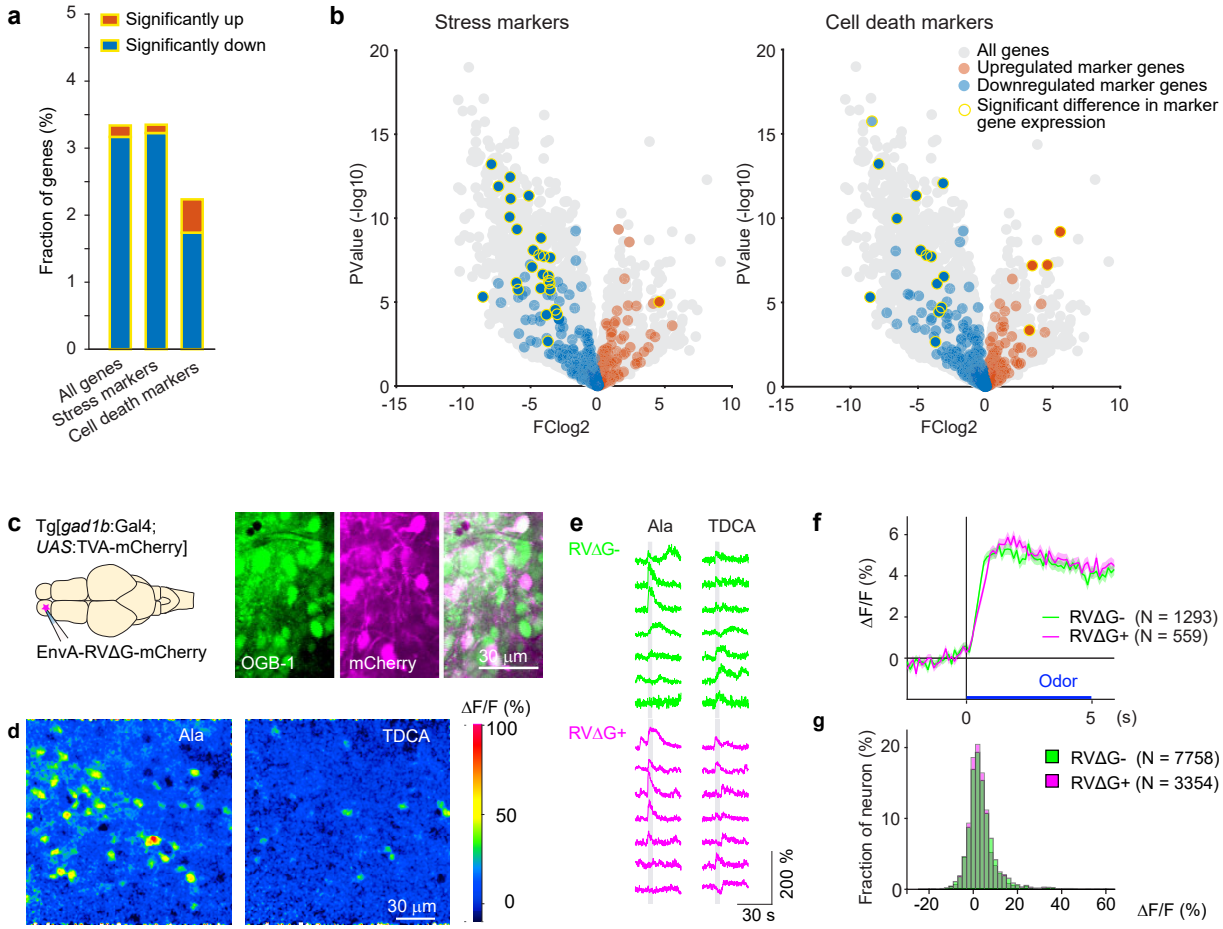


**Fig 3. Effects of RV infection on neuronal health and function**

(a) Fraction of genes that were significantly up- or down-regulated genes in RVΔG-infected cells out of all 19'819 genes, out of the 471 stress markers (GO:0033554), and out of the 651 cell-death markers (GO:0008219). Differences in expression level were considered significant when abs(logFC (fold change)) >3, log(counts per million reads mapped) >3, and FDR<0.05 . The FDR (False Discovery Rate) corrects for multiple testing.

(b) Volcano plots displaying differential gene expression in RVΔG-infected and uninfected cells. Colored dots indicate stress markers (left) and cell death markers (right) (orange: upregulated, blue: downregulated). Yellow outline depicts statistically significant difference in expression level.

(c) OGB-1 labeling and mCherry expression in the deep (granule cell) layer of the adult zebrafish OB after injection of EnvA-RVΔG-mCherry into the OB of Tg[gad1b:Gal4; UAS:TVA-mCherry] fish and bolus loading of OGB-1.

(d) Ca2+ signals evoked by two different odors in the same optical plane (single trials). Odors: alanine (Ala), taurode-oxycholic acid (TDCA).

(e) Randomly selected responses of seven infected (magenta) neurons and seven uninfected (green) neurons from the same optical plane to two odors (single trials).

(f) Odor-evoked Ca2+ signals of infected (N = 559) and uninfected (N = 1293) OB cells from N = 4 fish, averaged over all odors (N = 6) and repetitions (N = 3 for each odor). Shading indicates s.e.m.; bar indicates odor stimulation.

(g) Distribution of response amplitudes in non-infected and infected cells to different odors (N = 6), averaged over trials (N = 3). Distributions of were not significantly different (p = 0.24, Kolmogorov–Smirnov test ).

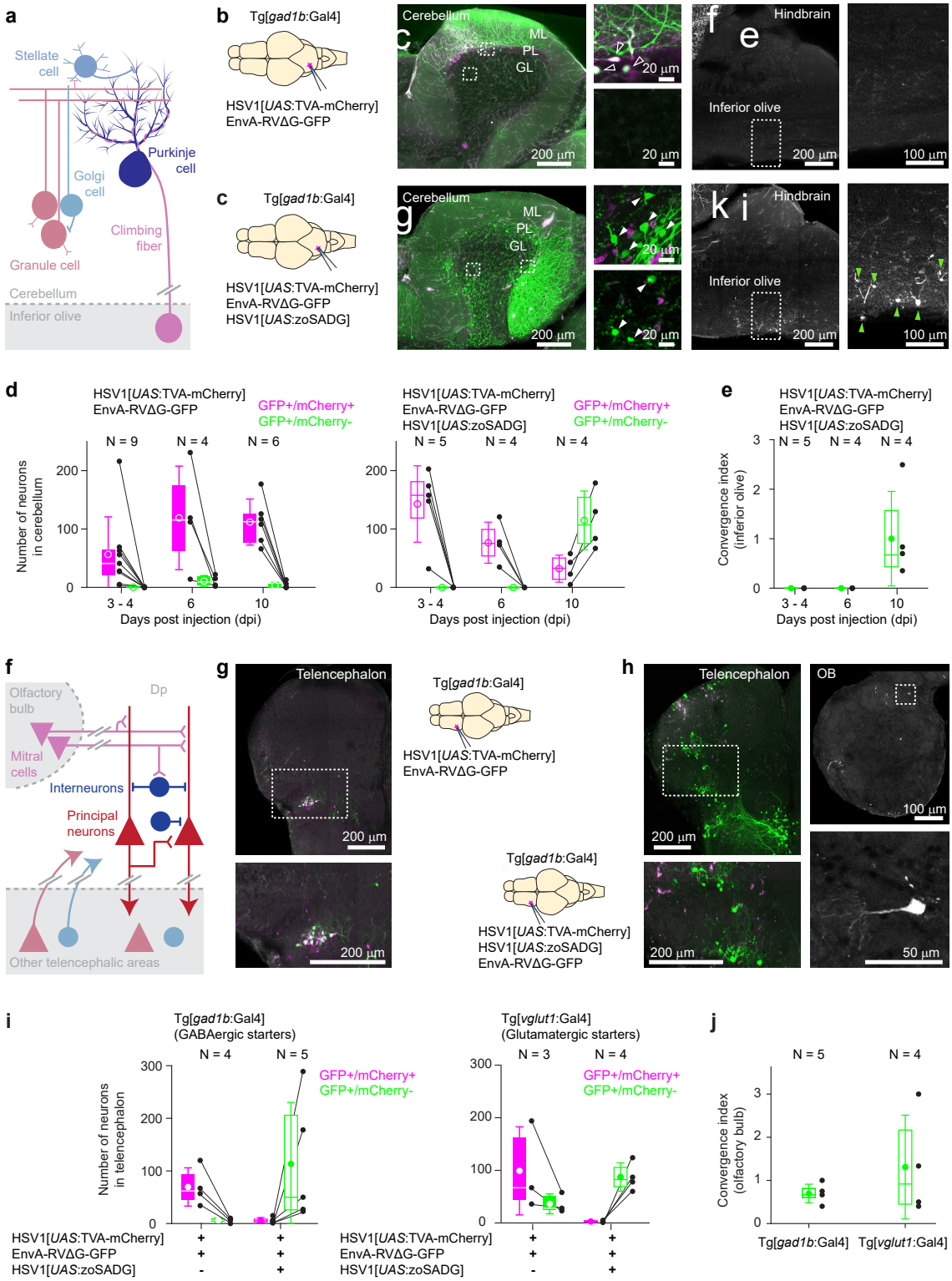


**Fig 4. Transneuronal tracing using pseudotyped rabies virus in adult zebrafish**

(a) Schematic of the cerebellar circuit. Glutamatergic neurons are shown in red colors, GABAergic neurons in blue colors. Purkinje cells receive extra-cerebellar input exclusively from the inferior olive.

(b) Co-injection of EnvA-RVΔG-GFP and HSV1[UAS:TVA-mCherry] into the cerebellum of Tg[gad1b:Gal4] fish in the absence of glycoprotein. Left: schematic. Center: expression of TVA-mCherry (magenta) and GFP (green) in the cerebellum. Regions in the Purkinje and granular layers (dashed rectangles) are enlarged. Unfilled white arrowheads indicate GFP+/mCherry+ neurons. Right: expression of GFP in the hindbrain. Region covering the inferior olive (dashed rectangle) is enlarged. Expression of GFP was restricted to putative starter neurons; no expression was detected in the inferior olive. ML: molecular layer; PL: Purkinje layer; GL: granular layer.

(c) Same as in (b) but the glycoprotein (zoSADG) was supplied to starter neurons in trans by co-injection of HSV1[UAS:zoSADG]. Filled white arrowheads indicate GFP+/mCherry- neurons. Note expression of GFP in putative granule cells and in neurons of the inferior olive, indicating transneuronal spread.

(d) Number of neurons that expressed GFP and mCherry (putative starter neurons) or GFP alone (putative presynaptic neurons) at different time points after injection of EnvA-RVΔG and HSV1[UAS:TVA-mCherry] into the cerebellum of Tg[gad1b:Gal4] fish. Left: without glycoprotein; right: with trans-complementation of zoSADG in starter neurons. Note that labeling of putative presynaptic neurons emerged between 6 and 10 days post injection only when zoSADG was trans-complemented in starter neurons. In all plots, black dots represent data from individual fish, box plot indicates median and the 25th and 75th percentiles, circles and error bars indicate mean and s.d. over individual fish. N: number of fish.

(e) Convergence index for the projection from the inferior olive to the cerebellum at different time points. The convergence index is the numerical ratio of transneuronally labeled neurons (GFP+/mCherry- neurons in the inferior olive) and putative starter cells in the cerebellum (GFP+/mCherry+ Purkinje neurons). N: number of fish.

(f) Schematic of the putative circuitry in telencephalic area Dp. Glutamatergic neurons are shown in red colors, GABAergic neurons in blue colors. Long-range projections from mitral cells in the olfactory bulb terminate on glutamatergic neurons and on GABAergic interneurons in Dp. Additional long-range projections originate in other telencephalic areas.

(g) Co-injection of EnvA-RVΔG and HSV1[UAS:TVA-mCherry] into Dp of Tg[gad1b:Gal4] fish in the absence of glycoprotein. Coronal section through the injected telencephalic hemisphere at the level of Dp. Area outlined by dashed rectangle is enlarged. Co-expression of GFP (green) and mCherry (magenta) indicates starter cells.

(h) Same as in (g) but with trans-complementation of zoSADG in starter neurons by co-injection of HSV1[UAS:zoSADG]. Left: coronal section through the injected telencephalic hemisphere. Right: coronal section through the ipsilateral OB. Expression of GFP only (green) indicates transneuronally labeled neurons.

(i) Number of neurons in the telencephalon that expressed GFP and mCherry (putative starter neurons) or GFP alone (putative presynaptic neurons) after injection of EnvA-RVΔG and HSV1[UAS:TVA-mCherry] into Dp with (+) or without (-) trans-complementation with zoSADG in starter neurons (HSV1[UAS:zoSADG]). Left: injection into Tg[gad1b:Gal4] fish; right: injection into Tg[vglut1:Gal4] fish (right). Expression was analyzed 10 days post injection. N: number of fish.

(j) Convergence index for the projection of transneuronally labeled neurons in the OB to Dp when EnvA-RVΔG was targeted to GABAergic neurons (viral injections into Tg[gad1b:Gal4] fish) or to glutamatergic neurons (injections into Tg[vglut1:Gal4] fish) in Dp. Expression was analyzed at 10 days post injection. N: number of fish.

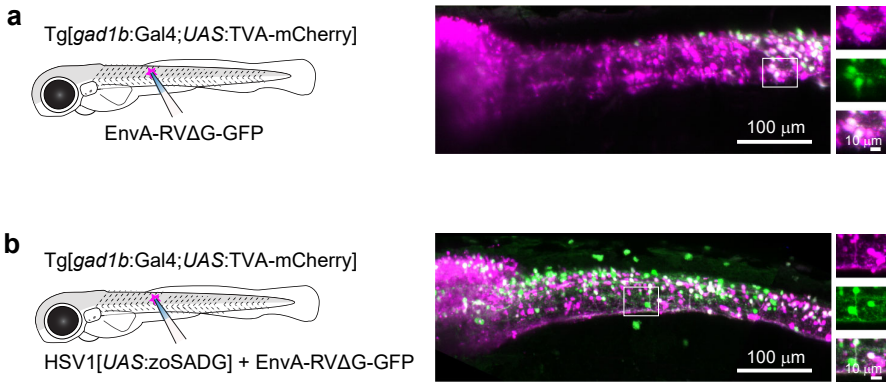


**Fig 5. Transneuronal tracing using pseudotyped rabies virus in zebrafish larvae**
(a) Expression of GFP (green) and TVA-mCherry (red) 6 days after injection of EnvA-RVΔG-GFP into the spinal cord of Tg[gad1b:Gal4;UAS:TVA-mCherry] fish at 7 dpf. Boxed region is enlarged on the right.
(b) Same after co-injection of EnvA-RVΔG-GFP and HSV1[UAS:zoSADG] into the spinal cord of Tg[gad1b:Gal4;UAS:TVA-mCherry] fish at 7 dpf.

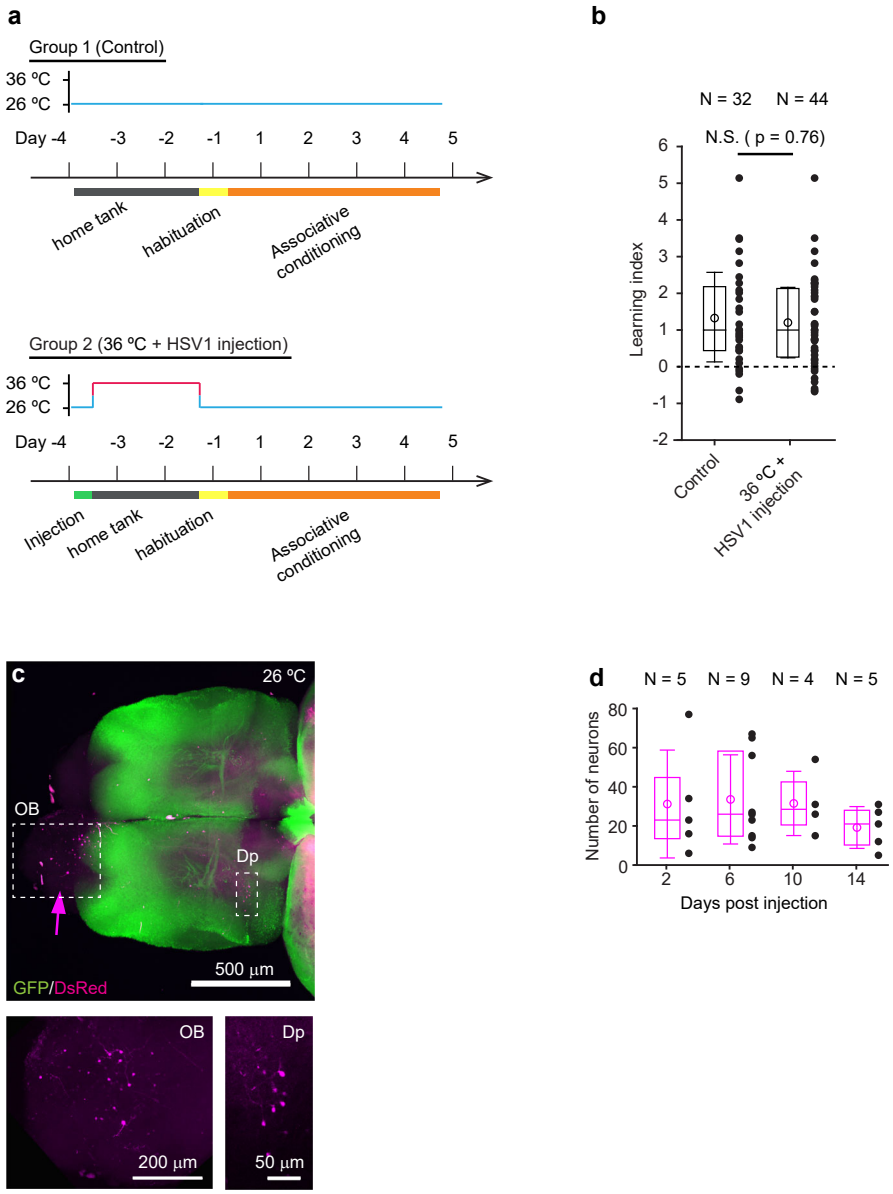


**Fig S1. Temperature-dependence and time course of HSV1-mediated gene expression**

(a) Sequence of virus injections, temperature changes and associative conditioning to assess effects of experimental manipulations on discrimination learning.

(b) Learning index (behavioral discrimination score) on the last day of training. Plot symbols represent data from individual fish; box plots show median and 25th and 75th percentiles, circles and error bars indicate mean and s.d. over individual fish. N: number of fish. Performance was not significantly different between groups (p = 0.76, Wilcoxon rank sum test)

(c) Expression of DsRed (magenta) six days after injection of HSV1[LTCMV:DsRed] into the OB (arrow) of an adult Tg[vglut1:GFP] fish kept at 26 ºC (maximum projection of confocal stack). Boxed areas (OB and Dp) are enlarged below. The number of DsRed-expressing neurons is low compared to DsRed expression at 36 ºC (Fig. 1).

(d) DsRed expression in the dorsal telencephalon at different timepoints after injection of HSV1[LTCMV:DsRed] into the ipsilateral OB. Fish were kept at 36 ºC. Black dots represent data from individual fish, box plot indicates median and 25th and 75th percentiles, circles and error bars indicate mean and s.d. over individual fish. N: number of fish.

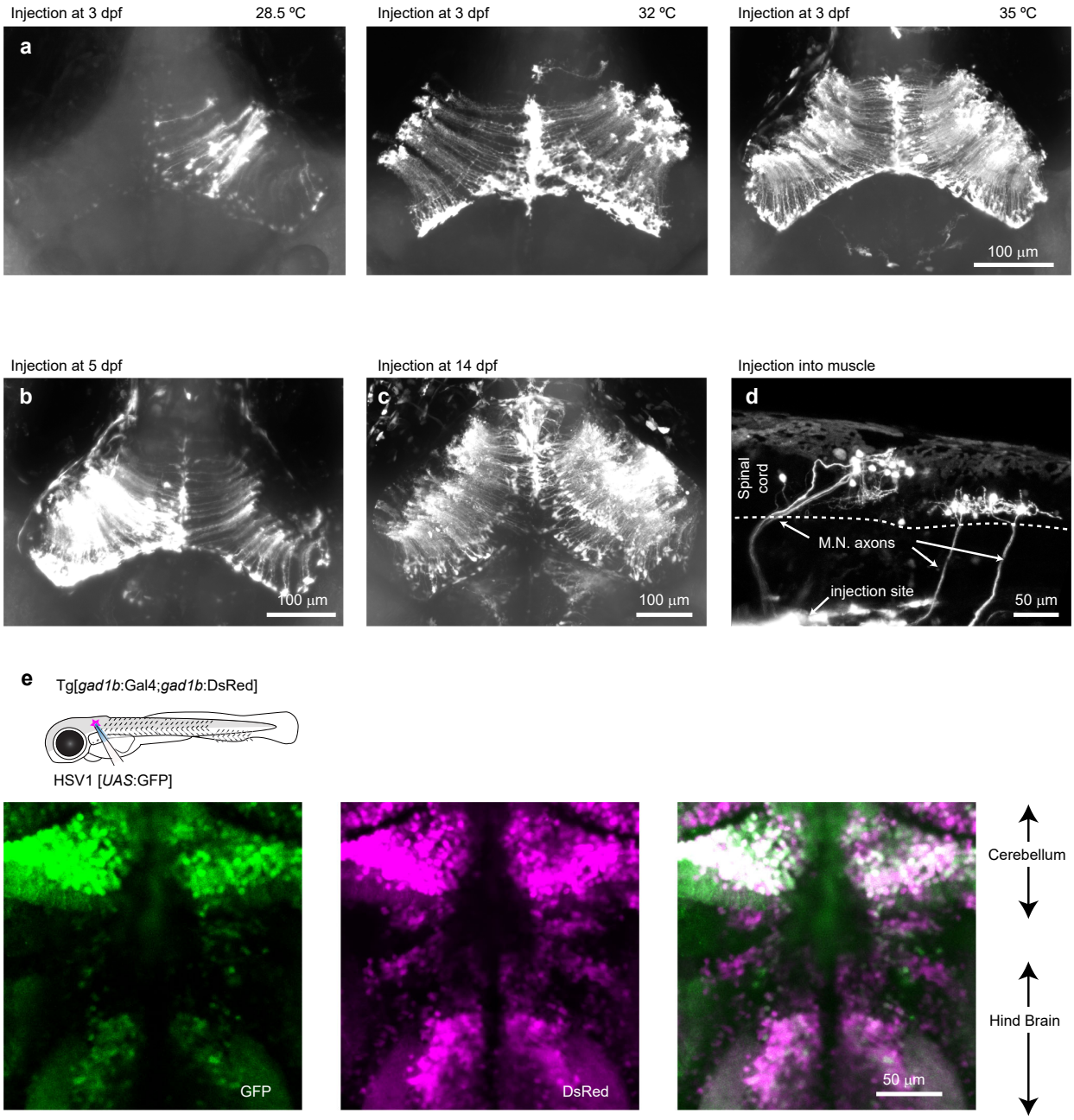


**Fig S2. HSV1-mediated gene delivery in larvae zebrafish and Gal4/UAS**

(a) Expression of GFP 48 h after injection of HSV1[LTCMV:GFP] into the optic tectum of zebrafish larvae (3 dpf; maximum intensity projection of confocal stack). Larvae were kept after the injection at 28.5, 32 or 35 ºC.

(b) Expression of GFP 48 h after injection of HSV1[LTCMV:GFP] into the optic tectum of a larva at 5 dpf (maximum intensity projection of confocal stack). The larva was kept after the injection at 35 ºC.

(c) Expression of GFP 48 h after injection of HSV1[LTCMV:GFP] into the optic tectum of a larva at 14 dpf (maximum intensity projection of confocal stack). The larva was kept after the injection at 35 ºC.

(d) Expression of GFP 48 h after injection of HSV1[LTCMV:GFP] into trunk muscles at 7 dpf (maximum intensity projection of confocal stack). The larva was kept after the injection at 35 ºC. Note retrograde labeling of motor neurons (M.N.).

(e) Expression of GFP 48 h after injection of HSV1[UAS:GFP] into the hindbrain of a Tg[gad1b:Gal4; gad1b:DsRed] larva at 7 dpf (maximum intensity projection of confocal stack). The larva was kept after the injection at 35 ºC. Note co-localization of DsRed and GFP in hindbrain and cerebellum.

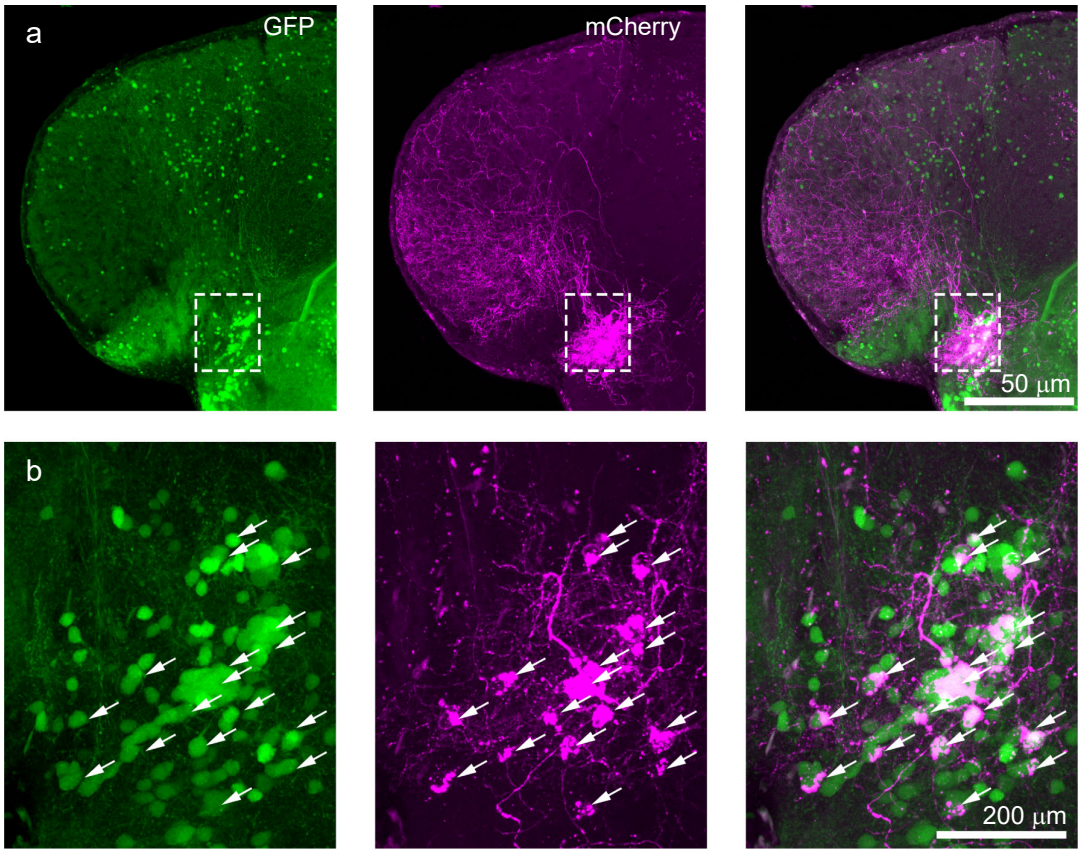


**Fig S3. Targeting of GABAergic neurons in the telencephalon**
(a) Coronal section through the telencephalon at the level of Dp after injection of HSV1[UAS:TVA-mCherry] into Tg[gad1b:Gal4; gad1b:GFP] double transgenic fish. The injection was targeted to a volume around Dp. mCherry was expressed predominantly in a cluster of GFP-positive neurons associated with Dp. Note long-range projections of mCherry-expressing neurons to multiple telencephalic areas.
(b) Enlargements of boxed region in (a). Arrows indicate GFP+/mCherry+ neurons.

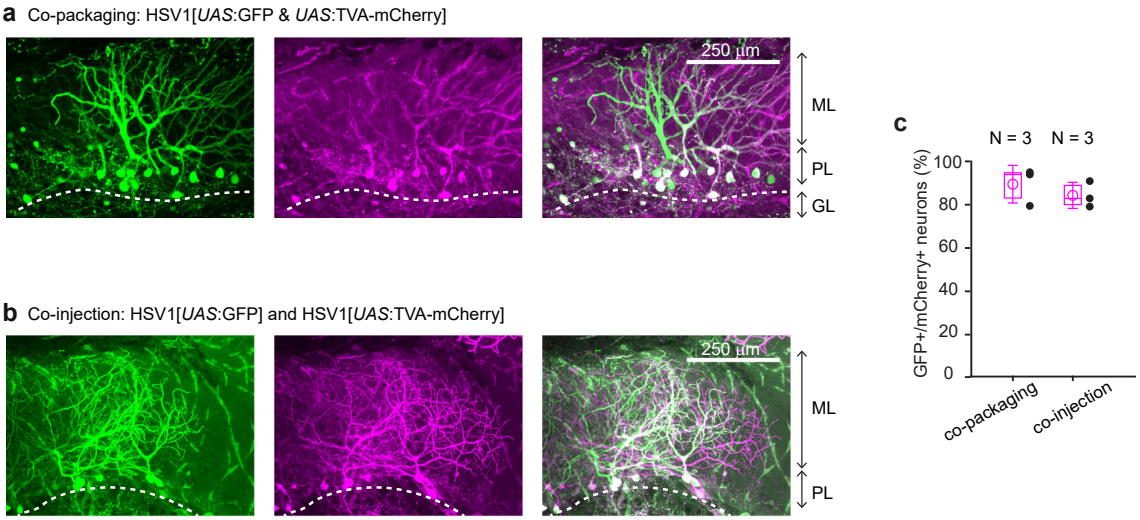


**Fig S4. Co-packaging of 2 different viruses does not facilitate co-infection of 2 viruses.**
(a) Expression of GFP and mCherry after injection of HSV1[UAS:GFP & UAS:TVA-mCherry] into the cerebellum of Tg[gad1b:Gal4] fish. In this virus, two expression constructs, UAS:GFP and UAS:TVA-mCherry, are packaged into the same virus particles. Expression is observed in Purkinje neurons and in putative Golgi cells. Note high rate of co-expression of GFP and mCherry. ML: molecular layer; PL: Purkinje layer; GL: granular layer.
(b) Expression of GFP and mCherry in the Purkinje layer after co-injection of two independent viruses (HSV1[UAS:GFP] and HSV1[UAS:TVA-mCherry]) into the cerebellum of Tg[gad1b:Gal4] fish. Note that the rate of co-expression was high even though GFP and mCherry were delivered by separate viruses. Note also that the overall expression was sparse, implying that co-expression was unlikely to occur by chance.
(c) Percentage of GFP and mCherry-expressing neurons among all fluorescent neurons. Filled circles represent data from individual fish, box plot indicates median and the 25th and 75th percentiles, and open circles indicate mean over individual fish. N: number of fish.

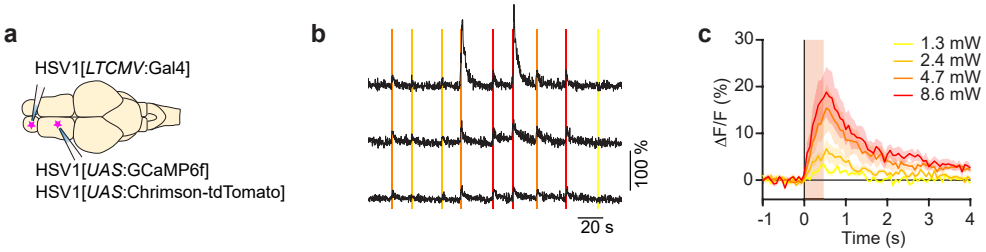


**Fig S5. Optogenetic manipulations using HSV1**

(a) Schematic: injection of HSV1[LTCMV:Gal4] into the OB and subsequent co-injection of HSV1[UAS:GCaMP6f] and HSV1[UAS:Chrimson-tdTomato] into the dorsal telencephalon of wt fish.

(b) Simultaneously recorded calcium transients evoked by optical stimulation of different light intensity (vertical lines) in three example neurons.

(c) Mean change GCaMP6f evoked by optical stimulation of different light intensity (N = 11 neurons; 11 ¬– 18 light stimuli at each intensity). Shading shows SEM is over cell.

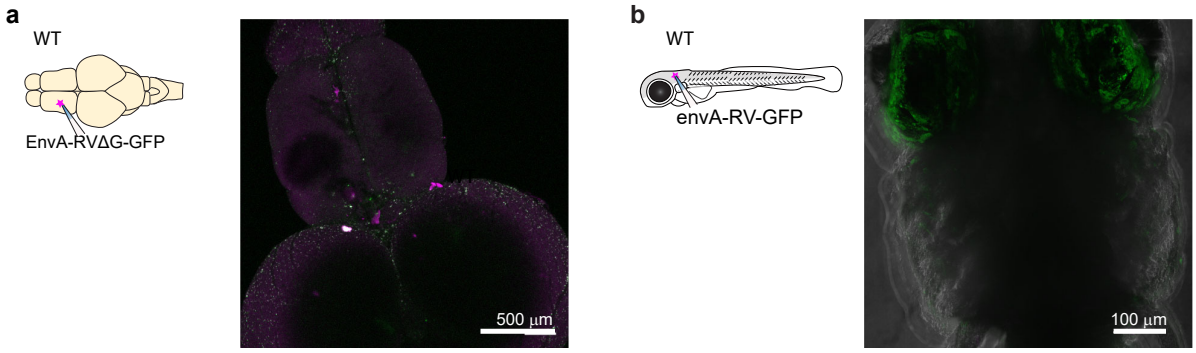


**Fig S6. Injection of pseudotyped rabies virus does not infect neurons in the absence of TVA**
(a) Absence of expression after injection of EnvA-RVΔG-GFP into the telencephalon of adult wt fish.
(b) Absence of expression after injection of EnvA-RVΔG-GFP into the optic tectum of wt fish at 7 dpf.

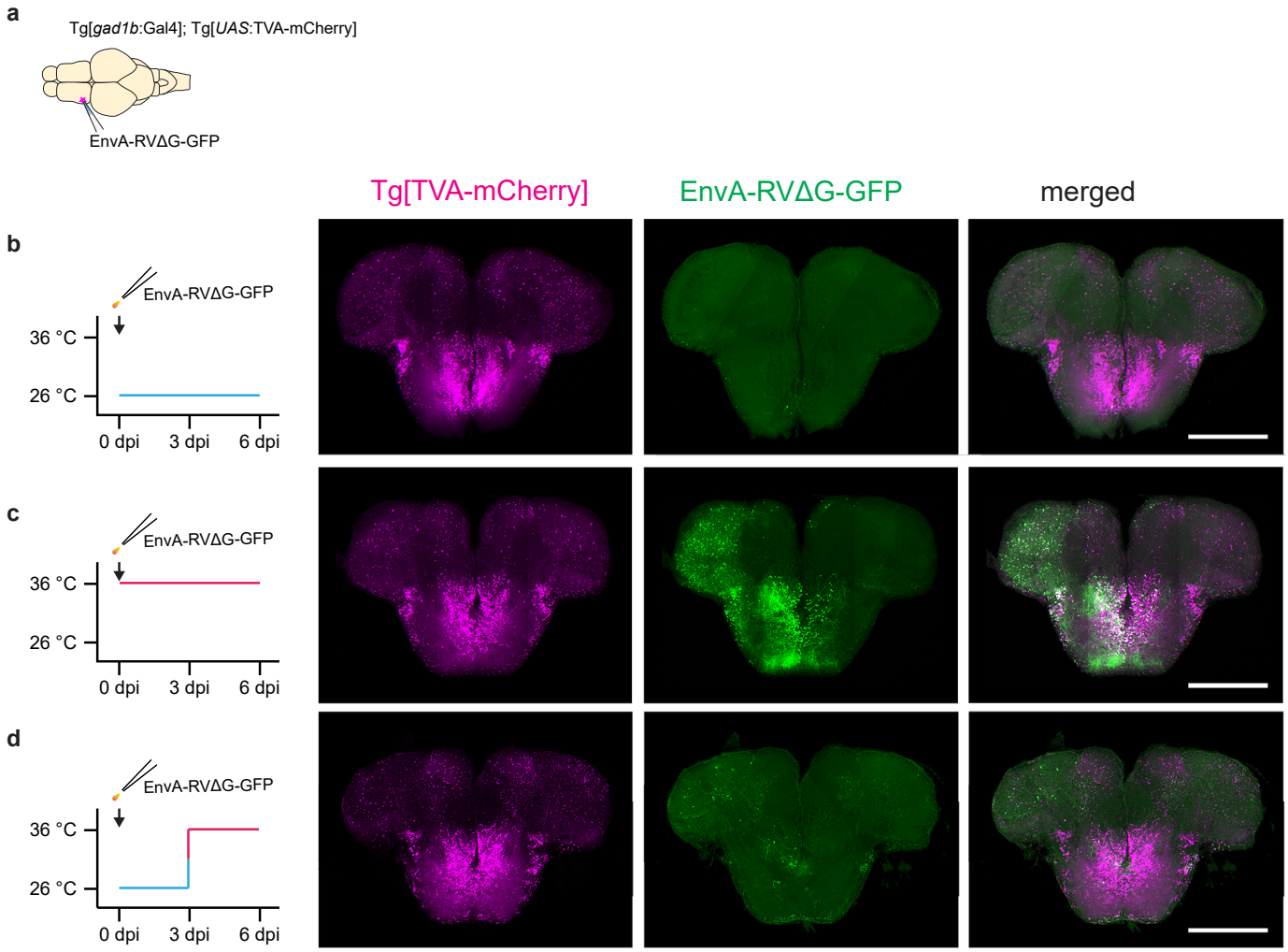


**Fig S7. Temperature-dependence of infection by rabies virus**

(a) Experimental scheme: Rabies virus (EnvA-RVΔG-GFP) was injected into the telencephalon of transgenic fish expressing TVA-mCherry in GABAergic neurons (Tg[gad1b:Gal4; UAS:TVA-mCherry]).

(b) Expression of TVA-mCherry and GFP when fish were kept at 26 ºC for 6 days after injection. Note almost complete absence of GFP expression.

(c) Expression of TVA-mCherry and GFP when fish were kept at 36 ºC for 6 days after injection. Note strong GFP expression.

(d) Expression of TVA-mCherry and GFP six days after injection when the housing temperature was increased from 26 ºC to 36 ºC 3 days after injection. GFP expression was weak and sparse.

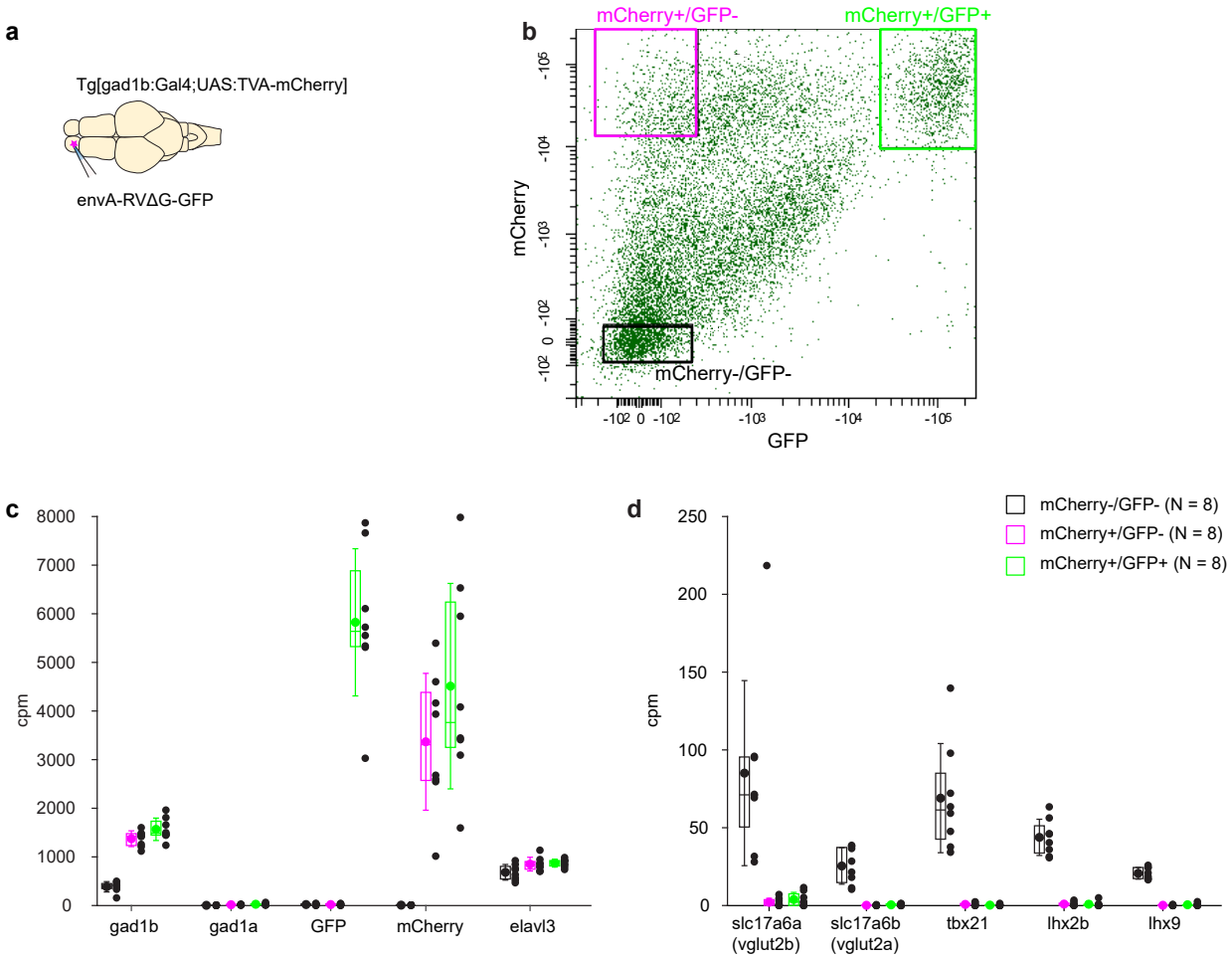


**Fig S8. Analysis of gene expression in GABAergic neurons**

(a) Schematic: injection of EnvA-RVΔG-GFP into the OB of adult Tg[gad1b:Gal4;UAS:TVA-mCherry] fish.

(b) Example of FACS analysis of GFP and mCherry expression. Boxes depict cells selected as mCherry+/GFP+ (EnvA-RVΔG-GFP infected gad1b neurons), mCherry+/GFP- (non-infected gad1b neurons), mCherry-/GFP- (negative control containing other OB cells). gad1b is one of two isoforms of gad1 that are expressed differentially in GABAergic neurons.

(c) Expression of marker genes (x-axis) in infected gad1b neurons (mCherry+/GFP+; green), non-infected gad1b neurons (mCherry+/GFP-; magenta), and other OB cells (mCherry-/GFP-; black). Cells classified as gad1b-positive by fluorescence markers, but not other cells, expressed gad1b but not gad1a, the other gad1 isoform. Expression of fluorescent marker genes followed the detection of fluorescent markers by FACS. The neuronal marker elav3 was present in all three pools. Plot symbols represent data from individual samples; box plots show median and 25th and 75th percentiles, circles and error bars indicate mean and s.d. over individual samples (N = 8 samples).

(d) Expression of negative markers for GABAergic neurons. The selected marker genes (slc17a6a, slc17a6b, tbx21, lhx2b and lhx9) should be expressed in mitral cells of the OB and other excitatory neurons but not in GABAergic neurons. Consistent with this expectation, expression of all negative markers was low or absent in pools of gad1b cells selected by FACS (N = 8 samples).

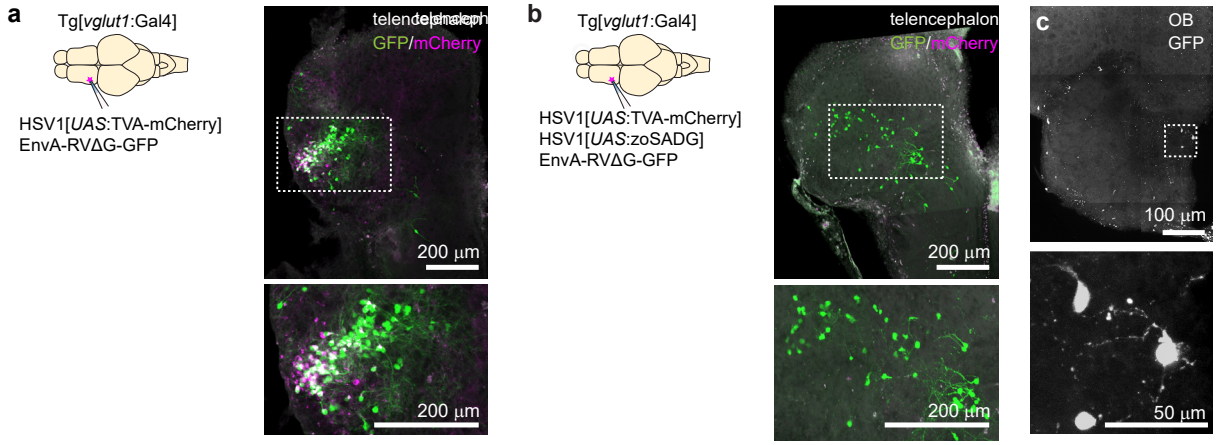


**Fig S9. Transneuronal tracing using pseudotyped rabies virus from vglut1+ neurons in Dp in adult zebrafish**

(a) Co-injection of EnvA-RVΔG-GFP and HSV1[UAS:TVA-mCherry] into Dp of Tg[vglut1:Gal4] fish in the absence of glycoprotein. Coronal section through the injected telencephalic hemisphere at the level of Dp. Area outlined by dashed rectangle is enlarged. Co-expression of GFP (green) and mCherry (magenta) indicates starter cells.

(b) Same as in (a) but with trans-complementation of zoSADG in starter neurons by co-injection of HSV1[UAS:zoSADG]. Left: coronal section through the injected telencephalic hemisphere. Right: coronal section through the ipsilateral olfactory bulb. Expression of GFP only (green) indicates transneuronally labeled neurons.

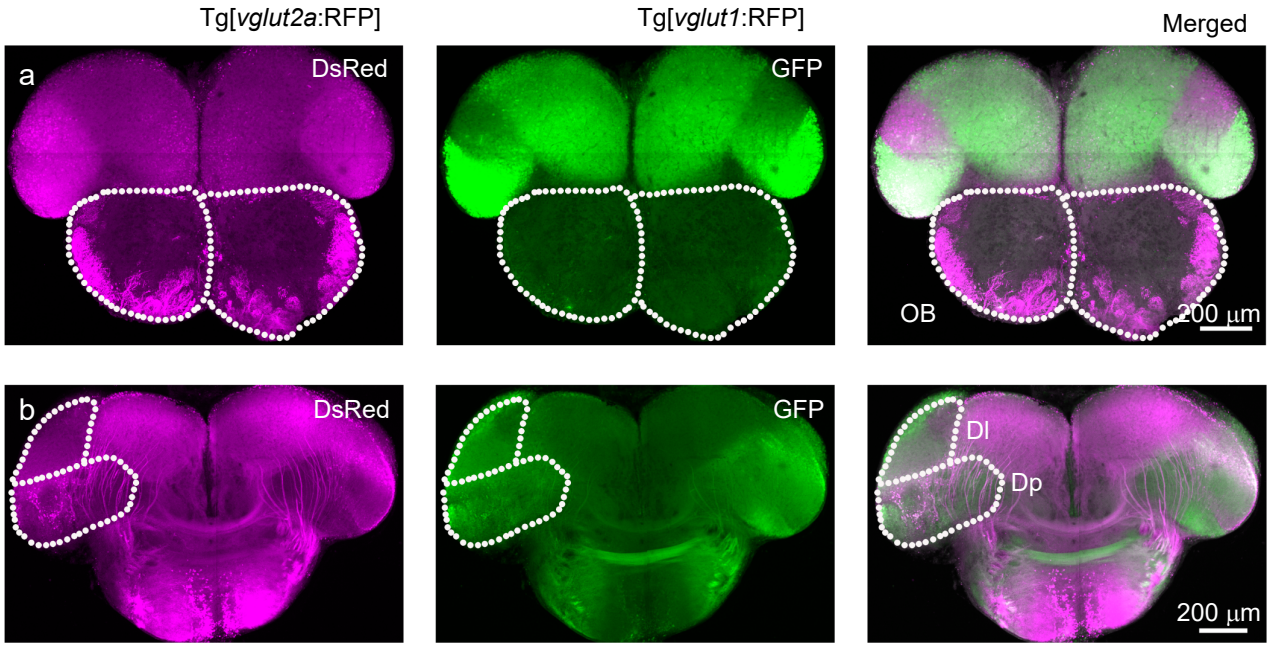


**Fig S10. Expression pattern of vglut1 and vglut2 in olfactory bulb and Dp**
(a) Coronal cross sections through the OB and anterior telencephalon from Tg[vglut2a:RFP; vglut1:GFP] double transgenic fish. Note that vglut2a (magenta) is expressed by axons of olfactory sensory neurons innervating glomeruli in the OB and by a subset of mitral cells, while expression of vglut1 (green) in the OB is weak or absent. Dotted lines outline OBs.
(b) More posterior coronal cross sections through the telencephalon of the same fish at the level of Dp. Note that expression of vglut2a and vglut1 in the telencephalon are largely complementary. Neurons in Dp express primarily vglut1. Dotted areas indicate the dorsal lateral telencephalic area (Dl) and Dp.

**Table 1**

| Promoter | Transgene | Transgene description | Comments |
|---|---|---|---|
| LTCMV | GFP | Green fluorescent protein | Fig. S2 |
| | DsRed | Red fluorescent protein | Fig. 1b, Fig. S2c |
| | mCherry | Red fluorescent protein | |
| | tdTomato | Red fluorescent protein | |
| | tagBFP-CAAX | Blue fluorescent protein, membrane targeted | |
| | Venus-CAAX | Yellow fluorescent protein (YFP), membrane targeted | |
| | TVA-mCherry | TVA-mCherry fusion | |
| | GCamp6s | Green flourescent calcium indicator | |
| | Gal4 | Gal4 | Fig. 2e, Fig. S5 |
| | ChR2-YFP | Channelrhodopsin-2-YFP fusion | |
| | ChR2-mCherry | ChR2-mCherry fusion | |
| | eNpHR3.0 | Halorhodopsin | |
| | H2B_GCamp6s | Green flourescent calcium indicator, targeted to nucleus | |
| | jGCamp7s | Green flourescent calcium indicator | |
| | jGCamp7b | Green flourescent calcium indicator | Fig. S1 b |
| UAS | GFP | Green fluorescent protein | Fig. 2b, Fig. S2e, Fig. S4 |
| | mCherry | Red fluorescent protein | |
| | tagBFP-CAAX | Blue fluorescent protein, membrane targeted | |
| | Venus-CAAX | Yellow fluorescent protein (YFP), membrane targeted | Fig. 2d |
| | GCamp6f | Green flourescent calcium indicator | Fig. S5 |
| | Chrimson-tdTomato | Chrimson-tdTomato fusion | Fig. S5 |
| | Jaws-mRuby | Jaws-mRuby fusion | |
| | TVA-mCherry | TVA-mCherry fusion | Fig. 2e, Fig 4, Fig. S3, Fig. S4, Fig. S9 |
| | zoSADG | glycoprotein for rabies tracing | Fig4, Fig5, Fig. S9 |
| | TeNT-GFP | tetanus toxin light chain fused with GFP | Movie 4 |
| | DT(Diphtheria toxin) | diphteria toxin | |

**Table 2**

| primaryID | secondaryI | logFC | logCPM | PValue | FDR | marker genes | up/down |
|---|---|---|---|---|---|---|---|
| blk | 2699 | -8.55359 | 3.676689 | 4.88E-06 | 0.000114 | stress/death marker | down |
| pycard | 916 | -7.91768 | 6.028085 | 6.07E-14 | 2.94E-11 | stress/death marker | down |
| crip1 | 1171 | -5.13301 | 6.208011 | 4.64E-12 | 8.89E-10 | stress/death marker | down |
| cd74b | 1071 | -4.80341 | 10.0098 | 8.15E-09 | 4.61E-07 | stress/death marker | down |
| cd74a | 1273 | -4.36402 | 10.47257 | 1.59E-08 | 8.08E-07 | stress/death marker | down |
| socs3a | 1935 | -4.0175 | 6.369958 | 1.92E-08 | 9.53E-07 | stress/death marker | down |
| anxa1a | 1317 | -3.70614 | 3.829076 | 0.002201 | 0.019825 | stress/death marker | down |
| nck1a | 1736 | -3.58713 | 4.058904 | 7.73E-07 | 2.31E-05 | stress/death marker | down |
| apoeb | 1718 | -7.39177 | 9.457418 | 1.28E-12 | 3.19E-10 | stress marker | down |
| caspa | 1542 | -6.56129 | 3.604579 | 8.50E-11 | 9.53E-09 | stress marker | down |
| tnfaip8l2a | 2999 | -6.52287 | 4.579522 | 3.59E-13 | 1.18E-10 | stress marker | down |
| caspb | 1819 | -6.49 | 6.385322 | 6.89E-12 | 1.29E-09 | stress marker | down |
| tnfsf10l | 6065 | -6.05507 | 3.205281 | 7.12E-07 | 2.17E-05 | stress marker | down |
| kita | 3558 | -5.92947 | 3.361018 | 1.80E-06 | 4.77E-05 | stress marker | down |
| gsdmeb | 2380 | -4.88661 | 4.555983 | 8.11E-08 | 3.24E-06 | stress marker | down |
| bnip4 | 1401 | -4.24925 | 3.11159 | 1.51E-06 | 4.08E-05 | stress marker | down |
| casp22 | 1164 | -4.22537 | 4.434146 | 1.50E-09 | 1.11E-07 | stress marker | down |
| lgals3b | 1678 | -4.1048 | 4.698176 | 2.26E-07 | 7.85E-06 | stress marker | down |
| gsdmea | 2051 | -3.81746 | 3.240636 | 5.71E-05 | 0.000945 | stress marker | down |
| pak2a | 2569 | -3.66208 | 4.849555 | 2.89E-07 | 9.72E-06 | stress marker | down |
| si:ch211-6 | 1149 | -3.64003 | 4.54818 | 5.38E-07 | 1.70E-05 | stress marker | down |
| tradd | 1302 | -3.54664 | 3.278696 | 1.82E-06 | 4.82E-05 | stress marker | down |
| ngfrb | 1974 | -3.53524 | 4.579012 | 2.23E-08 | 1.10E-06 | stress marker | down |
| dnase2b | 1363 | -3.31229 | 3.082677 | 4.85E-05 | 0.00083 | stress marker | down |
| prkcdb | 6370 | -3.16048 | 4.454486 | 2.88E-05 | 0.00053 | stress marker | down |
| bida | 917 | -3.01785 | 5.5786 | 5.34E-05 | 0.000897 | stress marker | down |
| mcamb | 3597 | -8.41473 | 5.820929 | 1.80E-16 | 4.23E-13 | cell death marker | down |
| cdk1 | 1367 | -6.56203 | 4.325484 | 1.05E-10 | 1.11E-08 | cell death marker | down |
| csrp1a | 2786 | -3.44261 | 4.812245 | 3.59E-05 | 0.000641 | cell death marker | down |
| neil3 | 2301 | -3.25707 | 3.685709 | 2.00E-05 | 0.000387 | cell death marker | down |
| rmi2 | 2164 | -3.13634 | 6.819279 | 8.49E-13 | 2.29E-10 | cell death marker | down |
| ccnd1 | 2826 | -3.08015 | 4.219045 | 2.95E-07 | 9.89E-06 | cell death marker | down |
| tnfrsf9a | 1514 | 4.579845 | 5.164639 | 9.66E-06 | 0.000207 | stress | up |
| nfe2l1a | 3303 | 3.262241 | 4.401034 | 0.000447 | 0.005445 | celldeath | up |
| sesn2 | 2194 | 3.473355 | 5.379293 | 6.45E-08 | 2.65E-06 | celldeath | up |
| nfe2l2b | 3002 | 4.602282 | 3.492498 | 6.01E-08 | 2.49E-06 | celldeath | up |
| ppp1r15b | 2374 | 5.54702 | 4.987662 | 6.44E-10 | 5.44E-08 | celldeath | up |
| calhm6 | 1503 | -10.39 | 4.351855 | 8.98E-18 | 4.93E-14 | | |
| si:ch211-1 | 1511 | -10.271 | 3.261507 | 2.14E-09 | 1.45E-07 | | |
| si:dkey-14 | 1358 | -10.1629 | 3.959676 | 2.06E-12 | 4.60E-10 | | |
| sla1a | 1350 | -10.0414 | 4.302244 | 4.15E-17 | 1.37E-13 | | |
| si:dkeyp-8 | 1795 | -9.91392 | 3.616256 | 1.07E-09 | 8.43E-08 | | |
| csf1ra | 3459 | -9.60321 | 6.558032 | 1.03E-19 | 1.69E-15 | | |
| si:dkey-25 | 1744 | -9.564 | 3.105679 | 5.59E-11 | 6.77E-09 | | |

| | | | | | |
|---|---|---|---|---|---|
| pdk2b | 2368 | -9.51768 | 3.090735 | 1.42E-09 | 1.06E-07 |
| cmklr1 | 1157 | -9.40585 | 4.534274 | 3.51E-14 | 2.05E-11 |
| sb:cb81 | 2447 | -9.37527 | 4.232372 | 3.79E-17 | 1.37E-13 |
| stoml3b | 1193 | -9.2643 | 3.289006 | 1.15E-14 | 8.83E-12 |
| zgc:10171 | 1451 | -9.11748 | 3.342702 | 4.38E-14 | 2.22E-11 |
| c1qc | 930 | -9.08859 | 8.200282 | 6.64E-16 | 1.22E-12 |
| zgc:17391 | 1007 | -9.08576 | 4.634535 | 1.53E-12 | 3.65E-10 |
| il10ra | 3764 | -9.0722 | 5.715717 | 2.95E-15 | 3.10E-12 |
| si:dkey-32 | 5121 | -9.03052 | 4.856579 | 2.85E-16 | 5.88E-13 |
| si:dkey-5n | 810 | -9.02918 | 6.885871 | 1.18E-14 | 8.83E-12 |
| kif23 | 3960 | -8.97105 | 3.341794 | 1.10E-07 | 4.17E-06 |
| si:ch211-2 | 646 | -8.97032 | 3.0444 | 5.20E-09 | 3.10E-07 |
| bin1b | 2143 | -8.9085 | 4.098503 | 3.77E-14 | 2.07E-11 |
| tgm2l | 2543 | -8.89724 | 3.159136 | 5.49E-12 | 1.04E-09 |
| rhoga | 809 | -8.74729 | 3.093063 | 1.99E-14 | 1.42E-11 |
| cfbl | 2575 | -8.56078 | 3.934788 | 1.97E-07 | 7.03E-06 |
| entpd1 | 2659 | -8.48709 | 6.351139 | 7.66E-18 | 4.93E-14 |
| csf1rb | 2894 | -8.37452 | 3.276585 | 1.35E-12 | 3.32E-10 |
| p2ry12 | 1371 | -8.33272 | 3.360911 | 2.25E-13 | 8.24E-11 |
| c1qa | 1133 | -8.26953 | 7.133016 | 6.73E-13 | 1.95E-10 |
| lpcat2 | 2803 | -8.20867 | 3.298753 | 5.99E-09 | 3.51E-07 |
| si:ch211-1 | 2166 | -8.19908 | 4.439234 | 1.15E-13 | 4.73E-11 |
| tlr8b | 2406 | -8.19408 | 4.043758 | 6.75E-13 | 1.95E-10 |
| ccr12a | 1113 | -8.17951 | 5.740079 | 2.45E-15 | 3.10E-12 |
| zgc:17209 | 3071 | -8.09484 | 3.768059 | 3.12E-12 | 6.50E-10 |
| si:ch1073- | 913 | -8.0804 | 3.63831 | 5.37E-05 | 0.000899 |
| si:dkey-18 | 1738 | -8.07066 | 3.816518 | 5.67E-09 | 3.35E-07 |
| plcg2 | 4465 | -8.00751 | 4.947682 | 1.47E-11 | 2.41E-09 |
| zgc:11249 | 1977 | -8.00113 | 7.268004 | 5.43E-15 | 4.71E-12 |
| sema4aa | 1971 | -7.99144 | 3.622184 | 5.86E-11 | 7.00E-09 |
| si:ch211-2 | 1720 | -7.92341 | 3.625703 | 1.77E-11 | 2.68E-09 |
| c1qb | 940 | -7.91322 | 7.500759 | 1.38E-13 | 5.42E-11 |
| lgals3bpa | 1977 | -7.86465 | 6.817372 | 3.60E-14 | 2.05E-11 |
| itga4 | 2270 | -7.83543 | 4.118082 | 1.13E-13 | 4.73E-11 |
| si:ch211-1 | 5290 | -7.78794 | 3.71111 | 5.41E-08 | 2.32E-06 |
| mfap4 | 1150 | -7.76643 | 3.54577 | 5.47E-10 | 4.79E-08 |
| tlr21 | 3055 | -7.71987 | 5.062953 | 2.71E-14 | 1.69E-11 |
| im:715403 | 1050 | -7.71657 | 3.29163 | 2.15E-09 | 1.46E-07 |
| si:rp71-68 | 2212 | -7.70411 | 4.73623 | 3.21E-12 | 6.53E-10 |
| havcr1 | 1184 | -7.7005 | 6.641428 | 2.62E-13 | 9.38E-11 |
| f11r.1 | 1749 | -7.65514 | 3.721817 | 1.05E-13 | 4.73E-11 |
| si:dkeyp-1 | 839 | -7.60183 | 4.522757 | 8.60E-09 | 4.77E-07 |
| si:dkey-1h | 1705 | -7.56723 | 4.309768 | 6.97E-09 | 4.02E-07 |
| itgae.1 | 2608 | -7.54668 | 5.480978 | 1.22E-11 | 2.08E-09 |
| si:dkeyp-6 | 6213 | -7.54631 | 5.15099 | 3.89E-14 | 2.07E-11 |
| dnase1l4.2 | 3425 | -7.53575 | 4.848219 | 1.84E-11 | 2.75E-09 |
| lgals3bpb | 1994 | -7.47349 | 11.77677 | 2.45E-14 | 1.65E-11 |

| | | | | | |
|---|---|---|---|---|---|
| fam83ha | 7192 | -7.46836 | 3.029466 | 2.40E-12 | 5.20E-10 |
| ccl34b.1 | 503 | -7.46171 | 10.04738 | 4.44E-14 | 2.22E-11 |
| si:ch211-2 | 1654 | -7.38678 | 3.651934 | 8.28E-08 | 3.30E-06 |
| gpat3 | 2637 | -7.3775 | 3.294922 | 1.19E-10 | 1.23E-08 |
| apoc1 | 783 | -7.36563 | 8.70788 | 5.70E-11 | 6.85E-09 |
| fut7 | 1275 | -7.35632 | 3.696356 | 2.30E-09 | 1.55E-07 |
| ms4a17a.6 | 962 | -7.34765 | 6.158979 | 1.07E-13 | 4.73E-11 |
| wasa | 2502 | -7.34092 | 4.248075 | 8.52E-14 | 4.01E-11 |
| cx32.2 | 1071 | -7.30629 | 4.567917 | 1.49E-10 | 1.47E-08 |
| lgals9l1 | 2201 | -7.26349 | 7.963593 | 6.64E-15 | 5.47E-12 |
| ikbke | 2508 | -7.26117 | 3.388682 | 3.14E-09 | 2.02E-07 |
| si:dkey-7i4 | 1564 | -7.25879 | 3.816286 | 6.66E-08 | 2.72E-06 |
| adam8a | 3251 | -7.25647 | 3.147203 | 2.11E-08 | 1.05E-06 |
| arhgap27 | 4401 | -7.21943 | 5.045676 | 1.91E-13 | 7.15E-11 |
| myo1f | 3684 | -7.21098 | 4.320156 | 2.17E-11 | 3.16E-09 |
| trim33l | 4150 | -7.20774 | 3.382336 | 6.81E-10 | 5.69E-08 |
| gpr18 | 945 | -7.20009 | 5.424085 | 3.95E-11 | 5.29E-09 |
| si:dkey-23 | 2429 | -7.12827 | 5.224191 | 8.22E-10 | 6.74E-08 |
| anxa4 | 1485 | -7.10838 | 5.404433 | 3.31E-13 | 1.14E-10 |
| kcnj10a | 1843 | -7.09252 | 3.071384 | 1.77E-09 | 1.26E-07 |
| tk1 | 2754 | -7.07147 | 3.175439 | 1.01E-09 | 8.09E-08 |
| zgc:12310 | 1985 | -7.05689 | 5.896833 | 1.81E-12 | 4.15E-10 |
| mrc1b | 3699 | -7.04138 | 6.294669 | 2.49E-11 | 3.60E-09 |
| inpp5d | 2826 | -7.01212 | 6.080787 | 1.53E-13 | 5.87E-11 |
| si:dkey-33 | 2802 | -6.99607 | 3.304151 | 1.02E-10 | 1.10E-08 |
| il1fma | 1744 | -6.99208 | 3.003249 | 1.56E-09 | 1.14E-07 |
| slc43a3b | 2532 | -6.99121 | 4.267088 | 1.70E-11 | 2.62E-09 |
| lpxn | 1249 | -6.9908 | 3.413242 | 8.37E-08 | 3.32E-06 |
| ncf1 | 2133 | -6.97863 | 5.396604 | 1.61E-11 | 2.56E-09 |
| tpst2 | 2939 | -6.9511 | 3.355849 | 5.34E-11 | 6.61E-09 |
| edaradd | 1887 | -6.9351 | 3.606989 | 1.24E-06 | 3.42E-05 |
| itgae.2 | 3070 | -6.90987 | 4.978628 | 7.65E-12 | 1.42E-09 |
| fybb | 2969 | -6.90743 | 5.096577 | 7.95E-13 | 2.18E-10 |
| si:ch211-1 | 778 | -6.89614 | 4.194368 | 4.59E-13 | 1.45E-10 |
| cxcr3.2 | 1893 | -6.89313 | 5.745659 | 8.75E-12 | 1.60E-09 |
| ptk2ba | 3201 | -6.87709 | 3.866064 | 6.66E-09 | 3.85E-07 |
| si:dkey-33i | 1891 | -6.87032 | 4.640381 | 3.37E-11 | 4.70E-09 |
| esco2 | 2339 | -6.87023 | 3.001886 | 1.96E-11 | 2.88E-09 |
| dok2 | 1591 | -6.8158 | 3.373412 | 1.59E-12 | 3.74E-10 |
| ptpn6 | 825 | -6.8136 | 5.664735 | 1.76E-11 | 2.68E-09 |
| gpr183a | 1448 | -6.79298 | 5.014105 | 3.53E-12 | 6.93E-10 |
| fxyd1 | 1072 | -6.77715 | 4.504522 | 2.92E-12 | 6.25E-10 |
| si:zfos-741 | 1108 | -6.77401 | 4.537165 | 2.50E-14 | 1.65E-11 |
| rgs18 | 1694 | -6.76696 | 5.686287 | 1.52E-11 | 2.43E-09 |
| smc4 | 4193 | -6.73144 | 3.796677 | 8.61E-08 | 3.41E-06 |
| cyba | 1033 | -6.72796 | 6.847746 | 3.59E-15 | 3.41E-12 |
| prkacba | 2483 | -6.715 | 4.405069 | 5.49E-08 | 2.34E-06 |

| | | | | | |
|---|---|---|---|---|---|
| zgc:12301( | 4414 | -6.69991 | 3.7256 | 1.32E-10 | 1.34E-08 |
| si:dkey-27l | 1009 | -6.67355 | 3.128548 | 3.70E-10 | 3.39E-08 |
| ikzf1 | 2301 | -6.63884 | 4.76291 | 3.44E-07 | 1.14E-05 |
| abo | 1238 | -6.63256 | 3.998867 | 1.03E-07 | 3.98E-06 |
| cd4-1 | 2043 | -6.61853 | 4.048068 | 8.18E-05 | 0.00129 |
| slc7a7 | 2395 | -6.61253 | 3.768626 | 6.18E-11 | 7.33E-09 |
| clic1 | 2440 | -6.58656 | 6.704249 | 3.35E-12 | 6.69E-10 |
| itgb2 | 3489 | -6.57167 | 6.740088 | 5.27E-13 | 1.58E-10 |
| ccdc88b | 5067 | -6.56981 | 4.294944 | 6.52E-09 | 3.79E-07 |
| skap2 | 1524 | -6.55845 | 4.776501 | 3.75E-10 | 3.41E-08 |
| si:ch211-1! | 920 | -6.54565 | 4.186354 | 2.54E-11 | 3.60E-09 |
| zgc:15331 | 827 | -6.54449 | 4.965433 | 4.01E-13 | 1.30E-10 |
| cd22 | 1834 | -6.49337 | 3.257232 | 9.46E-09 | 5.16E-07 |
| gmip | 3356 | -6.39194 | 4.812563 | 7.35E-11 | 8.59E-09 |
| rac2 | 1163 | -6.36626 | 6.795421 | 1.18E-12 | 2.98E-10 |
| gsto2 | 1088 | -6.3644 | 6.076688 | 3.59E-13 | 1.18E-10 |
| ctsk | 1639 | -6.36243 | 5.55315 | 4.80E-11 | 6.18E-09 |
| capgb | 1902 | -6.35208 | 5.903055 | 4.77E-11 | 6.18E-09 |
| grapa | 1419 | -6.32967 | 3.970559 | 8.29E-11 | 9.47E-09 |
| kif11 | 3677 | -6.31907 | 3.116131 | 1.13E-10 | 1.18E-08 |
| krt18b | 1889 | -6.29179 | 5.724327 | 8.57E-11 | 9.54E-09 |
| coro1a | 1813 | -6.29029 | 8.894132 | 1.83E-15 | 2.74E-12 |
| ltb4r | 3752 | -6.26428 | 3.297134 | 1.14E-09 | 8.95E-08 |
| myo1g | 2997 | -6.25781 | 4.760754 | 1.41E-10 | 1.42E-08 |
| arpc1b | 1702 | -6.24955 | 7.992704 | 3.72E-15 | 3.41E-12 |
| wipf1a | 1851 | -6.23643 | 4.762151 | 2.78E-08 | 1.33E-06 |
| cxcl11.5 | 259 | -6.23483 | 3.440395 | 1.33E-08 | 7.07E-07 |
| zgc:19372! | 516 | -6.2333 | 5.626308 | 1.16E-12 | 2.98E-10 |
| tprg1 | 1587 | -6.22348 | 3.960485 | 3.01E-08 | 1.43E-06 |
| grn1 | 1618 | -6.21813 | 6.383974 | 1.68E-10 | 1.63E-08 |
| itm2bb | 1505 | -6.21482 | 7.694584 | 7.37E-16 | 1.22E-12 |
| knl1 | 5496 | -6.21044 | 3.376769 | 1.15E-06 | 3.23E-05 |
| si:ch73-38( | 1529 | -6.20687 | 3.906146 | 1.16E-09 | 9.09E-08 |
| grna | 4163 | -6.16682 | 7.455984 | 1.14E-12 | 2.97E-10 |
| spi1a | 2287 | -6.16146 | 5.984179 | 1.26E-13 | 5.05E-11 |
| fam117ab | 2156 | -6.15802 | 3.014125 | 9.45E-09 | 5.16E-07 |
| hck | 7256 | -6.12147 | 6.314793 | 1.12E-13 | 4.73E-11 |
| zgc:11021( | 871 | -6.1172 | 3.175557 | 5.16E-10 | 4.57E-08 |
| ssuh2.4 | 1248 | -6.11585 | 3.454477 | 1.41E-09 | 1.05E-07 |
| zgc:11054( | 1584 | -6.11066 | 3.983982 | 1.50E-08 | 7.74E-07 |
| fgl2a | 2524 | -6.10368 | 3.452771 | 1.82E-09 | 1.28E-07 |
| ano6 | 4205 | -6.09562 | 4.561703 | 2.53E-11 | 3.60E-09 |
| wipf1b | 4085 | -6.09487 | 4.573721 | 6.47E-10 | 5.44E-08 |
| unc93b1 | 2489 | -6.09204 | 4.834007 | 3.70E-11 | 5.04E-09 |
| klhl6 | 2488 | -6.09164 | 3.446584 | 2.74E-08 | 1.32E-06 |
| samsn1a | 2760 | -6.09047 | 5.631879 | 1.36E-11 | 2.26E-09 |
| tnfsf10 | 1879 | -6.07853 | 4.21198 | 2.10E-10 | 2.01E-08 |

| | | | | | |
|---|---|---|---|---|---|
| hlx1 | 1489 | -6.04149 | 3.333557 | 8.23E-07 | 2.43E-05 |
| dnase2 | 3476 | -6.01074 | 3.54114 | 4.63E-10 | 4.17E-08 |
| csf2rb | 2322 | -5.99683 | 4.956642 | 1.90E-09 | 1.33E-07 |
| si:dkey-21 | 982 | -5.99598 | 4.282768 | 8.64E-10 | 7.04E-08 |
| fcer1g | 491 | -5.98436 | 6.143764 | 2.88E-13 | 1.01E-10 |
| itpr3 | 8687 | -5.96891 | 3.5609 | 5.63E-07 | 1.76E-05 |
| itgb7 | 2440 | -5.95446 | 4.050192 | 1.03E-07 | 3.98E-06 |
| rgs14a | 2583 | -5.93934 | 3.503998 | 1.56E-08 | 8.01E-07 |
| ms4a17a.1 | 1054 | -5.90552 | 5.553394 | 3.17E-12 | 6.53E-10 |
| si:ch211-1 | 650 | -5.89343 | 3.789355 | 1.64E-09 | 1.19E-07 |
| ttk | 3330 | -5.89199 | 3.740549 | 1.36E-08 | 7.14E-07 |
| enpp1 | 3932 | -5.86953 | 6.924821 | 1.94E-11 | 2.88E-09 |
| kel | 2890 | -5.86268 | 3.560545 | 4.29E-08 | 1.91E-06 |
| slc29a1b | 4805 | -5.86213 | 3.133898 | 1.26E-09 | 9.67E-08 |
| ptprja | 5618 | -5.85364 | 4.649104 | 4.49E-08 | 1.98E-06 |
| mpeg1.1 | 2634 | -5.83591 | 6.795263 | 8.39E-11 | 9.47E-09 |
| atp6v0e1 | 836 | -5.78222 | 4.925977 | 2.56E-11 | 3.60E-09 |
| si:dkey-10 | 838 | -5.73796 | 3.023258 | 1.15E-06 | 3.24E-05 |
| dnph1 | 667 | -5.7363 | 3.293293 | 1.34E-08 | 7.08E-07 |
| si:ch211-7 | 1840 | -5.73159 | 6.159251 | 5.38E-11 | 6.61E-09 |
| me1 | 2067 | -5.71822 | 3.020836 | 2.68E-08 | 1.30E-06 |
| ponzr1 | 1435 | -5.71062 | 7.74013 | 1.45E-11 | 2.39E-09 |
| grn2 | 783 | -5.70132 | 3.968429 | 3.98E-08 | 1.80E-06 |
| zgc:17150 | 1295 | -5.69589 | 3.463775 | 1.86E-08 | 9.31E-07 |
| si:ch211-2 | 1370 | -5.68653 | 3.129444 | 2.75E-08 | 1.32E-06 |
| rin3 | 5791 | -5.68382 | 3.422524 | 2.61E-08 | 1.27E-06 |
| fabp11a | 674 | -5.67152 | 4.462765 | 1.33E-06 | 3.64E-05 |
| si:ch73-22 | 926 | -5.6658 | 5.215537 | 3.17E-07 | 1.06E-05 |
| si:ch211-1 | 6759 | -5.63294 | 3.493092 | 2.22E-07 | 7.73E-06 |
| zgc:11033 | 1040 | -5.60424 | 4.419098 | 3.87E-11 | 5.22E-09 |
| si:dkey-26 | 3382 | -5.6029 | 3.23936 | 1.38E-09 | 1.04E-07 |
| zgc:10178 | 1582 | -5.59431 | 3.23463 | 1.58E-08 | 8.07E-07 |
| aplnrb | 2087 | -5.57484 | 4.617176 | 8.00E-09 | 4.56E-07 |
| f13a1b | 3162 | -5.57336 | 4.345208 | 9.51E-09 | 5.17E-07 |
| slc3a2a | 2079 | -5.57244 | 5.751776 | 1.69E-09 | 1.22E-07 |
| cxcl8b.1 | 714 | -5.54711 | 3.685568 | 0.000248 | 0.00334 |
| eef1da | 1607 | -5.53799 | 7.740961 | 5.00E-13 | 1.56E-10 |
| gnpda1 | 1346 | -5.53174 | 4.24265 | 1.06E-10 | 1.12E-08 |
| alox5ap | 1304 | -5.5002 | 3.698811 | 5.52E-08 | 2.34E-06 |
| wee2 | 2245 | -5.47644 | 3.158668 | 1.50E-08 | 7.75E-07 |
| si:ch211-2 | 1205 | -5.47061 | 4.161078 | 7.25E-09 | 4.15E-07 |
| ahnak | 20569 | -5.44864 | 4.482993 | 3.09E-09 | 2.00E-07 |
| dhrs9 | 1351 | -5.44507 | 3.51788 | 2.33E-08 | 1.14E-06 |
| blnk | 3517 | -5.43461 | 5.202384 | 2.05E-09 | 1.41E-07 |
| arhgap17b | 1904 | -5.42888 | 4.531299 | 1.79E-09 | 1.27E-07 |
| mpzl2b | 1608 | -5.42569 | 3.951077 | 7.09E-08 | 2.87E-06 |
| grap2a | 1829 | -5.41182 | 6.070648 | 5.16E-11 | 6.54E-09 |

| | | | | | |
|---|---|---|---|---|---|
| tlr3 | 3161 | -5.40996 | 5.517135 | 6.58E-07 | 2.03E-05 |
| lpar5a | 1571 | -5.39378 | 4.690987 | 3.35E-09 | 2.12E-07 |
| hcls1 | 2495 | -5.38296 | 6.006668 | 3.50E-10 | 3.22E-08 |
| apbb1ip | 3287 | -5.36059 | 5.594083 | 4.49E-08 | 1.98E-06 |
| gpr65 | 1331 | -5.33736 | 3.25469 | 5.62E-08 | 2.37E-06 |
| plekhf1 | 1225 | -5.33663 | 4.539008 | 5.69E-10 | 4.96E-08 |
| antxr1c | 6703 | -5.33535 | 3.73568 | 8.14E-08 | 3.25E-06 |
| tlcd1 | 1076 | -5.33352 | 3.023806 | 3.76E-08 | 1.73E-06 |
| rgn | 1490 | -5.33302 | 3.174138 | 4.31E-09 | 2.62E-07 |
| notch1a | 6096 | -5.31687 | 3.961899 | 7.39E-10 | 6.09E-08 |
| adcy7 | 10228 | -5.29656 | 4.911045 | 9.24E-11 | 1.01E-08 |
| pfn1 | 1540 | -5.29118 | 10.69854 | 1.07E-12 | 2.83E-10 |
| wasf2 | 3321 | -5.29117 | 4.361607 | 3.22E-09 | 2.06E-07 |
| rnaset2l | 995 | -5.2852 | 6.427019 | 1.49E-11 | 2.41E-09 |
| pik3r5 | 2823 | -5.28036 | 3.436336 | 3.51E-07 | 1.16E-05 |
| si:dkey-27i | 706 | -5.27799 | 7.121681 | 3.37E-12 | 6.69E-10 |
| wasb | 1735 | -5.26685 | 6.276717 | 4.91E-08 | 2.13E-06 |
| itpkcb | 3844 | -5.25908 | 3.168152 | 1.12E-06 | 3.16E-05 |
| si:ch211-2 | 2048 | -5.24928 | 7.477174 | 3.48E-11 | 4.82E-09 |
| kpna2 | 1933 | -5.24507 | 4.908564 | 5.72E-10 | 4.96E-08 |
| gstt1a | 1674 | -5.22965 | 3.658929 | 2.19E-07 | 7.66E-06 |
| si:ch73-24 | 2779 | -5.22912 | 4.513749 | 3.86E-08 | 1.76E-06 |
| il2rga | 1135 | -5.22598 | 5.548132 | 2.63E-09 | 1.73E-07 |
| ampd3b | 3081 | -5.22563 | 4.235599 | 3.11E-08 | 1.47E-06 |
| cyfip1 | 4645 | -5.2206 | 5.930294 | 1.50E-10 | 1.48E-08 |
| ostf1 | 3322 | -5.21755 | 3.474732 | 3.45E-09 | 2.15E-07 |
| pparg | 1581 | -5.21527 | 3.78603 | 4.92E-09 | 2.95E-07 |
| rbp4 | 1122 | -5.18913 | 4.240103 | 0.000482 | 0.005812 |
| mtmr8 | 3126 | -5.17214 | 3.863115 | 2.68E-08 | 1.30E-06 |
| rhogb | 1957 | -5.17203 | 5.441925 | 1.19E-11 | 2.03E-09 |
| rgl1 | 4786 | -5.16981 | 3.335712 | 8.71E-08 | 3.44E-06 |
| ephx2 | 2170 | -5.15157 | 3.472828 | 1.10E-06 | 3.12E-05 |
| stx7l | 2408 | -5.14742 | 3.220775 | 1.25E-07 | 4.69E-06 |
| ifi30 | 1041 | -5.14192 | 6.001759 | 1.81E-09 | 1.28E-07 |
| stx11a | 1526 | -5.14187 | 4.863036 | 6.32E-09 | 3.70E-07 |
| snx33 | 4452 | -5.12527 | 3.990311 | 8.31E-09 | 4.64E-07 |
| plk1 | 2538 | -5.08974 | 4.207503 | 3.59E-07 | 1.18E-05 |
| snx9b | 2965 | -5.08741 | 4.626339 | 1.11E-07 | 4.23E-06 |
| abi3a | 2447 | -5.08691 | 4.931541 | 1.25E-10 | 1.28E-08 |
| tacc3 | 3275 | -5.07545 | 3.463467 | 2.69E-07 | 9.13E-06 |
| chaf1b | 2548 | -5.02924 | 3.145242 | 2.16E-06 | 5.60E-05 |
| slco2b1 | 2782 | -5.00378 | 5.011461 | 3.65E-09 | 2.26E-07 |
| si:ch211-1 | 972 | -5.00336 | 6.013044 | 8.30E-09 | 4.64E-07 |
| top2a | 2839 | -4.98978 | 3.906693 | 1.38E-08 | 7.22E-07 |
| rasgrp4 | 3443 | -4.9744 | 5.005735 | 5.91E-09 | 3.48E-07 |
| arhgap4a | 2964 | -4.97419 | 4.490722 | 1.22E-06 | 3.39E-05 |
| myh9a | 6842 | -4.96904 | 3.874687 | 9.27E-08 | 3.62E-06 |

| | | | | | |
|---|---|---|---|---|---|
| lifrb | 3101 | -4.96743 | 3.673836 | 6.69E-07 | 2.06E-05 |
| adap2 | 1291 | -4.96277 | 4.105948 | 1.05E-07 | 4.01E-06 |
| xpnpep2 | 2837 | -4.96094 | 3.555436 | 9.20E-07 | 2.64E-05 |
| myd88 | 1485 | -4.94839 | 4.502204 | 1.35E-08 | 7.10E-07 |
| pitpnaa | 1799 | -4.93084 | 4.364783 | 2.79E-08 | 1.33E-06 |
| si:ch211-2 | 2945 | -4.92927 | 5.831847 | 3.89E-08 | 1.76E-06 |
| f13a1a.1 | 3541 | -4.90229 | 4.260768 | 0.000575 | 0.006744 |
| cdh30 | 2492 | -4.89217 | 3.0878 | 5.37E-05 | 0.000899 |
| prkcq | 2128 | -4.88934 | 3.555412 | 8.19E-06 | 0.000181 |
| ctsl.1 | 1434 | -4.87462 | 3.325039 | 0.0027 | 0.023449 |
| irf5 | 2539 | -4.87107 | 3.074134 | 1.95E-06 | 5.09E-05 |
| zgc:10172 | 915 | -4.86052 | 3.764231 | 6.14E-08 | 2.53E-06 |
| si:dkey-18 | 3441 | -4.83741 | 4.911856 | 2.31E-07 | 7.99E-06 |
| nutf2l | 833 | -4.83191 | 4.562038 | 5.56E-08 | 2.35E-06 |
| flvcr2b | 2505 | -4.82902 | 4.328858 | 8.34E-07 | 2.45E-05 |
| itprid2 | 4552 | -4.76987 | 4.819814 | 9.39E-10 | 7.59E-08 |
| tmc8 | 3177 | -4.75391 | 3.629136 | 5.67E-06 | 0.000131 |
| lcp2a | 2034 | -4.7439 | 5.638843 | 2.98E-10 | 2.78E-08 |
| map3k1 | 4122 | -4.74336 | 4.806579 | 1.58E-07 | 5.82E-06 |
| jac2 | 1016 | -4.73677 | 5.445929 | 0.000827 | 0.009069 |
| glb1l | 2095 | -4.71537 | 4.901345 | 8.24E-09 | 4.64E-07 |
| fli1b | 2827 | -4.71029 | 5.927144 | 8.92E-07 | 2.58E-05 |
| ppp1r18 | 4779 | -4.70587 | 4.511345 | 4.47E-09 | 2.70E-07 |
| sh3bp2 | 1485 | -4.7015 | 4.584956 | 7.65E-07 | 2.30E-05 |
| lrrc8da | 5389 | -4.69889 | 4.268579 | 3.11E-06 | 7.67E-05 |
| igf2b | 3385 | -4.69883 | 5.111442 | 9.74E-09 | 5.28E-07 |
| jac3 | 1289 | -4.684 | 3.635914 | 0.00061 | 0.007053 |
| si:dkey-25 | 5084 | -4.68241 | 3.185553 | 6.97E-05 | 0.001123 |
| snx22 | 1066 | -4.66849 | 3.909313 | 3.29E-09 | 2.10E-07 |
| plxnc1 | 3171 | -4.6396 | 4.783128 | 3.18E-10 | 2.95E-08 |
| si:dkey-20 | 3053 | -4.6307 | 4.145849 | 2.33E-08 | 1.14E-06 |
| si:dkey-17 | 2451 | -4.62265 | 5.142877 | 1.97E-06 | 5.13E-05 |
| cd82b | 3342 | -4.61856 | 3.96336 | 1.14E-05 | 0.000238 |
| arhgef10 | 4004 | -4.61737 | 3.074743 | 2.36E-07 | 8.11E-06 |
| si:dkey-18 | 1380 | -4.59616 | 5.821332 | 1.80E-10 | 1.73E-08 |
| ms4a17a.9 | 2247 | -4.58961 | 3.848891 | 5.96E-08 | 2.48E-06 |
| uap1l1 | 1911 | -4.56385 | 4.248701 | 4.82E-07 | 1.53E-05 |
| mfng | 1857 | -4.55618 | 5.889677 | 6.98E-07 | 2.14E-05 |
| anxa2a | 1639 | -4.53833 | 4.161123 | 8.92E-06 | 0.000193 |
| kctd12.2 | 1479 | -4.53759 | 6.042336 | 7.00E-13 | 1.95E-10 |
| cfp | 5130 | -4.5368 | 5.4558 | 7.62E-11 | 8.85E-09 |
| anxa5b | 1913 | -4.52723 | 3.862974 | 6.52E-06 | 0.000148 |
| ccl34b.8 | 533 | -4.51707 | 5.784373 | 0.000129 | 0.001914 |
| mhc2a | 1590 | -4.51251 | 8.414729 | 5.33E-08 | 2.29E-06 |
| si:dkeyp-6 | 6843 | -4.51068 | 4.785306 | 1.68E-06 | 4.49E-05 |
| rin2 | 6162 | -4.4969 | 4.44012 | 1.08E-08 | 5.75E-07 |
| niban1b | 3364 | -4.49176 | 3.289794 | 7.88E-08 | 3.17E-06 |

| | | | | | |
|---|---|---|---|---|---|
| tmcc3 | 3507 | -4.47317 | 4.856199 | 3.67E-09 | 2.26E-07 |
| capn2b | 2454 | -4.4521 | 3.261582 | 4.14E-05 | 0.000723 |
| si:ch73-23 | 862 | -4.43896 | 4.420901 | 5.51E-08 | 2.34E-06 |
| ehd4 | 2052 | -4.43713 | 5.558764 | 1.46E-07 | 5.39E-06 |
| galnt6 | 3301 | -4.43627 | 3.622361 | 4.16E-06 | 9.90E-05 |
| dnajc5gb | 2669 | -4.43348 | 3.793567 | 5.93E-08 | 2.48E-06 |
| timd4 | 1424 | -4.42573 | 3.223874 | 1.31E-05 | 0.000269 |
| zgc:153654 | 2161 | -4.39584 | 6.492608 | 9.65E-08 | 3.74E-06 |
| olig1 | 1477 | -4.38947 | 4.94993 | 1.07E-08 | 5.74E-07 |
| gnsb | 1934 | -4.38784 | 3.294982 | 1.21E-06 | 3.35E-05 |
| ace2 | 2870 | -4.38385 | 3.37079 | 1.49E-05 | 0.0003 |
| glud1a | 2482 | -4.37718 | 6.423205 | 2.11E-12 | 4.64E-10 |
| jak3 | 3612 | -4.37386 | 3.247807 | 8.31E-07 | 2.45E-05 |
| ccr9a | 1856 | -4.36801 | 5.381074 | 8.79E-07 | 2.57E-05 |
| si:ch73-24 | 2336 | -4.36209 | 4.87447 | 2.25E-07 | 7.83E-06 |
| dnase1l1 | 1741 | -4.35644 | 4.600647 | 1.15E-11 | 2.02E-09 |
| tuba8l3 | 1556 | -4.35176 | 4.692818 | 8.00E-08 | 3.21E-06 |
| man2a1 | 4037 | -4.34766 | 3.92296 | 9.03E-07 | 2.60E-05 |
| rnaseka | 1000 | -4.3441 | 4.573851 | 9.48E-10 | 7.62E-08 |
| btk | 2634 | -4.30352 | 4.279735 | 4.64E-06 | 0.000109 |
| mhc1zja | 1388 | -4.28632 | 3.227249 | 2.18E-06 | 5.64E-05 |
| lgals9l3 | 2454 | -4.28251 | 7.326678 | 1.84E-09 | 1.29E-07 |
| tagapb | 2316 | -4.28188 | 6.45975 | 6.98E-08 | 2.83E-06 |
| pitpnc1b | 2094 | -4.28134 | 3.36557 | 2.28E-06 | 5.85E-05 |
| rhof | 1448 | -4.25959 | 4.226267 | 8.56E-05 | 0.001343 |
| unc13d | 4192 | -4.25092 | 4.649695 | 1.93E-06 | 5.07E-05 |
| prg4a | 1999 | -4.25092 | 5.443901 | 9.37E-12 | 1.70E-09 |
| si:dkey-26 | 1360 | -4.25086 | 4.822505 | 1.30E-09 | 9.89E-08 |
| bcam | 2220 | -4.2465 | 3.043259 | 7.20E-07 | 2.19E-05 |
| cldnk | 1729 | -4.24176 | 3.685421 | 2.67E-06 | 6.70E-05 |
| slc43a1a | 2967 | -4.24014 | 3.212915 | 9.30E-06 | 0.0002 |
| si:dkey-18 | 7434 | -4.23639 | 5.113268 | 1.58E-06 | 4.25E-05 |
| spi1b | 2376 | -4.22694 | 6.058692 | 3.02E-09 | 1.98E-07 |
| tmem176l | 4764 | -4.21548 | 3.610698 | 2.82E-05 | 0.00052 |
| mob1a | 1647 | -4.20275 | 6.432844 | 5.36E-11 | 6.61E-09 |
| cdk2 | 1734 | -4.1989 | 3.374312 | 7.34E-08 | 2.96E-06 |
| gpr17 | 1020 | -4.1837 | 4.243183 | 2.35E-05 | 0.000443 |
| arhgap31 | 4378 | -4.18077 | 3.226644 | 9.02E-07 | 2.60E-05 |
| cabz01093 | 5437 | -4.17787 | 3.042953 | 1.62E-06 | 4.34E-05 |
| mag | 2496 | -4.17651 | 4.633782 | 1.07E-05 | 0.000225 |
| nkx2.2a | 1791 | -4.1739 | 3.087585 | 9.24E-05 | 0.001425 |
| si:dkey-68 | 1192 | -4.17122 | 3.738474 | 1.10E-05 | 0.000232 |
| anxa3b | 1864 | -4.16644 | 6.912076 | 1.82E-08 | 9.17E-07 |
| cnn2 | 2452 | -4.16501 | 5.572361 | 5.76E-10 | 4.97E-08 |
| ncf4 | 2216 | -4.15616 | 3.765017 | 6.07E-08 | 2.51E-06 |
| rbck1 | 2809 | -4.14877 | 3.095654 | 1.93E-06 | 5.06E-05 |
| gnaia | 3744 | -4.14553 | 5.307481 | 3.44E-09 | 2.15E-07 |

| | | | | | |
|---|---|---|---|---|---|
| cyth4b | 1752 | -4.12273 | 3.904627 | 3.67E-06 | 8.89E-05 |
| mpz | 3017 | -4.11663 | 7.069336 | 4.53E-09 | 2.72E-07 |
| si:ch73-264 | 1747 | -4.10983 | 3.112336 | 3.58E-05 | 0.00064 |
| si:dkey-206 | 2209 | -4.10883 | 3.764472 | 2.09E-06 | 5.42E-05 |
| sult1st1 | 1614 | -4.10863 | 3.09415 | 6.90E-07 | 2.12E-05 |
| si:dkey-22 | 1731 | -4.09626 | 4.823491 | 1.18E-06 | 3.31E-05 |
| cmtm3 | 1705 | -4.08909 | 4.288679 | 1.93E-07 | 6.93E-06 |
| cybb | 3495 | -4.07785 | 6.481948 | 1.31E-10 | 1.33E-08 |
| cdc25b | 3191 | -4.07471 | 5.301512 | 8.39E-11 | 9.47E-09 |
| cxcl11.7 | 514 | -4.07463 | 3.529502 | 7.31E-06 | 0.000163 |
| hhipl1 | 3000 | -4.07313 | 3.367543 | 4.51E-08 | 1.98E-06 |
| sox10 | 3205 | -4.07031 | 3.594972 | 8.75E-06 | 0.000191 |
| malt3 | 2006 | -4.05967 | 3.871727 | 5.73E-06 | 0.000133 |
| swap70b | 2777 | -4.0561 | 5.542431 | 8.67E-09 | 4.79E-07 |
| plp1b | 2150 | -4.0516 | 7.063861 | 4.21E-07 | 1.36E-05 |
| cdca8 | 1916 | -4.04963 | 3.09761 | 4.93E-05 | 0.000838 |
| sh3bp1 | 2819 | -4.04573 | 5.365886 | 7.57E-06 | 0.000168 |
| rgs13 | 1279 | -4.04065 | 5.09582 | 1.35E-07 | 5.04E-06 |
| cdc14ab | 4587 | -4.0341 | 3.353984 | 9.36E-06 | 0.000201 |
| si:ch73-33 | 1369 | -4.0291 | 3.645312 | 6.02E-06 | 0.000138 |
| serinc2 | 1963 | -4.0241 | 5.65218 | 2.78E-14 | 1.69E-11 |
| srgn | 1961 | -3.99485 | 7.406068 | 4.19E-09 | 2.57E-07 |
| lgals2a | 883 | -3.98491 | 8.299424 | 7.19E-17 | 1.98E-13 |
| si:ch211-1 | 3041 | -3.95922 | 6.385952 | 7.02E-06 | 0.000158 |
| tgfbi | 3037 | -3.94993 | 3.877888 | 0.000218 | 0.002973 |
| etv4 | 1974 | -3.93551 | 5.756378 | 4.21E-09 | 2.57E-07 |
| myo9b | 7892 | -3.93452 | 4.399617 | 5.66E-08 | 2.38E-06 |
| zgc:64051 | 1448 | -3.9329 | 7.547311 | 1.22E-05 | 0.000253 |
| mhc2dab | 1428 | -3.92296 | 4.947086 | 0.003762 | 0.030282 |
| si:dkey-18 | 851 | -3.90794 | 3.223749 | 3.82E-06 | 9.19E-05 |
| olig2 | 1684 | -3.9044 | 5.118098 | 1.97E-07 | 7.03E-06 |
| timp4.3 | 912 | -3.89369 | 5.457788 | 1.56E-08 | 7.99E-07 |
| si:dkeyp-1 | 1676 | -3.88993 | 5.978579 | 2.86E-06 | 7.17E-05 |
| s100a10b | 872 | -3.88792 | 6.075417 | 7.34E-07 | 2.23E-05 |
| arhgap12a | 3954 | -3.88379 | 3.574402 | 3.99E-08 | 1.80E-06 |
| npc2 | 1236 | -3.88183 | 7.490699 | 3.01E-15 | 3.10E-12 |
| itpka | 3108 | -3.86342 | 3.747536 | 5.37E-06 | 0.000125 |
| robo4 | 3715 | -3.85036 | 4.313533 | 8.34E-06 | 0.000183 |
| grap2b | 2396 | -3.847 | 5.56503 | 2.54E-07 | 8.65E-06 |
| si:dkey-17 | 12090 | -3.84563 | 4.325381 | 9.32E-08 | 3.63E-06 |
| ctsa | 748 | -3.84453 | 4.381696 | 3.93E-10 | 3.56E-08 |
| malt2 | 3148 | -3.8371 | 4.147979 | 0.000124 | 0.001843 |
| wdfy4 | 2886 | -3.8299 | 3.647256 | 5.04E-06 | 0.000118 |
| klf12a | 2479 | -3.82843 | 4.124118 | 4.01E-08 | 1.80E-06 |
| ehbp1l1b | 9265 | -3.82825 | 5.444675 | 3.19E-08 | 1.50E-06 |
| acsl4b | 3641 | -3.82697 | 3.036008 | 6.07E-06 | 0.000139 |
| aspm | 10507 | -3.80665 | 4.037961 | 1.01E-05 | 0.000214 |

| | | | | | |
|---|---|---|---|---|---|
| si:ch211-1( | 4277 | -3.78735 | 3.649657 | 3.38E-09 | 2.12E-07 |
| reep3a | 3865 | -3.77709 | 3.21264 | 7.27E-06 | 0.000163 |
| lrrfip1a | 6555 | -3.76733 | 4.923809 | 1.78E-07 | 6.52E-06 |
| dlgap5 | 3267 | -3.76275 | 3.258758 | 5.23E-05 | 0.000879 |
| ninj2 | 1002 | -3.76241 | 4.063325 | 2.64E-06 | 6.64E-05 |
| sypl2b | 1966 | -3.75626 | 5.252935 | 1.11E-05 | 0.000233 |
| sema5a | 4513 | -3.74902 | 6.670327 | 8.86E-11 | 9.73E-09 |
| si:ch73-86( | 1054 | -3.74737 | 3.701795 | 9.75E-06 | 0.000209 |
| foxj2 | 1598 | -3.73228 | 3.888745 | 4.87E-08 | 2.12E-06 |
| slc7a10b | 2242 | -3.72931 | 3.344854 | 6.29E-06 | 0.000143 |
| ctss2.1 | 1227 | -3.71608 | 7.510285 | 2.78E-08 | 1.33E-06 |
| aplnra | 1708 | -3.7147 | 5.50186 | 4.02E-07 | 1.32E-05 |
| si:cabz010 | 1023 | -3.70181 | 5.051546 | 4.70E-05 | 0.000809 |
| mki67 | 8187 | -3.68279 | 5.568542 | 1.12E-06 | 3.17E-05 |
| si:zfos-464 | 2116 | -3.68003 | 3.9506 | 0.000122 | 0.001816 |
| pygb | 2860 | -3.67725 | 3.484544 | 1.37E-05 | 0.000281 |
| zgc:10158 | 4188 | -3.67498 | 3.506911 | 2.51E-05 | 0.000471 |
| si:ch211-1 | 2249 | -3.65166 | 3.066744 | 9.27E-05 | 0.001428 |
| mapre1a | 1699 | -3.6467 | 6.701483 | 2.32E-15 | 3.10E-12 |
| si:dkey-76 | 2932 | -3.64382 | 3.41056 | 2.02E-05 | 0.00039 |
| elk3 | 2275 | -3.63811 | 4.58869 | 9.12E-08 | 3.57E-06 |
| spata2l | 2307 | -3.63613 | 3.077659 | 3.39E-05 | 0.000614 |
| snx10b | 2241 | -3.63464 | 3.521565 | 2.45E-06 | 6.20E-05 |
| zgc:11059 | 2333 | -3.62196 | 4.846818 | 1.04E-06 | 2.98E-05 |
| cgas | 810 | -3.61538 | 3.287647 | 0.000183 | 0.002558 |
| ctss2.2 | 1267 | -3.61405 | 6.579532 | 4.67E-07 | 1.49E-05 |
| cyp3c1 | 2217 | -3.61023 | 4.213902 | 1.86E-05 | 0.000364 |
| zfp36l1a | 1899 | -3.60736 | 6.941516 | 6.90E-13 | 1.95E-10 |
| syngr2a | 3500 | -3.6028 | 4.527218 | 1.68E-06 | 4.49E-05 |
| fzd2 | 2440 | -3.60191 | 5.849651 | 1.33E-09 | 1.01E-07 |
| epdl1 | 1983 | -3.59239 | 3.482754 | 2.77E-05 | 0.000513 |
| npsn | 1553 | -3.5739 | 3.676872 | 0.003639 | 0.029586 |
| il7r | 1617 | -3.57014 | 5.529228 | 0.001354 | 0.013509 |
| si:ch73-23 | 3659 | -3.56836 | 4.242986 | 1.11E-06 | 3.14E-05 |
| tcea3 | 2108 | -3.55634 | 4.129173 | 3.97E-06 | 9.52E-05 |
| asah1b | 1726 | -3.55355 | 6.565242 | 3.05E-12 | 6.44E-10 |
| rab44 | 6889 | -3.55272 | 4.773442 | 7.30E-10 | 6.08E-08 |
| jpt2 | 2146 | -3.54592 | 6.259813 | 1.44E-10 | 1.43E-08 |
| fam49ba | 2280 | -3.54554 | 5.335237 | 3.20E-08 | 1.50E-06 |
| ctbs | 1568 | -3.52992 | 3.573678 | 8.31E-06 | 0.000182 |
| tpp1 | 2198 | -3.52027 | 4.474223 | 1.25E-10 | 1.28E-08 |
| icn | 408 | -3.50698 | 4.94438 | 9.60E-06 | 0.000206 |
| cd59 | 1144 | -3.48787 | 7.798522 | 1.47E-05 | 0.000296 |
| rxraa | 1699 | -3.47169 | 4.362481 | 4.11E-08 | 1.85E-06 |
| bdh2 | 1719 | -3.44745 | 3.138041 | 2.31E-06 | 5.90E-05 |
| arhgef3l | 2286 | -3.44741 | 4.991602 | 2.86E-07 | 9.64E-06 |
| rilpl2 | 2009 | -3.44375 | 3.145831 | 0.000294 | 0.003832 |

| | | | | | |
|---|---|---|---|---|---|
| b3gnt3.4 | 1427 | -3.41535 | 3.545608 | 1.06E-05 | 0.000224 |
| si:ch73-158 | 2343 | -3.41057 | 4.978349 | 2.07E-06 | 5.37E-05 |
| draxin | 8513 | -3.41039 | 4.530343 | 3.73E-06 | 8.99E-05 |
| mov10b.2 | 3131 | -3.39212 | 4.92879 | 2.29E-06 | 5.88E-05 |
| eif4ebp3l | 1181 | -3.39051 | 3.353764 | 6.01E-06 | 0.000138 |
| sh2b3 | 1791 | -3.38558 | 3.651054 | 0.0002 | 0.002749 |
| tor4aa | 2819 | -3.36987 | 3.607388 | 0.000586 | 0.006828 |
| dennd2c | 3685 | -3.36923 | 3.394374 | 1.80E-05 | 0.000353 |
| arhgap15 | 1680 | -3.36856 | 4.054182 | 1.95E-09 | 1.35E-07 |
| paox1 | 2182 | -3.34843 | 3.470282 | 0.000155 | 0.002228 |
| mmp14b | 4473 | -3.34366 | 4.577592 | 1.30E-07 | 4.86E-06 |
| si:ch1073-3 | 1331 | -3.33492 | 4.230913 | 9.97E-06 | 0.000212 |
| cib1 | 1353 | -3.33478 | 4.834651 | 1.56E-06 | 4.21E-05 |
| tpx2 | 2748 | -3.319 | 3.176199 | 0.001733 | 0.016478 |
| si:ch1073-9 | 1924 | -3.3187 | 3.040662 | 1.11E-05 | 0.000232 |
| si:ch211-10 | 1005 | -3.31672 | 4.503534 | 0.004108 | 0.032401 |
| dock8 | 7072 | -3.30149 | 5.975038 | 4.79E-07 | 1.53E-05 |
| myrf | 5038 | -3.30071 | 3.166781 | 0.001581 | 0.015356 |
| peli2 | 2448 | -3.29891 | 3.425943 | 0.000579 | 0.006779 |
| pacc1 | 2017 | -3.29779 | 3.500781 | 0.0004 | 0.004946 |
| rgcc | 1661 | -3.29604 | 3.916799 | 1.89E-07 | 6.82E-06 |
| glipr1a | 828 | -3.29207 | 3.445232 | 1.35E-05 | 0.000278 |
| ugt8 | 5298 | -3.28093 | 4.009998 | 0.000653 | 0.007452 |
| smc2 | 4073 | -3.27565 | 3.847737 | 0.000267 | 0.003552 |
| p2ry10 | 1445 | -3.27489 | 3.024895 | 0.002565 | 0.022465 |
| rbm47 | 7222 | -3.27403 | 5.124896 | 3.35E-05 | 0.000609 |
| gzm3 | 802 | -3.26733 | 3.878358 | 0.003788 | 0.030405 |
| fa2h | 5711 | -3.26491 | 3.496754 | 0.00013 | 0.001922 |
| Sep-12 | 4427 | -3.26434 | 6.487622 | 5.21E-10 | 4.59E-08 |
| parvg | 1492 | -3.25983 | 5.40895 | 6.58E-07 | 2.03E-05 |
| prex1 | 7934 | -3.25416 | 5.8839 | 1.05E-06 | 2.99E-05 |
| ada2b | 2228 | -3.24834 | 3.00663 | 1.04E-06 | 2.97E-05 |
| ptbp1a | 4314 | -3.24445 | 4.976362 | 1.12E-05 | 0.000234 |
| cdca7a | 1741 | -3.21906 | 3.484806 | 0.000874 | 0.009497 |
| btr09 | 2511 | -3.19686 | 3.975973 | 1.81E-06 | 4.79E-05 |
| fhod1 | 5712 | -3.18398 | 3.245273 | 8.91E-05 | 0.001386 |
| p2rx7 | 1877 | -3.18015 | 5.087771 | 1.86E-07 | 6.75E-06 |
| cxcr4b | 1674 | -3.173 | 7.523554 | 3.13E-06 | 7.71E-05 |
| gab1 | 4453 | -3.16926 | 5.109654 | 5.30E-07 | 1.68E-05 |
| lpar5b | 1301 | -3.14392 | 3.574826 | 0.001611 | 0.015565 |
| litaf | 2374 | -3.14284 | 7.309642 | 1.94E-12 | 4.39E-10 |
| c7b | 2612 | -3.1418 | 5.586824 | 0.000144 | 0.002099 |
| txnipa | 2753 | -3.13304 | 7.369882 | 6.52E-11 | 7.67E-09 |
| si:dkey-237 | 5656 | -3.13301 | 4.550869 | 1.63E-10 | 1.59E-08 |
| sox9a | 1784 | -3.13135 | 3.823582 | 5.80E-06 | 0.000134 |
| tmem63a | 2958 | -3.12369 | 3.030938 | 0.003335 | 0.02764 |
| sash3 | 1558 | -3.12056 | 6.85863 | 3.13E-07 | 1.04E-05 |

| | | | | | |
|---|---|---|---|---|---|
| slc38a5a | 3639 | -3.11652 | 3.373367 | 0.000891 | 0.009641 |
| si:dkey-26 | 1250 | -3.10145 | 6.511819 | 4.01E-11 | 5.33E-09 |
| frmd4ba | 4516 | -3.0986 | 3.837903 | 1.71E-05 | 0.000337 |
| cspg5b | 3332 | -3.09541 | 3.150778 | 9.97E-05 | 0.001523 |
| cxcl32b.1 | 798 | -3.08104 | 4.926649 | 0.004967 | 0.037682 |
| ptprc | 3997 | -3.05266 | 6.820259 | 5.66E-09 | 3.35E-07 |
| bin2b | 2438 | -3.04751 | 5.528214 | 1.71E-05 | 0.000337 |
| zgc:15315 | 2503 | -3.03525 | 3.0317 | 0.002222 | 0.01995 |
| iqgap1 | 7680 | -3.02729 | 5.642788 | 2.60E-08 | 1.27E-06 |
| phf19 | 4073 | -3.02402 | 3.738168 | 0.000383 | 0.00477 |
| alox12 | 3595 | -3.00358 | 4.26455 | 5.94E-10 | 5.05E-08 |
| itpr2 | 5841 | -3.00032 | 5.340626 | 1.83E-08 | 9.20E-07 |
| ociad2 | 1483 | 3.00855 | 3.956523 | 2.14E-05 | 0.000408 |
| scube1 | 4038 | 3.030827 | 3.563031 | 0.006195 | 0.04448 |
| kitb | 2903 | 3.142948 | 3.517037 | 0.00053 | 0.006273 |
| fmnl3 | 5605 | 3.165834 | 4.077171 | 0.000187 | 0.00261 |
| tuft1a | 3237 | 3.284301 | 4.991177 | 9.14E-05 | 0.001415 |
| si:ch211-2 | 1424 | 3.743359 | 3.184179 | 0.000857 | 0.009347 |
| atf3 | 2701 | 3.830712 | 6.557653 | 1.98E-09 | 1.36E-07 |
| dynll1 | 1000 | 3.854694 | 11.04169 | 2.73E-15 | 3.10E-12 |
| scgn | 1605 | 3.863703 | 3.583968 | 0.001575 | 0.015309 |
| cd83 | 888 | 3.989025 | 6.171617 | 1.79E-06 | 4.76E-05 |
| si:ch73-33 | 1499 | 4.187793 | 6.28041 | 1.80E-05 | 0.000353 |
| homeza | 2117 | 4.220133 | 3.78839 | 8.97E-05 | 0.001392 |
| si:ch211-1 | 1057 | 4.306881 | 6.052418 | 7.30E-06 | 0.000163 |
| si:dkey-31 | 777 | 4.348411 | 3.703514 | 1.55E-07 | 5.73E-06 |
| hunk | 1830 | 4.519412 | 4.768265 | 6.87E-07 | 2.11E-05 |
| zgc:19410 | 777 | 4.615589 | 6.196546 | 4.34E-07 | 1.40E-05 |
| si:dkey-31 | 766 | 4.62671 | 4.273604 | 2.44E-07 | 8.38E-06 |
| si:ch211-2 | 1071 | 4.764516 | 4.677218 | 4.56E-05 | 0.000786 |
| insm1a | 1190 | 4.765792 | 3.080093 | 4.11E-07 | 1.34E-05 |
| traf3ip2l | 1765 | 4.923479 | 4.36792 | 6.87E-06 | 0.000155 |
| ifnphi1 | 823 | 5.408527 | 5.285983 | 3.87E-08 | 1.76E-06 |
| cxcl18b | 1101 | 6.878814 | 7.159051 | 1.76E-09 | 1.26E-07 |
| GFP1 | 720 | 8.134915 | 10.89424 | 5.12E-13 | 1.56E-10 |
| ifnphi2 | 546 | 9.144219 | 3.479161 | 3.78E-08 | 1.73E-06 |

**Table 3**

| GO term | Cluster frequency | Genome frequency | Corr. P-value | FDR | FALSE Pos. | Genes annotated to the term |
|---|---|---|---|---|---|---|
| immune system process | 104 of 529 genes, 19.7% | 1377 of 25457 genes, 5.4% | 6.72E-28 | 0.00% | 0 | cgas, ccl34b.1, c1qa, scube1, cd4-1, cxcl32b.1, ano6, cxcl11.5, ptk2ba, tnfsf10l, klhl6, rac2, cfp, ctsl.1, si:dkey-1h24.6, hlx1, blk, si:ch211-66k16.27, mhc2a, sh2b3, rgs18, slc7a7, fybb, tlr3, notch1a, ikzf1, c1qc, ccr9a, prg4a, unc93b1, p2ry12, igf2b, hck, mhc1zja, skap2, dok2, inpp5d, itgb2, cd74b, mfap4, gpr183a, ptpn6, zgc:123107, ifi30, cmklr1, ada2b, tlr8b, gpr65, cxcr3.2, ifnphi1, ctss2.1, caspb, jak3, il2rga, si:ch73-226l13.2, c7b, il1fma, pycard, zgc:153654, cyba, ifnphi2, spi1b, ccr12a, c1qb, ccl34b.8, tnfsf10, kita, ctss2.2, rhogb, wasb, myd88, cxcl18b, cdca7a, il7r, f11r.1, fam49ba, arpc1b spi1a, traf3ip2l, bdh2, cd74a, ephx2, csf1rb, cfbl, caspa, irf5, ctsk, rhoga, sla1a, lgals9l1, tnfaip8l2a, tlr21, cxcr4b, kitb, si:ch73-158p21.3, lgals9l3, cd83, adam8a, csf1ra, zgc:173915, lgals3b, mhc2dab, p2rx7, anxa1a |
| immune response | 61 of 529 genes, 11.5% | 712 of 25457 genes, 2.8% | 9.10E-18 | 0.00% | 0 | cgas, ccr12a, ccl34b.1, c1qb, c1qa, ccl34b.8, tnfsf10, cxcl32b.1, cxcl11.5, ptk2ba, kita, tnfsf10l, klhl6, ctss2.2, cfp, ctsl.1, si:dkey-1h24.6, myd88, blk, si:ch211-66k16.27, cxcl18b, mhc2a, fybb, tlr3, c1qc, ccr9a, prg4a, unc93b1, hck, traf3ip2l, mhc1zja, cd74a, cd74b, mfap4, cfbl, zgc:123107, ptpn6, gpr183a, caspa, cmklr1, tlr8b, cxcr3.2, ctsk, ctss2.1, sla1a, tnfaip8l2a, tlr21, caspb, cxcr4b, kitb, si:ch73-158p21.3, si:ch73-226l13.2, cd83, c7b, zgc:173915, csf1ra, il1fma, mhc2dab, pycard, anxa1a, zgc:153654 |
| regulation of immune system process | 42 of 529 genes, 7.9% | 460 of 25457 genes, 1.8% | 1.69E-12 | 0.00% | 0 | spi1b, cgas, c1qb, c1qa, ptk2ba, kita, klhl6, rac2, rhogb, wasb, si:dkey-1h24.6, myd88, blk, cdca7a, f11r.1, fam49ba, fybb, tlr3, c1qc, unc93b1, spi1a, igf2b, inpp5d, cd74a, cd74b, csf1rb, mfap4, cfbl, tlr8b, gpr65, ifnphi1, rhoga, lgals9l1, tlr21, cxcr4b, kitb, lgals9l3, c7b, csf1ra, zgc:173915, adam8a, anxa1a |
| cell migration | 52 of 529 genes, 9.8% | 818 of 25457 genes, 3.2% | 1.55E-09 | 0.00% | 0 | ccr12a, ccl34b.1, ccl34b.8, apoc1, cxcl32b.1, ano6, cxcl11.5, ptk2ba, kita, rac2, insm1a, nkx2.2a, lpxn, rhogb, wasb, myd88, cxcl18b, sema5a, plxnc1, fam83ha, ccr9a, csrp1a, sema4aa, inpp5d, itgb2, rhof, cnn2, gpr183a, cmklr1, coro1a, robo4, rgs14a, sox10, cxcr3.2, fmnl3, rhoga, fzd2, arhgap4a, cxcr4b, kitb, aplnra, itgb7, adam8a, csf1ra, aplnrb, mmp14b, lgals3b, p2rx7, anxa1a, ngfrb, olig2, cyba |
| cell chemotaxis | 22 of 529 genes, 4.2% | 160 of 25457 genes, 0.6% | 4.24E-09 | 0.00% | 0 | ccr12a, ccl34b.1, ccl34b.8, cxcl32b.1, ano6, cxcl11.5, gpr183a, ptk2ba, rac2, cmklr1, wasb, myd88, cxcl18b, cxcr3.2, cxcr4b, ccr9a, csf1ra, lgals3b, p2rx7, anxa1a, inpp5d, cyba |
| defense response | 40 of 529 genes, 7.6% | 542 of 25457 genes, 2.1% | 8.14E-09 | 0.00% | 0 | cgas, ccl34b.1, ccl34b.8, cxcl32b.1, cxcl11.5, ptk2ba, rac2, cybb, myd88, blk, si:ch211-66k16.27, cxcl18b, ncf1, tlr3, cd59, unc93b1, p2ry12, hck, mfap4, ptpn6, caspa, mpeg1.1 npsn, irf5, tlr8b, cxcr3.2, ifnphi1, sla1a, tnfaip8l2a, tlr21, caspb, cxcr4b, si:ch73-226l13.2, il1fma, adam8a, csf1ra, zgc:173915, pycard, anxa1a, ifnphi2 |
| cell motility | 53 of 529 genes, 10.0% | 888 of 25457 genes, 3.5% | 1.03E-08 | 0.00% | 0 | ccr12a, ccl34b.1, ccl34b.8, apoc1, cxcl32b.1, ano6, cxcl11.5, ptk2ba, kita, rac2, insm1a, nkx2.2a, lpxn, rhogb, wasb, myd88, cxcl18b, sema5a, plxnc1, fam83ha, ccr9a, csrp1a, sema4aa, inpp5d, itgb2, rhof, cnn2, gpr183a, cmklr1, coro1a, robo4, rgs14a, sox10, cxcr3.2, fmnl3, rhoga, fzd2, anxa5b, arhgap4a, cxcr4b, kitb, aplnra, itgb7, adam8a, csf1ra, aplnrb, mmp14b, lgals3b, p2rx7, anxa1a, ngfrb, olig2, cyba |
| localization of cell | 53 of 529 genes, 10.0% | 888 of 25457 genes, 3.5% | 1.03E-08 | 0.00% | 0 | ccr12a, ccl34b.1, ccl34b.8, apoc1, cxcl32b.1, ano6, cxcl11.5, ptk2ba, kita, rac2, insm1a, nkx2.2a, lpxn, rhogb, wasb, myd88, cxcl18b, sema5a, plxnc1, fam83ha, ccr9a, csrp1a, sema4aa, inpp5d, itgb2, rhof, cnn2, gpr183a, cmklr1, coro1a, robo4, rgs14a, sox10, cxcr3.2, fmnl3, rhoga, fzd2, anxa5b, arhgap4a, cxcr4b, kitb, aplnra, itgb7, adam8a, csf1ra, aplnrb, mmp14b, lgals3b, p2rx7, anxa1a, ngfrb, olig2, cyba |
| leukocyte chemotaxis | 19 of 529 genes, 3.6% | 121 of 25457 genes, 0.5% | 1.21E-08 | 0.00% | 0 | ccl34b.1, ccl34b.8, cxcl32b.1, ano6, cxcl11.5, gpr183a, ptk2ba, rac2, wasb, myd88, cxcl18b, cxcr3.2, cxcr4b, csf1ra, lgals3b, p2rx7, inpp5d, anxa1a, cyba |
| leukocyte migration | 22 of 529 genes, 4.2% | 169 of 25457 genes, 0.7% | 1.29E-08 | 0.00% | 0 | ccl34b.1, ccl34b.8, cxcl32b.1, ano6, cxcl11.5, gpr183a, ptk2ba, rac2, rhogb, wasb, myd88, cxcl18b, cxcr3.2, rhoga, cxcr4b, adam8a, csf1ra, lgals3b, p2rx7, anxa1a, inpp5d, cyba |
| cell activation | 25 of 529 genes, 4.7% | 253 of 25457 genes, 1.0% | 2.20E-07 | 0.00% | 0 | cd74b, cd4-1, gpr183a, kita, si:dkey-1h24.6, myd88, blk, il7r, cxcr3.2, ptbp1a, fam49ba, im:7154036, lgals9l1, arpc1b, ikzf1, kitb, lgals9l3, jak3, p2ry12, igf2b, cd83, il2rga, anxa1a, skap2, cd74a |

| | | | | | | |
|---|---|---|---|---|---|---|
| movement of cell or subcellular component | 64 of 529 genes, 12.1% | 1303 of 25457 genes, 5.1% | 2.56E-07 | 0.00% | 0 | ccl34b.1, cxcl32b.1, ano6, cxcl11.5, ptk2ba, rac2, lpxn, wipf1b, ccr9a, csrp1a, inpp5d, sema4aa, itgb2, myo1g, cnn2, gpr183a, kif11, cmklr1, kif23, cxcr3.2, fzd2, aplnra, aplnrb, mmp14b, ngfrb, olig2, cyba, ccr12a, cyfip1, apoc1, ccl34b.8, kita, insm1a, nkx2.2a, draxin, wasb, rhogb, myd88, cxcl18b, wasa, sema5a, plxnc1, fam83ha, myo9b, wipf1a, rhof, coro1a, mcamb, rgs14a, robo4, sox10, fmnl3, rhoga, arhgap4a, anxa5b, myo1f, kitb, cxcr4b, itgb7, csf1ra, adam8a, lgals3b, anxa1a, p2rx7 |
| response to stimulus | 205 of 529 genes, 38.8% | 6725 of 25457 genes, 26.4% | 4.13E-07 | 0.00% | 0 | rab44, cgas, ccl34b.1, c1qa, scube1, cd4-1, cyth4b, ano6, cxcl11.5, atf3, entpd1, rac2, si:dkey-32n7.4, cfp, si:dkey-1h24.6, dock8, cybb, si:ch211-66k16.27, edaradd, mhc2a, sh2b3, rasgrp4, arhgap15, fybb, tlr3, notch1a, cd59, blnk, neil3, mhc1zja, csrp1a, hunk, sema4aa, lpar5b, si:ch211-246e12.3, rxraa, tagapb, cdk2, p2ry10, lpar5a, cnn2, f13a1b, mpeg1.1, gpr183a, ptpn6, zgc:123107, npsn, cmklr1, tlr8b, gpr65, cxcr3.2, apbb1ip, ifnphi1, ninj2, ctss2.1, im:7154036, caspb, esco2, gpr17, aplnra, sesn2, si:ch73-226l13.2, plcg2, zgc:153654, rgl1, lgals2a, ttk, itga4, bnip4, itgae.2, c1qb, ccl34b.8, tnfsf10, tradd, kita, insm1a, nkx2.2a, ostf1, draxin, myd88, gpr18, il7r, plxnc1, pak2a, cd74a, peli2, rbck1, cfbl, rgn, caspa, crip1, socs3a, irf5, fcer1g, lcp2a, ctsk, il10ra, nfe2l1a, sla1a, arhgap12a, arhgap4a, rin3, tnfaip8l2a, cxcr4b, timp4.3, kitb, si:ch73-158p21.3, mtmr8, itgb7, p2rx7, anxa1a, tuft1a, pik3r5, cxcl32b.1, btk, ptk2ba, adcy7, klhl6, tnfsf10l, lpxn, ltb4r, ctsl.1, blk, ncf1, si:dkey-188i13.6, rgs18, c1qc, ccr9a, prg4a, p2ry12, unc93b1, hck, igf2b, prex1, inpp5d, itgb2, prkcq, cd74b, mfap4, ccnd1, si:dkey-265e15.2, sh3bp2, iqgap1, ptbp1a, f13a1a.1, fzd2, arhgef3l, si:dkey-188i13.8, slc7a10b, jak3, si:ch1073-90m23.1, il2rga, c7b, il1fma, aplnrb, pycard, si:ch211-191c10.1, lifrb, ngfrb, ifnphi2, cyba, ccr12a, cyfip1, arhgap31, si:dkey-172h23.2, ctss2.2, rbp4, wasb, rhogb, ppp1r15b, sult1st1, cxcl18b, rin2, si:ch211-241f5.3, arhgap17b, sema5a, prkacba, bida, fam83ha, myo9b, traf3ip2l, mfng, cdk1, tgfbi, rhof, csf1rb, rmi2, arhgap27, robo4, mcamb, rgs14a, rhoga, slc38a5a, tlr21, ptprja, gmip, nfe2l2b, cd83, adam8a, csf1ra, zgc:173915, si:dkey-204f11.64, lgals3b, mhc2dab, gnaia |
| leukocyte activation | 23 of 529 genes, 4.3% | 228 of 25457 genes, 0.9% | 8.04E-07 | 0.00% | 0 | cd74b, cd4-1, gpr183a, kita, si:dkey-1h24.6, myd88, blk, il7r, cxcr3.2, fam49ba, lgals9l1, arpc1b, ikzf1, kitb, lgals9l3, jak3, p2ry12, igf2b, cd83, il2rga, anxa1a, skap2, cd74a |
| immune effector process | 22 of 529 genes, 4.2% | 211 of 25457 genes, 0.8% | 1.02E-06 | 0.00% | 0 | cd74b, cgas, mfap4, c1qb, c1qa, cfbl, gpr183a, rac2, irf5, myd88, tlr8b, blk, cxcr3.2, ifnphi1, tlr3, c1qc, cd83, c7b, zgc:173915, anxa1a, cd74a, ifnphi2 |
| myeloid leukocyte migration | 18 of 529 genes, 3.4% | 144 of 25457 genes, 0.6% | 2.01E-06 | 0.00% | 0 | ccl34b.1, ccl34b.8, cxcl32b.1, cxcl11.5, rac2, rhogb, wasb, myd88, cxcl18b, cxcr3.2, rhoga, cxcr4b, csf1ra, lgals3b, inpp5d, anxa1a, p2rx7, cyba |
| positive regulation of biological process | 102 of 529 genes, 19.3% | 2709 of 25457 genes, 10.6% | 2.93E-06 | 0.00% | 0 | cgas, ccl34b.1, c1qa, pik3r5, cd4-1, cxcl32b.1, ano6, tnfsf10l, klhl6, rac2, si:dkey-1h24.6, cdc14ab, blk, tpx2, fybb, tlr3, myrf, notch1a, c1qc, unc93b1, igf2b, sema4aa, lpar5b, rxraa, cd74b, cdc25b, cdk2, mfap4, p2ry10, foxj2, lpar5a, scgn, gpr183a, ccnd1, si:dkey-206d17.12, trim33l, tlr8b, gpr65, ptbp1a, si:ch211-113a14.18, arhgef3l, caspb, etv4, esco2, gpr17, aplnra, sesn2, c7b, aplnrb, wasf2, pycard, olig2, lgals2a, spi1b, bnip4, c1qb, ccl34b.8, tradd, kita, si:dkey-172h23.2, nkx2.2a, wasb, ppp1r15b, gpr18, myd88, wasa, il7r, sema5a, bida, fam49ba, plxnc1, arpc1b, fam83ha, pak2a, traf3ip2l, ptprc, cd74a, rbck1, csf1rb, cfbl, casp22, caspa, robo4, sox10, nfe2l1a, pparg, sox9a, lgals9l1, pfn1, swap70b, tlr21, cxcr4b, kitb, lgals9l3, nfe2l2b, adam8a, csf1ra, zgc:173915, lgals3b, apoeb, anxa1a, top2a |
| locomotion | 55 of 529 genes, 10.4% | 1108 of 25457 genes, 4.4% | 3.85E-06 | 0.00% | 0 | cyfip1, ccr12a, ccl34b.1, ccl34b.8, apoc1, cxcl32b.1, ano6, cxcl11.5, ptk2ba, kita, rac2, insm1a, nkx2.2a, lpxn, draxin, rhogb, wasb, myd88, cxcl18b, sema5a, plxnc1, fam83ha, ccr9a, csrp1a, sema4aa, inpp5d, itgb2, rhof, cnn2, gpr183a, cmklr1, coro1a, robo4, rgs14a, sox10, cxcr3.2, fmnl3, rhoga, fzd2, anxa5b, arhgap4a, cxcr4b, kitb, aplnra, itgb7, adam8a, csf1ra, aplnrb, mmp14b, lgals3b, p2rx7, anxa1a, ngfrb, olig2, cyba |
| lymphocyte activation | 20 of 529 genes, 3.8% | 199 of 25457 genes, 0.8% | 1.16E-05 | 0.00% | 0 | cd74b, cd4-1, gpr183a, kita, si:dkey-1h24.6, blk, il7r, fam49ba, lgals9l1, arpc1b, ikzf1, kitb, lgals9l3, jak3, cd83, il2rga, igf2b, anxa1a, skap2, cd74a |
| positive regulation of response to stimulus | 46 of 529 genes, 8.7% | 871 of 25457 genes, 3.4% | 1.32E-05 | 0.00% | 0 | lgals2a, cgas, ccl34b.1, c1qb, c1qa, ccl34b.8, pik3r5, cd4-1, cxcl32b.1, tradd, kita, si:dkey-172h23.2, tnfsf10l, klhl6, si:dkey-1h24.6, myd88, gpr18, blk, il7r, bida, fybb, tlr3, c1qc, unc93b1, igf2b, traf3ip2l, lpar5b, cd74a, cd74b, rbck1, mfap4, cfbl, p2ry10, gpr183a, robo4, tlr8b, gpr65, arhgef3l, tlr21, cxcr4b, kitb, gpr17, c7b, csf1ra, zgc:173915, anxa1a |
| leukocyte differentiation | 16 of 529 genes, 3.0% | 129 of 25457 genes, 0.5% | 1.87E-05 | 0.00% | 0 | spi1b, csf1rb, gpr183a, kita, ada2b, blk, il7r, slc7a7, arpc1b, ikzf1, kitb, spi1a, jak3, il2rga, csf1ra, anxa1a |

| | | | | | | |
|---|---|---|---|---|---|---|
| granulocyte migration | 16 of 529 genes, 3.0% | 129 of 25457 genes, 0.5% | 1.87E-05 | 0.00% | 0 | ccl34b.1, ccl34b.8, cxcl32b.1, cxcl11.5, rac2, rhogb, wasb, myd88, cxcl18b, rhoga, cxcr4b csf1ra, lgals3b, inpp5d, anxa1a, cyba |
| macrophage chemotaxis | 7 of 529 genes, 1.3% | 16 of 25457 genes, 0.1% | 2.46E-05 | 0.00% | 0 | rac2, csf1ra, lgals3b, wasb, p2rx7, cyba, cxcr3.2 |
| positive regulation of immune system process | 25 of 529 genes, 4.7% | 318 of 25457 genes, 1.2% | 2.47E-05 | 0.00% | 0 | cd74b, cgas, mfap4, c1qb, c1qa, cfbl, klhl6, rac2, si:dkey-1h24.6, myd88, blk, tlr8b, fam49ba, fybb, tlr3, tlr21, c1qc, unc93b1, igf2b, c7b, zgc:173915, csf1ra, adam8a, anxa1a, cd74a |
| T cell activation | 15 of 529 genes, 2.8% | 115 of 25457 genes, 0.5% | 2.68E-05 | 0.00% | 0 | cd74b, fam49ba, arpc1b, lgals9l1, cd4-1, ikzf1, gpr183a, lgals9l3, jak3, igf2b, cd83, si:dkey-1h24.6, anxa1a, il7r, cd74a |
| chemotaxis | 31 of 529 genes, 5.9% | 473 of 25457 genes, 1.9% | 3.49E-05 | 0.00% | 0 | cyfip1, ccr12a, ccl34b.1, ccl34b.8, cxcl32b.1, ano6, cxcl11.5, gpr183a, ptk2ba, rac2, cmklr1, nkx2.2a, draxin, robo4, rhogb, wasb, myd88, cxcl18b, cxcr3.2, sema5a, rhoga, plxnc1, cxcr4b, ccr9a, csf1ra, lgals3b, p2rx7, anxa1a, inpp5d, sema4aa, cyba |
| innate immune response | 23 of 529 genes, 4.3% | 282 of 25457 genes, 1.1% | 4.74E-05 | 0.00% | 0 | cgas, mfap4, ccl34b.1, ccl34b.8, cxcl32b.1, caspa, ptpn6, ptk2ba, myd88, blk, tlr8b, si:ch211-66k16.27, cxcr3.2, sla1a, tlr3, tnfaip8l2a, tlr21, caspb, unc93b1, hck, zgc:173915, csf1ra, pycard |
| macrophage migration | 7 of 529 genes, 1.3% | 18 of 25457 genes, 0.1% | 6.62E-05 | 0.00% | 0 | rac2, csf1ra, lgals3b, wasb, p2rx7, cyba, cxcr3.2 |
| taxis | 31 of 529 genes, 5.9% | 490 of 25457 genes, 1.9% | 7.80E-05 | 0.00% | 0 | cyfip1, ccr12a, ccl34b.1, ccl34b.8, cxcl32b.1, ano6, cxcl11.5, gpr183a, ptk2ba, rac2, cmklr1, nkx2.2a, draxin, robo4, rhogb, wasb, myd88, cxcl18b, cxcr3.2, sema5a, rhoga, plxnc1, cxcr4b, ccr9a, csf1ra, lgals3b, p2rx7, anxa1a, inpp5d, sema4aa, cyba |
| regulation of cell motility | 22 of 529 genes, 4.2% | 273 of 25457 genes, 1.1% | 0.00011 | 0.00% | 0 | cnn2, gpr183a, ptk2ba, kita, rac2, robo4, rhogb, wasb, sema5a, rhoga, plxnc1, arhgap4a, anxa5b, fam83ha, cxcr4b, kitb, adam8a, csf1ra, anxa1a, inpp5d, sema4aa, ngfrb |
| regulation of cell migration | 21 of 529 genes, 4.0% | 254 of 25457 genes, 1.0% | 0.00015 | 0.00% | 0 | cnn2, gpr183a, ptk2ba, kita, rac2, robo4, rhogb, wasb, sema5a, rhoga, plxnc1, arhgap4a, fam83ha, cxcr4b, kitb, adam8a, csf1ra, anxa1a, inpp5d, sema4aa, ngfrb |
| regulation of leukocyte migration | 10 of 529 genes, 1.9% | 53 of 25457 genes, 0.2% | 0.00019 | 0.00% | 0 | rhoga, ptk2ba, cxcr4b, rac2, csf1ra, adam8a, wasb, rhogb, anxa1a, inpp5d |
| regulation of response to stimulus | 72 of 529 genes, 13.6% | 1829 of 25457 genes, 7.2% | 0.00019 | 0.00% | 0 | cgas, ccl34b.1, c1qa, pik3r5, cd4-1, cxcl32b.1, cyth4b, btk, cxcl11.5, ptk2ba, tnfsf10l, klhl6, rac2, si:dkey-1h24.6, blk, fybb, tlr3, c1qc, unc93b1, igf2b, inpp5d, sema4aa, lpar5b si:ch211-246e12.3, cd74b, mfap4, p2ry10, cnn2, gpr183a, tlr8b, gpr65, ptbp1a, ifnphi1, arhgef3l, gpr17, aplnra, sesn2, si:ch1073-90m23.1, c7b, aplnrb, lgals2a, c1qb, ccl34b.8, kita, tradd, si:dkey-172h23.2, draxin, gpr18, myd88, il7r, arhgap17b, sema5a, bida, traf3ip2l, mfng, cd74a, peli2, rbck1, cfbl, rmi2, rgn, socs3a, robo4, sla1a, ptprja, tlr21, cxcr4b, kitb, zgc:173915, csf1ra, lgals3b, anxa1a |
| positive regulation of intracellular signal transduction | 26 of 529 genes, 4.9% | 384 of 25457 genes, 1.5% | 0.00025 | 0.00% | 0 | cd74b, cgas, rbck1, ccl34b.1, p2ry10, ccl34b.8, pik3r5, cd4-1, cxcl32b.1, gpr183a, tradd, kita, si:dkey-172h23.2, robo4, myd88, gpr18, gpr65, il7r, bida, arhgef3l, kitb, gpr17, traf3ip2l, igf2b, lpar5b, cd74a |
| granulocyte chemotaxis | 13 of 529 genes, 2.5% | 101 of 25457 genes, 0.4% | 0.00028 | 0.00% | 0 | ccl34b.1, ccl34b.8, cxcl32b.1, cxcl11.5, cxcr4b, rac2, csf1ra, lgals3b, wasb, myd88, anxa1a, cxcl18b, inpp5d |
| response to cytokine | 19 of 529 genes, 3.6% | 221 of 25457 genes, 0.9% | 0.00033 | 0.00% | 0 | cd74b, csf1rb, ccl34b.1, ccl34b.8, cd4-1, cxcl32b.1, cxcl11.5, kita, irf5, cxcl18b, cxcr3.2, il10ra, timp4.3, kitb, il2rga, csf1ra, anxa1a, lifrb, cd74a |
| neutrophil migration | 14 of 529 genes, 2.6% | 122 of 25457 genes, 0.5% | 0.0004 | 0.00% | 0 | rhoga, ccl34b.1, ccl34b.8, cxcl32b.1, cxcl11.5, cxcr4b, rac2, lgals3b, rhogb, wasb, myd88, cxcl18b, inpp5d, cyba |
| regulation of locomotion | 22 of 529 genes, 4.2% | 296 of 25457 genes, 1.2% | 0.00047 | 0.00% | 0 | cnn2, gpr183a, ptk2ba, kita, rac2, robo4, rhogb, wasb, sema5a, rhoga, plxnc1, arhgap4a, anxa5b, fam83ha, cxcr4b, kitb, adam8a, csf1ra, anxa1a, inpp5d, sema4aa, ngfrb |
| regulation of cellular component movement | 22 of 529 genes, 4.2% | 296 of 25457 genes, 1.2% | 0.00047 | 0.00% | 0 | cnn2, gpr183a, ptk2ba, kita, rac2, robo4, rhogb, wasb, sema5a, rhoga, plxnc1, arhgap4a, anxa5b, fam83ha, cxcr4b, kitb, adam8a, csf1ra, anxa1a, inpp5d, sema4aa, ngfrb |
| regulation of immune response | 22 of 529 genes, 4.2% | 298 of 25457 genes, 1.2% | 0.00053 | 0.00% | 0 | cd74b, cgas, mfap4, c1qb, c1qa, cfbl, kita, klhl6, si:dkey-1h24.6, myd88, blk, tlr8b, fybb, tlr3, tlr21, kitb, c1qc, unc93b1, c7b, zgc:173915, anxa1a, cd74a |

| | | | | | | |
|---|---|---|---|---|---|---|
| intracellular signal transduction | 74 of 529 genes, 14.0% | 1953 of 25457 genes, 7.7% | 0.00057 | 0.00% | 0 | cgas, tuft1a, ccl34b.1, pik3r5, cd4-1, cxcl32b.1, cyth4b, btk, adcy7, rac2, dock8, sh2b3, rasgrp4, blnk, ccr9a, igf2b, prex1, csrp1a, hunk, lpar5b, prkcq, si:ch211-246e12.3, cd74b, p2ry10, cnn2, gpr183a, cmklr1, si:dkey-265e15.2, gpr65, cxcr3.2, arhgef3l, gpr17, aplnra, jak3, sesn2, si:ch1073-90m23.1, aplnrb, plcg2, si:ch211-191c10.1, pycard, ngfrb, rgl1, ccr12a, ccl34b.8, arhgap31, kita, tradd, si:dkey-172h23.2, rhogb, gpr18, myd88, il7r, si:ch211-241f5.3, arhgap17b, prkacba, bida, pak2a, traf3ip2l, myo9b, cd74a, rbck1, rhof, rgn, crip1, socs3a, rgs14a, robo4, lcp2a, rhoga, ptprja, cxcr4b, gmip, kitb, mtmr8 |
| gliogenesis | 15 of 529 genes, 2.8% | 145 of 25457 genes, 0.6% | 0.0006 | 0.00% | 0 | olig1, sox9a, slc7a7, myrf, swap70b, notch1a, gpr183a, tuba8l3, plp1b, nkx2.2a, csf1ra, sox10, anxa1a, il7r, olig2 |
| regulation of intracellular signal transduction | 36 of 529 genes, 6.8% | 684 of 25457 genes, 2.7% | 0.00063 | 0.00% | 0 | cgas, ccl34b.1, ccl34b.8, pik3r5, cd4-1, cxcl32b.1, cyth4b, tradd, kita, si:dkey-172h23.2, myd88, gpr18, il7r, arhgap17b, bida, igf2b, traf3ip2l, lpar5b, cd74a, si:ch211-246e12.3, cd74b, rbck1, p2ry10, gpr183a, rgn, cnn2, robo4, gpr65, arhgef3l, ptprja, kitb, gpr17, sesn2, aplnra, si:ch1073-90m23.1, aplnrb |
| response to stress | 68 of 529 genes, 12.9% | 1743 of 25457 genes, 6.8% | 0.00063 | 0.00% | 0 | cgas, ccl34b.1, cxcl32b.1, ano6, cxcl11.5, ptk2ba, rac2, cybb, blk, si:ch211-66k16.27, ncf1, tlr3, cd59, unc93b1, p2ry12, igf2b, hck, neil3, csrp1a, cd74b, mfap4, lpar5a, f13a1b, mpeg1.1, ptpn6, ccnd1, npsn, tlr8b, cxcr3.2, ifnphi1, ninj2, f13a1a.1, im:7154036, fzd2, caspb, esco2, sesn2, si:ch73-226l13.2, il1fma, pycard, ifnphi2, ttk, lgals2a, ccl34b.8, insm1a, ppp1r15b, myd88, cxcl18b, pak2a, cd74a, cdk1, rmi2, caspa, crip1, irf5, socs3a, mcamb, nfe2l1a, il10ra, sla1a, tnfaip8l2a, tlr21, cxcr4b, nfe2l2b, adam8a, csf1ra, zgc:173915, anxa1a |
| cytokine-mediated signaling pathway | 17 of 529 genes, 3.2% | 187 of 25457 genes, 0.7% | 0.00065 | 0.00% | 0 | cd74b, csf1rb, ccl34b.1, ccl34b.8, cd4-1, cxcl32b.1, cxcl11.5, kita, irf5, cxcl18b, cxcr3.2, il10ra, kitb, il2rga, csf1ra, lifrb, cd74a |
| regulation of developmental process | 44 of 529 genes, 8.3% | 942 of 25457 genes, 3.7% | 0.00089 | 0.00% | 0 | lgals2a, spi1b, cyfip1, ano6, ptk2ba, enpp1, rac2, slc3a2a, rhogb, myd88, cdca7a, f11r.1, grn2, sema5a, plxnc1, notch1a, pak2a, spi1a, igf2b, rbm47, sema4aa, cdk1, cdc25b, csf1rb, rhof, gpr183a, ccnd1, grn1, socs3a, sox10, gpr65, ptbp1a, fmnl3, rhoga, sox9a, swap70b, cxcr4b, grna, aplnra, csf1ra, aplnrb, kctd12.2, anxa1a, olig2 |
| positive regulation of immune response | 20 of 529 genes, 3.8% | 259 of 25457 genes, 1.0% | 0.0009 | 0.00% | 0 | cd74b, cgas, mfap4, c1qb, c1qa, cfbl, klhl6, si:dkey-1h24.6, myd88, blk, tlr8b, fybb, tlr3, tlr21, c1qc, unc93b1, c7b, zgc:173915, anxa1a, cd74a |
| leukocyte activation involved in immune response | 8 of 529 genes, 1.5% | 36 of 25457 genes, 0.1% | 0.00094 | 0.00% | 0 | cd74b, gpr183a, cd83, blk, myd88, anxa1a, cxcr3.2, cd74a |
| cellular response to cytokine stimulus | 17 of 529 genes, 3.2% | 193 of 25457 genes, 0.8% | 0.00103 | 0.00% | 0 | cd74b, csf1rb, ccl34b.1, ccl34b.8, cd4-1, cxcl32b.1, cxcl11.5, kita, irf5, cxcl18b, cxcr3.2, il10ra, kitb, il2rga, csf1ra, lifrb, cd74a |
| positive regulation of cytosolic calcium ion concentration | 16 of 529 genes, 3.0% | 176 of 25457 genes, 0.7% | 0.00144 | 0.00% | 0 | itpr2, ccr12a, p2ry10, cmklr1, gpr18, gpr65, cxcr3.2, ptbp1a, cxcr4b, ccr9a, gpr17, aplnra, aplnrb, itpr3, p2rx7, lpar5b |
| cell activation involved in immune response | 8 of 529 genes, 1.5% | 38 of 25457 genes, 0.1% | 0.00147 | 0.00% | 0 | cd74b, gpr183a, cd83, blk, myd88, anxa1a, cxcr3.2, cd74a |
| response to external stimulus | 50 of 529 genes, 9.5% | 1161 of 25457 genes, 4.6% | 0.00162 | 0.00% | 0 | cgas, cyfip1, ccr12a, ccl34b.1, ccl34b.8, cxcl32b.1, ano6, cxcl11.5, ptk2ba, atf3, rac2, nkx2.2a, draxin, rhogb, wasb, myd88, blk, cxcl18b, ncf1, sema5a, plxnc1, tlr3, cd59, ccr9a, inpp5d, sema4aa, cfbl, gpr183a, mpeg1.1, npsn, cmklr1, socs3a, irf5, robo4, tlr8b, cxcr3.2, ctsk, ifnphi1, rhoga, tlr21, caspb, cxcr4b, sesn2, csf1ra, lgals3b, pycard, p2rx7, anxa1a, ifnphi2, cyba |
| inflammatory response | 19 of 529 genes, 3.6% | 246 of 25457 genes, 1.0% | 0.00172 | 0.00% | 0 | ccl34b.1, ccl34b.8, cxcl32b.1, cxcl11.5, myd88, tlr8b, si:ch211-66k16.27, cxcl18b, tlr3, tlr21, caspb, cxcr4b, p2ry12, si:ch73-226l13.2, adam8a, csf1ra, il1fma, pycard, anxa1a |

| | | | | | | |
|---|---|---|---|---|---|---|
| oligodendrocyte differentiation | 9 of 529 genes, 1.7% | 52 of 25457 genes, 0.2% | 0.00177 | 0.00% | 0 | olig1, sox9a, myrf, swap70b, plp1b, nkx2.2a, sox10, olig2, il7r |
| regulation of cytosolic calcium ion concentration | 17 of 529 genes, 3.2% | 207 of 25457 genes, 0.8% | 0.00273 | 0.00% | 0 | itpr2, ccr12a, p2ry10, scgn, cmklr1, gpr18, gpr65, cxcr3.2, ptbp1a, cxcr4b, ccr9a, gpr17, aplnra, aplnrb, itpr3, p2rx7, lpar5b |
| hemopoiesis | 29 of 529 genes, 5.5% | 520 of 25457 genes, 2.0% | 0.00279 | 0.00% | 0 | spi1b, ephx2, csf1rb, scube1, gpr183a, kita, ada2b, myd88, hlx1, blk, gpr65, cdca7a, il7r, sh2b3, f11r.1, rgs18, slc7a7, arpc1b, notch1a, ikzf1, kitb, jak3, spi1a, il2rga, csf1ra, bdh2, anxa1a, dok2, itgb2 |
| regulation of multicellular organismal process | 47 of 529 genes, 8.9% | 1090 of 25457 genes, 4.3% | 0.00336 | 0.00% | 0 | lgals2a, spi1b, cgas, apoc1, ano6, ptk2ba, enpp1, myd88, blk, cdca7a, grn2, f11r.1, sema5a, plxnc1, tlr3, notch1a, pak2a, spi1a, sema4aa, cd74a, cdk1, cd74b, cdc25b, csf1rb, gpr183a, cnn2, ccnd1, grn1, socs3a, sox10, tlr8b, gpr65, sox9a, lgals9l1, anxa5b, swap70b, cxcr4b, grna, lgals9l3, aplnra, csf1ra, aplnrb, eif4ebp3l, apoeb, kctd12.2, anxa1a, olig2 |
| Rac protein signal transduction | 6 of 529 genes, 1.1% | 20 of 25457 genes, 0.1% | 0.00373 | 0.00% | 0 | arhgap17b, rac2, rhoga, robo4, rhogb, si:ch211-246e12.3 |
| hematopoietic or lymphoid organ development | 29 of 529 genes, 5.5% | 532 of 25457 genes, 2.1% | 0.00438 | 0.00% | 0 | spi1b, ephx2, csf1rb, scube1, gpr183a, kita, ada2b, myd88, hlx1, blk, gpr65, cdca7a, il7r, sh2b3, f11r.1, rgs18, slc7a7, arpc1b, notch1a, ikzf1, kitb, jak3, spi1a, il2rga, csf1ra, bdh2, anxa1a, dok2, itgb2 |
| glial cell differentiation | 13 of 529 genes, 2.5% | 131 of 25457 genes, 0.5% | 0.00572 | 0.00% | 0 | olig1, sox9a, slc7a7, myrf, swap70b, notch1a, tuba8l3, plp1b, nkx2.2a, csf1ra, sox10, il7r, olig2 |
| small GTPase mediated signal transduction | 22 of 529 genes, 4.2% | 344 of 25457 genes, 1.4% | 0.00581 | 0.00% | 0 | rhof, p2ry10, cyth4b, arhgap31, si:dkey-172h23.2, rac2, robo4, rhogb, dock8, gpr18, gpr65, arhgap17b, rhoga, rasgrp4, arhgef3l, gpr17, si:ch1073-90m23.1, myo9b, lpar5b, ngfrb, rgl1, si:ch211-246e12.3 |
| neutrophil chemotaxis | 11 of 529 genes, 2.1% | 94 of 25457 genes, 0.4% | 0.00647 | 0.00% | 0 | ccl34b.1, ccl34b.8, cxcl32b.1, cxcl11.5, cxcr4b, rac2, lgals3b, wasb, myd88, cxcl18b, inpp5d |
| immune system development | 29 of 529 genes, 5.5% | 543 of 25457 genes, 2.1% | 0.00652 | 0.00% | 0 | spi1b, ephx2, csf1rb, scube1, gpr183a, kita, ada2b, myd88, hlx1, blk, gpr65, cdca7a, il7r, sh2b3, f11r.1, rgs18, slc7a7, arpc1b, notch1a, ikzf1, kitb, jak3, spi1a, il2rga, csf1ra, bdh2, anxa1a, dok2, itgb2 |
| regulation of neutrophil migration | 6 of 529 genes, 1.1% | 22 of 25457 genes, 0.1% | 0.00694 | 0.00% | 0 | rac2, rhoga, rhogb, wasb, cxcr4b, inpp5d |
| positive regulation of cellular process | 80 of 529 genes, 15.1% | 2322 of 25457 genes, 9.1% | 0.00751 | 0.00% | 0 | cgas, ccl34b.1, pik3r5, cd4-1, cxcl32b.1, tnfsf10l, rac2, cdc14ab, blk, tpx2, myrf, notch1a, igf2b, sema4aa, lpar5b, rxraa, cd74b, cdc25b, cdk2, p2ry10, foxj2, scgn, gpr183a, ccnd1, si:dkey-206d17.12, trim33l, gpr65, ptbp1a, si:ch211-113a14.18, arhgef3l, caspb, etv4, esco2, gpr17, aplnra, sesn2, aplnrb, wasf2, pycard, olig2, lgals2a, bnip4, ccl34b.8, tradd, kita, si:dkey-172h23.2, nkx2.2a, wasb, ppp1r15b, gpr18, myd88, wasa, il7r, sema5a, bida, fam49ba, plxnc1, arpc1b, fam83ha, pak2a, traf3ip2l, ptprc, cd74a, rbck1, csf1rb, casp22, caspa, robo4, sox10, nfe2l1a, pparg, sox9a, pfn1, swap70b, kitb, nfe2l2b, csf1ra, adam8a, anxa1a, top2a |